Force and centre of pressure measurements during ice hockey skating with a regular and a modified ice hockey skate

By:

Chau Le Ngoc

Department of Kinesiology and Physical Education

McGill University, Montreal, QC

December 2012

A thesis submitted to McGill University in partial fulfillment of the requirements of the degree of Masters of Science

Acknowledgements

I would like to thank my supervisor, Dr. René Turcotte who has given me an opportunity to pursue graduate studies. Thank you for your guidance and your motivation. I would also like to thank my co-supervisor Dr. David Pearsall who has given a lot of support on my project. Thanks to our research assistant, Yannick who has spent a tremendous amount of time in helping me with my project with his technical expertise and his advice. I also have to thank all my colleagues Cam, Marc, Lisa, Leo, Ryan and Sam who have always been there to help and assist me. Thanks to Sylvain and Lasse who have helped me with pilot work and testing. Finally, thanks to all my friends and family for their continued support.

Table of Contents

Abstract

Force and centre of pressure (COP) were measured during a forward skating task on ice using a standard hockey skate and a modified skate with an altered tendon guard and eyelet configuration which allows for increased dorsiflexion and plantarflexion. The objective of this study was to determine if those skate design changes would result in biomechanical changes in the skaters during forward skating. Both left and right skates were instrumented with a calibrated strain gauge force transducer system to measure forces and with an insole system used to measure the COP during the forward skating task. The modified skate showed a reduction of 14.5-24.3 mm in total anterior-posterior COP excursion ($p < .05$). This suggests that the modified skate changes the biomechanics of the skaters. However, a full body kinematic study might be needed in order to study the exact biomechanical changes.

Abrégé

La force et le centre de poussée (CDP) ont été mesurés pendant le patinage sur glace en ligne droite en utilisant des patins de hockey standards et des patins de hockey modifiés avec un protecteur du tendon d'Achille plus flexible et une configuration différente des oeillets pour lacets permettant une plus grande dorsiflexion et flexion plantaire de la cheville. Le but de cette étude était de déterminer si ces changements de construction de patins ont une influence sur le mouvement biomécanique des patineurs pendant le patinage sur glace en ligne droite. Les patins gauches et droites ont été instrumentés avec un système d'estimation de la force calibré et avec un système de capteurs de pression en dessous de la semelle pour mesurer le CDP. L'utilisation du patin modifié s'est manifestée par une réduction de 14.5 à 24.3 mm du déplacement total du CDP dans la direction antéro-postérieure ($p < .05$). Celà suggère que l'utilisation du patin modifié a un effet sur la biomécanique des patineurs. Cependant, une étude cinématique du corps au complet serait peut-être nécéssaire afin d'étudier les changements biomécaniques exacts.

List of Figures

List of Tables

1. Introduction

1.1 Thesis Outline

The purpose of this thesis is to compare skaters using a standard ice hockey skate to a modified ice hockey skate by looking at kinematic and kinetic (centre of pressure measurements). Chapter 1 presents the thesis outline, the definition of the nomenclature, the rationale for this study, hypotheses, limitations and delimitations of the study and a description of the variables investigated. Chapter 2 provides a review of literature related mostly to the history of hockey and the ice skate, the classification of hockey skills and factors affecting performance, an analysis of skating analysis kinematics and kinetics. Chapter 3 defines the methodology of the thesis research. This section includes the presentation of the subjects, a complete and detailed research protocol, the explanation of all equipment utilized including the calibration procedure, the statistical methods as well as a description of the data acquisition and processing. Chapter 4 presents the results of the study. Chapter 5 will contain a discussion of the previously presented results.

1.2 Operational Definitions

Centre of Pressure: Instantaneous point of application of the ground reaction force

Regular skate: A standard Bauer One95 ice hockey skate

Modified skate: A One95 ice hockey skate including a modified flexible Achilles tendon guard and a modified eyelet placement at the metatarsal guard allowing for increased plantarflexion and dorsiflexion

Kinematics: The area of biomechanics that describes movement without consideration of the forces leading to that motion

Kinetics: The area of biomechanics concerned with the forces that produce given movements

Skating Stride: The biphasic motion of skating, which begins when the foot contacts the ice with the blade and progresses through glide, push-off, and recovery of the ipsilateral limb (Upjohn, Turcotte, Pearsall, & Loh, 2008)

Stride Phases: 1. Initial Contact: Initial blade to skating surface contact.
2. Glide: Following initial contact, the phase of the stride in which no propulsion is occurring. The orientation of the blade of the skate on the ice is steering the body movement.
3. Push-Off: Following the glide, the phase in which the blade turns outwards, creating propulsion from extension of the hip, knee, and ankle
4. Swing: Flexion of the non-weight bearing limb, allowing it to swing forward to begin the next stride.

1.3 Rationale

Despite the increasing popularity of the sport of ice hockey, there have not been many studies investigating the biomechanics of ice hockey skating. Ice hockey research has mostly been focused on the physiology of training and conditioning, skill development, safety and injury prevention (D. J. Pearsall, Turcotte, & Murphy, 2000). Skating is a fundamental skill in ice hockey (Bracko, 2001) and previous research has demonstrated that significant improvements in skating performance can be achieved by improved skate design (de Koning, Houdijk, de Groot, & Bobbert, 2000). The ice skate has constantly evolved throughout history and with technological advances, improvements in skate design have become evident in recent years (Formenti & Minetti, 2007). The most significant development in ice skating may be the klapskate designed with a hinge under the anterior part of the skate boot. The development of the klapskate has revolutionized the sport of speed skating resulting in improved ice skating performance (de Koning, et al., 2000; Houdijk et al., 2000).

Forward skating is used by ice hockey players in many situations during a game. The ice skating stride consists of two phases: single support and double support. The total time of the stride is composed of approximately 18% double support and 82% single support. Propulsion starts approximately halfway through the single support phase and lasts until the end of the subsequent double-support phase. Propulsion begins with hip external rotation and initial extension of the hip and knee and ends with full knee extension, hip hyperextension and plantar flexion (Marino & Weese, 1979). Forward skating performance is dependent on the ability to accelerate in two or three strides, and short periods of high intensity skating (Marino, 1983).

Speed skating skills can be defined as closed, while in ice hockey, skating skills can be defined as open because hockey players have to react to the environment they are playing in. However, the skating mechanics are similar in both sports, especially for forward skating. The studies on the klapskate in speed skating have revealed the importance of increased ankle range of motion in skating performance (de Koning, et al., 2000). One study compared push-off mechanics with a conventional fixed blade skate and a klapskate. The study showed that the klapskate allowed for an increase in skating velocity of 5% which can be explained by an increase in work per stroke and stroke frequency. The difference in work per stroke occurs during the final 50 ms of the push-off phase (Houdijk, et al., 2000). As well, the conventional skate did not allow the skater to fully extend the knee and ankle joints before the skate was lifted at the beginning of recovery phase. Kinematic analysis using skate models have suggested that the type of hockey skate an athlete wears can affect the range of motion of the ankle and subtalar joint during the skating stride (Hoshizaki, 1989). The conventional skate boot in ice hockey restricts range of motion at the ankle and thus there is potential for increasing that range of motion which might result in a better skate design. However, further studies are needed in order to examine if that increased range of motion would benefit the ice hockey player.

Previous work has demonstrated that strain gauges could be used on ice to measure vertical and medial-lateral forces acting on the skate during ice hockey skating. This system allowed skaters to use a natural skating motion and did not affect the integrity of the hockey skate construction or design characteristics. However, the configuration of the strain gauge system did not reveal the forces produced at the extreme

front and back of the skate or where the force was applied under the foot (Stidwill et al, 2009). That system was used to compare the kinetics between the two skate models: a Bauer One95 and a modified Bauer One95 with a flexible tendon guard which allows for increased ankle range of motion. Comparison of the skate models revealed that the modified skate allowed for gains in plantarflexion and net plantar/dorsiflexion range of motion when compared to the standard skate model. A greater kinetic output via an increase in medial-lateral force generation was also observed. Peak force occurred later during plantarflexion, suggesting that the increased range of motion resulted in a more prolonged force generation during a given skating stride. As a result, there was a 14 to 20% increase in work and power output although this increase was not statistically significant (Lachaîne, 2010).

However, the location and the manner of the application of force in the skate during skating are still unknown. In order to further examine these differences between the two skate models, a centre of pressure study is needed. The development of a system that would allow the tracking of the plantar center of pressure (COP) during skating maneuvers on ice would further our understanding of method and the timing of force generation during skating tasks on ice. The plantar centre of pressure can be defined as the origin of the ground reaction force vector acting on the plantar surface of the foot, or more specifically, the location in the skate boot where the foot is applying force. The COP is a variable that has been used as a measure of balance, foot function and treatment efficacy (Chesnin, Selby-Silverstein, & Besser, 2000). An evaluation of the COP and how it is applied during skating would help elaborate our understanding of skating mechanics and could also be used to evaluate the effects of skate design on some aspects

of skating mechanics. This has potential application to performance and improving skate design.

This study will compare two different skate models by examining both the forces acting on the skates as well as the plantar centre of pressure during skating. The two skate models used will be a Bauer One95 and a modified Bauer One95 with a modified tendon guard and eyelet configuration designed specifically to permit increased dorsiflexion and plantar flexion. The forces will be measured using a strain gauge system on the blade holder and the plantar centre of pressure will be measured using pressure sensors on an insole system.

Concurrent validity and reliability of COP measurements using an insole instrumented with FSA sensors and COP measured on a force plate will be assessed. A Bertec force plate (4060-10, Bertec, Columbus, OH) will be used to validate the COP measured with the Force Sensitive Application Array (FSA) sensors (Vista Medical, Winnipeg, Manitoba). The system will then be used quantify the center of pressure during forward skating in the two different types of skates. Force measurements will be measured using the strain gauge system developed by Stidwill et al. (2009). By quantifying the plantar centre of pressure during skating, this study will allow a better understanding of how plantar forces are generated during ice hockey skating.

1.4 Purpose

The purpose of this study is to determine the effect of a skate with a modified boot design designed specifically to permit increased dorsiflexion and plantarflexion on skating mechanics. The centre of pressure as well as the forces exerted on the skates during a forward skating task will be measured.

1.5. Research Hypotheses

It is hypothesized that the modified skates will allow for greater COP excursion, especially in the AP direction, during the execution of the forward skating task as compared to the regular skate. The ML centre of pressure excursion should not be affected as much as the skate modifications have a greater impact on dorsiflexion and plantarflexion which will affect the AP centre of pressure. It is expected that there will be no statistically significant differences in the kinetic values, as shown in previous studies.

1.6 Limitations

- There is a discrete amount of sensors which does not cover the whole area of the insole limiting the mapping of pressure measurement in the skate.

- The subjects will not be wearing full ice hockey equipment, thus possibly affecting the kinetics and kinematics of the skating stride.

1.7 Delimitations

- The study will only examine certain aspects of skating: forward linear skating acceleration, constant velocity and deceleration

- Only experienced male skaters will be studied.

- Only subjects fitting sizes 8.5 and 9 skates (equivalent to shoe size 10-10.5) will be studied.

2. Review of Literature

2.1 History of Ice Skating and Ice Hockey

Throughout history, human beings have developed tools that make better use of their neuromuscular system to allow for a more energy efficient way of travelling. Such examples are bicycles, skis and ice skates. Humans started ice skating more than 3000 years ago (Formenti & Minetti, 2007). It is hypothesized that ice skating was first developed as a more energy efficient means of locomotion. The first ice skates were made of animal bones and were discovered by archaeologists in cold North European countries such as Finland, the Netherlands, Sweden and Norway. Most of the skates were found in areas where water covers more than 5% of the land's surface (Formenti & Minetti, 2007, 2008). It has been suggested that these skates would allow travelling over frozen lakes instead of avoiding them. In a time where survival depended on saving energy to hunt for food, skating on bones might have helped humans survive by reducing the cost of locomotion. Later, approximately in the 13th century in The Netherlands, a few skates made of wood with a metal blade fixed under the boot were developed. Competitive ice skating might have existed as early as the 16th and 17th century (de Koning, et al., 2000). By the 18th century, the ice skate had evolved to include a longer blade, providing easier balance control. In the 19th century, boots were screwed on a metal frame, which allowed for easier and safer travelling. This basic design was used to construct typical speed skates that have been used by high performance speed skaters for at least a century (de Koning, et al., 2000). Advances in technology have since allowed the development of longer and thinner blades. The most significant development in ice skating might be the klapskate. The klapskate possesses a hinge under the anterior part of

the foot which allows for a more powerful plantar flexion which helps increase the skater's impulse through a longer skating stroke.

Although ice skating originated in Northern Europe, the sport of ice hockey is believed to have originated in Canada in the 1880s. The rules of ice hockey were influenced by English, Scottish and Irish immigrants. Since then, the game of ice hockey has evolved at a fast pace and has increased in popularity. The game has become more sophisticated and expensive to play due to technical innovations in equipment design and facilities as well as improvement in training, coaching and game strategies. (D. J. Pearsall, et al., 2000).

2.2 Classification of Skills in Ice Hockey

Because the game of ice hockey is played under specialized conditions, most notably a low friction surface, it requires a unique set of skills compared to other team sports. The skills in ice hockey are primarily goal oriented and the timing and the movement patterns are a secondary function to the achievement of the task. To determine a player's skill, both the objectives and the player's movements have to be considered. Some skills in hockey can be considered closed while other skills can be considered open. The skills might be considered closed in that certain features of the environment are constant such as the rink dimensions and the equipment. However, the skills are more often considered open. The performance of a skill depends on the changing surroundings such as the positions of other players and whether they are moving or not. Because, ice hockey is often played in open conditions, perception, decision making and reaction time are as important as the movement in defining skills levels. Several qualities such as

timing, anticipation, direction, balance, accuracy, rhythm, speed, versatility, agility and reaction time can therefore be used to define skill level in ice hockey (D. J. Pearsall, et al., 2000).

General movement patterns in ice hockey include skating, stick handling and checking. The variations and subsets of these skills can be found in figure 2. There are a variety of skills and techniques used by hockey players which are used in an ever-changing environment. This makes ice hockey an exciting sport to play and watch (D. J. Pearsall, et al., 2000).

Skating Skills			
Linear - forward - backwards	**Angular** external (change in direction of movement) - crossover - forward - backwards -parallel blade pivot internal (change in body orientation) -longitudinal axis - front to back - back to front	**Starts** forward - forward - crossover - side - running backwards - straight - crossover	**Stops** forward - snowplow - two foot - one foot - front or rear "T" - running backwards - snowplow - two foot - one foot (rear) side (parallel) - two foot - one foot (front)

Figure 2.1: Classification of hockey skills (adapted from Pearsall, 2000)

2.3. Biomechanics of Ice Skating

Ice hockey is a dynamic and fast-paced team sport because it is played on an ice surface which allows the players to perform movements with great agility and speed. The single most important skill for an ice hockey player is ice skating. Performance in ice skating can depend on many biomechanical factors. However, there has been limited research on the biomechanics of ice hockey skating. An understanding of the biomechanics of the ice skating is important to performance, injury prevention and skate design. Most of the research on ice skating has looked primarily at the kinematic aspect of successful skating performance (Lafontaine, 2007; Upjohn, Turcotte, Pearsall & Loh, 2008). Obviously, a combination of kinematic and kinetic parameters would provide better insight on the biomechanics of ice skating. However, there have been a limited number of studies attempting to measure forces on the ice due to the nature of the environment and other technical difficulties such as portability and data storage. Some studies have looked at the kinetics of skating through the use of strain gauges, however sensor fragility, limited capacity to record force data and the need to add major modifications to the skate made this technology unpractical (de Boer et al., 1987; de Koning, 1992; Gagnon, Doré & Lamontagne, 1983; Jobse, 1990). Researchers then attempted to investigate forces during ice hockey skating while maintaining the integrity of the skate. Stidwill et al. (2009) demonstrated that strain gauges could be used on-ice to measure vertical and medial-lateral forces during ice hockey skating. The system enabled for a natural skating motion, and did not affect the structural integrity of the hockey skates. However, the configuration of the strain gauge system could not reveal the forces

produced at the extreme front and back of the skate and it did not reveal where the force was applied under the foot (Stidwill, 2009).

2.3.1 Kinematics of Skating

The kinematics of ice skating have not been extensively studied due to difficulties associated with capturing motion on ice. The lack of accuracy and the large field of view required are some of the technical challenges that researchers have to overcome (Lafontaine, 2007; Upjohn, et al., 2008). However, there are several studies investigating the kinematics of ice skating. Most of the research has in kinematics has been done on lower limbs only.

Marino published a number of studies focusing on the kinematics of the acceleration phase of skating. These studies used a video camera to derive two-dimensional data and could only offer a gross description of the forward skating movement as well as identify a few performance variables. One of these studies (Marino, 1977) using 10 skaters ranged from moderately skilled to highly skilled has examined different kinematic variables over three different skating velocities. An increase in skating velocity resulted in an increase in stride rate which corresponded to a decrease in both single and double support times. However, double support time decreased more relative to single support time. For a slow skating speed (3.75 m/s), double support time consisted of 44% of the total stride time. For a fast skating speed (6.92 m/s), double support time consisted only of 30% of total stride time. On the other hand, stride length did not change significantly. Therefore, skating velocity was more dependent on stride rate ($r = 0.76$) than stride velocity ($r = 0.05$). Close to 60% of the variation in velocity

was due to the variation in stride rate (Marino, 1977). Marino and Weese (1979) followed this study with another to further their understanding of the kinematics of the ice skating stride. For this study, the researchers used four highly skilled performers. Each subject had tight fitting sweat suits and their segmental end points were marked. They performed three trials of maximal velocity skating though a designated filming area. The mean horizontal velocity for the skaters was 8.78 m/sec. The mean stride rate was 3.54 strides per second and the mean stride length was 2.48 meters. The mean single support time was .234 seconds and the mean double support time was .052 seconds. It was concluded that on average, the total time of the stride was composed of approximately 18% double support and 82% single support. The highly skilled participants were able to generate propulsion during both periods of double support and single support. Propulsion starts approximately halfway through the single support phase and lasts until the end of the subsequent double-support phase. Propulsion begins with hip external rotation and initial extension of the hip and knee and ends with full knee extension, hip hyperextension and plantar flexion (Marino & Weese, 1979).

Marino (1979) also looked at the kinematics of forward acceleration. The acceleration pattern during the first 6 meters of skating was studied. Four subjects ranging from moderately skilled to highly skilled were used. A typical observation was a high initial acceleration during the first 1.25 seconds. For three out of the four subjects, the acceleration levels then diminished gradually until periods of deceleration began. Overall, there was positive acceleration during the first 1.75 seconds despite alternate periods of single and double support. While this study did not have many subjects, Marino was able to confirm that propulsion could occur during both single and double

support phases of the stride. They were able to maintain a positive acceleration throughout a period during which at least three strides were taken. During the first few strides, a large percentage of time is spent on single support, on average 85.3% (Marino, 1979).

A similar study on acceleration patterns was later published by Marino (Marino, 1983). Once again, the subjects' acceleration phase after a front start during the first 6 meters was studied. In this study, 69 male subjects with widely varying skill levels were used and many more kinematic variables such as stride length, vertical displacement of the recovery foot, joint angles, trunk lean angle and propulsive angle of the skate blade were studied. It was found that for a skating start with a high rate of acceleration, the stride pattern included: "a high stride rate, significant forward lean at the point of touchdown relatively short single support periods, and placement of the recovery foot almost directly beneath the body rather than in front of it at the end of the single support period" (Marino, 1983). The studies by Marino offered important insights on skating kinematics. However, most the research was done on the acceleration phase of skating and could only provide a gross description of the motions or identify factors that affect performance (Lafontaine, 2007). These studies were also limited because they only used two dimensional video analyses.

In addition to the studies conducted by Marino, there have been several studies conducted to identify performance variances in speed skating. Ingen Schenau et al. (1985) examined elite female speed skaters during an international competition. They found that speed skaters control their speed mainly by changing their stroke frequency and not by changing the amount of work per stroke. The better skaters gained potential

energy during their glide phase and showed a more horizontally directed push-off (Van Ingen Schenau, de Groot, & de Boer, 1985). De Boer et al. compared stroke mechanics between elite and trained male speed skaters. They found that better skaters showed a higher power production while having the same stroke frequency. They found several mechanical factors that could predict speed skating performance. The faster skaters reached a higher angular velocity at the knee and the time during which the knee was extended was shorter. The better push-off of the better skaters was characterized by a larger gliding time which resulted in a more effectively directed push-off force (de Boer, Schermerhorn, Gademan, De Groot, & van Ingen Schenau, 1986). Ingen Schenau et al. (1989) concluded that elite skaters possessed the following characteristics: a smaller pre-extension knee angle, mainly caused by a more horizontal upper leg position, a considerably higher amount of work per stroke and slightly higher stroke frequency, a higher knee extension velocity, a short lasting powerful push-off and a more horizontally directed push off (van Ingen Schenau, De Boer, & De Groot, 1989).

In a paper published in 1995, de Koning et al. described the speed skating stride as an evolution from running to gliding. Five elite speed skaters doing all out-starts over a distance of about 50 m were used. They were filmed using three high-speed cameras placed near the track and three dimensional coordinates were calculated. The study compared the second stroke to the eighth stroke and it was concluded that the mechanics of the first strokes of a sprints were significantly different than the mechanics of the later strokes. The first push-offs were more similar to running. During the push-off phase, the skate was perpendicular to the intended direction of travel due to external rotation of the leg and the force was applied on a fixed location on the ice as there was little

displacement of the skate, similarly to a running stride. By the eighth stride, the skate was gliding throughout the push-off phase and there was little external rotation; the push-off was more laterally directed. Gliding was defined as "the last instant when the foot moved backward relative to the body as fast as the body was moving forward relative to the ground." This occurred at a mean velocity of 6.7 m/s, after about six push-offs (de Koning, Thomas, Berger, de Groot, & van Ingen Schenau, 1995). The same research group revolutionized the sport of speed skating by developing the klapskate. The klapskate possesses a hinged skate blade holder that allows for powerful plantar flexion which helps increase the skater's impulse through a longer skating stroke (de Koning, et al., 2000; Houdijk, et al., 2000). The klapskate allows for an increase in skating velocity of 5% which can be explained by an increase in work per stroke and stroke frequency. The difference in work per stroke occurs during the final 50 ms of the push-off phase. (Houdijk, et al., 2000). The conventional skate does not allow the skater to fully extend the knee and ankle joints before the skate have to be lifted.

Pearsall and his co-workers examined foot and ankle kinematics during forward skating using biaxial electrogoniometers attached to the rear foot along the Achilles tendon inside the skate boot on both feet. The subjects had to perform forward skating in an ice hockey arena. The data was logged to a portable computer which was carried in a backpack creating a completely portable system. It was found that during single support of the glide phase, the ankle was in 7.1° of dorsiflexion with respect to the subject's neutral position with was taken during an on-ice standing position. During double support, dorsiflexion increased and reached an angle of 11.8° (D. J. Pearsall et al., 2001).

At the end of push off and at the moment the skate came off the ice, the subjects rapidly plantar flexed to a minimum of 1.9° of dorsiflexion. The foot was in dorsiflexion during the entire skating cycle. This was likely due to the position the skaters used described by van Ingen Schenau et al. (1989). van Ingen Schenau group revealed that speed skaters adopted a sitting position with the trunk in a forward lean, in order to minimize the effects of air resistance (van Ingen Schenau, et al., 1989). Also, van Ingen Schenau explained that a dorsiflexed skate was necessary to prevent scraping of the skate tip on the ice surface which would cause a large increase in ice frictional force. Throughout the glide phase, the foot was slightly everted with relatively little change in the ankle. As the skater approached double support and the foot was about to push off, the foot reached a maximal eversion of 7.1°. Once the foot reached swing phase, the ankle underwent inversion, exceeding the neutral position. In preparing for the gliding phase, the foot is in a near neutral position. While this study only used 3 subjects and looked at only one joint, it demonstrated a new technique of collecting ice skating kinematic data. Because the system was completely portable, it did not restrict the players' movements. With a camera system, it is difficult to establish a properly calibrated field of view with high resolution (D. J. Pearsall, et al., 2001). This study demonstrated that there are viable alternatives for capturing ice skating kinematics.

Lafontaine then investigated three-dimensional kinematics of the knee and ankle joints for three consecutive push-offs during ice hockey starts. Lafontaine used an innovative data collection system using a moving camera cart on guide rails (Lafontaine, 2007). The subjects had reflective markers attached to the right thigh, leg and skate boot. It was found that the range of motion in the knee and ankle joints increased as the skaters

gained speed. Knee flexion angles were the joint angles most affected by an increase in skating velocity. For the first push off, the skaters gradually increased their knee flexion during the first 70% of the push-off and followed with an extension during the last 30% of the task. Subjects kept their knees slightly flexed until the end of ice contact. During push-offs 2 and 3, the subjects initiated ice contact on a flexed leg and extended gradually over the duration of ice contact. The angle joint remained relatively stable. However, that could be attributed to the design of the skate boots which were very rigid (Lafontaine, 2007). However, that study was limited because of experimental difficulties. The skater was restricted to the field of view of the camera and the acceleration of the skater and the moving cart had to correspond. A further limitation of the study was that only capture one side of the body could be captured.

Upjohn et al (2008) examined the three-dimensional kinematics of the lower limbs during forward ice-skating. The subjects consisted of both low and high calibre skaters and studies were conducted using a skating treadmill. The subjects had to wear reflective markers placed on both sides of the body on the thighs, shanks and skates while being recorded with four synchronized digital video cameras. The problem of the large field of view required for skating task was removed by using a skating treadmill. Each participant completed trials of one minute at different speeds. The joint and limb segments angles were calculated. High calibre players were able to achieve a higher skating velocity compared to the lower calibre players while using the same stride rate. The researchers suggested that their higher skating speed was due to a greater stride length and stride width than low-calibre participants. In general, the high calibre skaters had a higher range of motion and rate of joint motion in both the sagittal and front planes

which contributed to a greater stride length. Furthermore, high-calibre skaters had greater limb excursion for the pelvis, thigh and foot. Thus, there was a greater lateral displacement of the lower limbs in high-calibre players (Upjohn, et al., 2008). In order to complete our understanding of forward hockey skating, a three-dimensional analysis of the skating stride is still needed.

A study analyzed the kinematics with a modified skate which possesses a flexible ankle guard to allow for more ankle dorsiflexion compared to a regular skate. There was a significant increase of 4º to 5º in plantarflexion range of motion and net dorsi-plantarflexion ankle range of motion(Lachaîne, 2010). The maximal plantarflexion during forward skating was 16.8º and for the outside and inside feet during crossovers 11.5º and 21.4º (Lachaîne, 2010). Moreover, at the time of peak force, the plantarflexion angle was significantly 5º higher with the modified skate. These results demonstrate that the skater was actively using the extra plantarflexion during ice contact pushoff. A study using a dynamometer testing hockey players in a seated position has shown that the modified skate allowed for substantial increases in ankle range of motion (14.8º , $p < .05$), particularly in the plantarflexion direction (12.6 º). However, no changes in inversion or eversion were found (David J. Pearsall, Paquette, Baig, Albrecht, & Turcotte, 2012).

2.3.2 Kinetics of Skating

Biomechanical research on ice skating has mostly focused on the kinematic variables that could influence skating performance. These studies were usually restricted to forward starts and forward skating (de Boer et al., 1987; Lafontaine, 2007; Marino,

1977, 1979; Marino & Weese, 1979; Upjohn, et al., 2008). Ideally, kinematic measures would have been combined with kinetic measures in order to provide more insight on the biomechanics of ice skating. However, measurements of forces during ice skating present unique technical challenges because of the ice environment (Stidwill, Turcotte, Dixon, & Pearsall, 2010). Traditional kinetic instruments such as force plates cannot be used. Instead, some studies on force measurements during skating have been done using strain gauges. These studies have used temperature compensated strain gauges as force transducers attached to an interconnected block assembly between the boot and blade of the speed skate (de Boer, et al., 1987; Jobse, Schuurhof, Cserep, Schreurs, & De Koning, 1990). The strain gauge system consisted of three subsystems: the instrumented skate, a microcomputer and the computer software. A temperature compensated strain gauge block assembly was placed between the blade and the boot of the skate. A load would cause a transformation to the measuring unit to which the Wheatstone bridge will produce a proportional electric signal. A transducer was placed in the middle of the unit to detect horizontal forces which would determine frictional force and transducers were positioned in the front and back of the unit to measure normal forces. This system was able to measure normal forces of up to 1400 N and frictional forces of up to 40 N. However, with the insertion of the system on the skate boot, the weight of the skate increased by 55% which would likely alter normal skating mechanics. The instrumented skates were wired to a microcomputer for data collection and storage. At a frequency of 200 Hz, the system could measure data for a maximum of 40 seconds. A combination of known loads was used to calibrate the system. A linear regression model was used to relate the known forces and the resulting electric signals (Jobse, et al., 1990).

Using that force measurement system, de Boer et al. (1987) found that the force measured at the front connection between the boot and the skate showed an increasing pattern towards the end of the stroke. Conversely, the force measured at the back connection showed a more or less decreasing pattern during the stroke. Therefore, during the stroke, the point of application of the total push-off vector moves forward with respect to the ankle joint (de Boer, et al., 1987). However, because of the orientations of the transducers, these studies could only measure horizontal forces and not medial-lateral forces. De Koning et al. later used the system to determine ice frictional properties during speed skating (de Koning, de Groot, & van Ingen Schenau, 1992).

A research group has recently developed a force transducer system for measurement of ice hockey skating force (Stidwill, et al., 2010). Similarly to the previous system, it consisted of three components: a hockey skate with strain gauges bonded to the blade holder, a portable data acquisition system, and post-processing software to convert micro-strain signals to force estimates. The system can accurately estimate the forces in vertical and medial-lateral forces without modification to the skate or any of its components. One gauge was used to measure the vertical strain and was oriented along the longitudinal axis of the blade holder's beam element. The medial-lateral strain was measured using two pairs of gauges. They were oriented parallel to the vertical axis of the blade holder along the front and back post. The wires were glued to the outer surface of the blade holder and were directed towards the back of the skate. These wires are then connected to a data acquisition device which can be put in a backpack worn by the subject. Testing has shown that the system could provide an accurate measure of medial-lateral, horizontal and vertical forces during ice skating. The strain gauges signals

produced a high linear relationship to known force values. This system allows for a rapid data collection as well as unencumbered skating (Stidwill, et al., 2010).

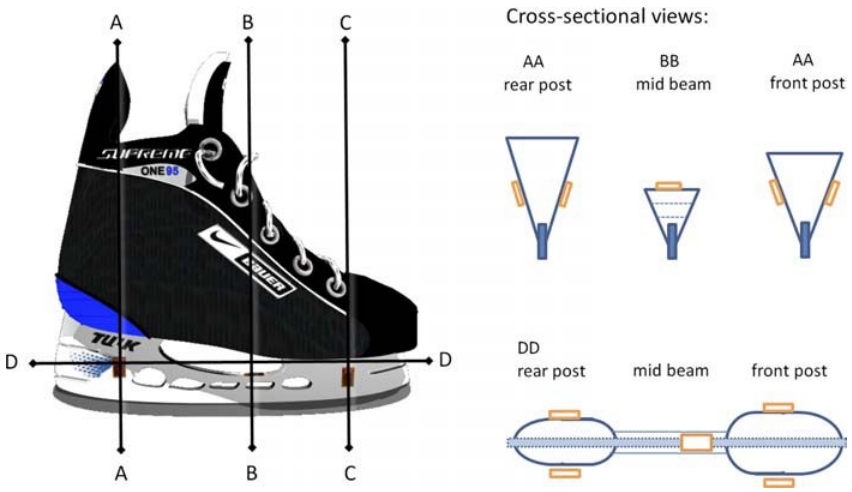

Figure 2.2: Representation of instrumented skate blade holder (top), and cross-sectional views of gauge locations (bottom). Gauges AML and PML are oriented vertically along each post, while gauge V is oriented longitudinally along the beam element of the blade holder (adapted from Stidwill et al., 2010)

That technology was used to compare the forces acting on the skate during forward and crossover skating between the modified One95 skate and a regular skate. It was found that the total average force tended to be greater with the modified One95 skate for all skating tasks by 5-8% of bodyweight. However, these differences were not significant. The medial-lateral force was significantly higher (7-10% of bodyweight) in forward skating. The total work during the skating tasks tended to be higher with the modified skate but the difference was not significant.

The system enabled for natural skating motion, and did not affect the integrity of the hockey skates. However, the configuration of the strain gauges system could not reveal the forces produced at the extreme front and back of the skate and it did not reveal where the force was applied under the foot (Stidwill, 2009). Therefore, it would be useful

to develop a portable and accurate system that would allow the measurement of force while also tracking the center of pressure (COP) during skating maneuvers on the ice.

2.4 Plantar Pressure

The foot is the terminal link of the kinematic chain in human locomotion. The foot first serves as a cushion of the impact forces during walking and running. Furthermore, the foot transfers forces produced by the muscles to the ground (Rosenbaum & Becker, 1997). Plantar pressure measurements allow us to measure the interactive force between the human body and the ground. Plantar pressure can be defined as the pressure on the plantar surface of the foot experienced during activity (Shu et al., 2010). Center of pressure (COP) on the plantar surface can also defined as the origin of the ground reaction force vector of external forces acting on the plantar surface of the foot. It can be used to measure balance and foot function (Chesnin, et al., 2000). The assessment of plantar pressure can have many applications. It can be used in the evaluation and design of footwear for people without impairment. Another application of plantar pressure is for clinical gait analysis. It can be used for the diagnosis and the assessment of different diseases such as diabetes mellitus, Hansen's disease, and rheumatoid arthritis where elevated pressure can cause injury or pain (Shu, et al., 2010). The last application is the use of plantar pressure assessment in athletic training in order to optimize sports performance. Footwear is widely believed to facilitate and enhance athletic performance (Cavanagh, Hewitt Jr, & Perry, 1992). After 2000, more studies have been reported on athletic plantar pressure such as soccer specific movements (Eils et al., 2004) and forefoot loading during running (Queen, Haynes, Hardaker, & Garrett,

2007). Pressure measurements can provide a better understanding of the effects of the shoe design on the mechanics of the foot. This has applications in both shoe design and clinical practice.

Several instruments can be used to measure COP including force plate, pressure plate and in-shoe pressure systems. Forces plate and pressure plates measure the COP at the shoe/floor interface. On the other hand, in-shoe pressure systems allow for the calculation at the foot/shoe interface which might be more representative of typical foot function (Cavanagh, et al., 1992; Shu, et al., 2010). In shoe pressure systems also offer the advantage of not being restricted to one area. There have been several studies assessing the characteristics of various pressure measurement systems. Several factors such as sensor accuracy and repeatability, sensor size, the number of sensors, sensor arrangement, sampling rate, and measurement context can affect the validity of calculating COP.

2.4.1 Types of Pressure Measurement Systems

A variety of plantar pressure measurement systems exist. The most important principle is that the act of measurement should not change the quantity being measured. Some systems use discrete sensors that act like coins placed inside the shoes and this might alter the local pressures. Other systems use matrix devices, which might change the coefficient of friction between the foot/shoe interface and act on their own to alter the pressure distribution. Moreover, almost most devices require trailing cables or the wearing of a package. These features can hinder the motion of the subject. There is a

wide variety of sensors which are commercially available and they vary greatly in cost and performance.

2.4.1.1 Types of Pressure Sensors

Capacitors

A capacitor is a device that stores charge. It is made of two conducting plates separated by diaelectric layer. The capacitance or ability to store charge is inversely proportional to plate separation. A capacitance based in-shoe pressure transducer will use a compressive diaelectric layer. By increasing the pressure, it will decrease the separation between the two plates which will increase capacitance. By measuring the instantaneous value of capacitance, the pressure can then be derived using a calibration curve.

Strain gauges

A strain gauge system used a material that changes its electrical resistance when subjected to mechanical stress. Strain gauges are usually thin metal foils and semiconductors such as silicon. Strain gauges are usually applied to a metal beam which can bend in proportion to applied force.

Piezo-electric methods

The piezoelectric effect is found in natural materials such as quartz and in manufactured materials such as PZT (lead zirconate titanate). It results in the generation of charge when the material is deformed. This charge occurs when the material is deformed due to the reordering of the atoms in the material. This charge can then be converted to a voltage proportional to the applied stress (Cavanagh, et al., 1992).

2.4.1.2 Discrete vs. Matrix Systems

Discrete transducers are usually placed at anatomically defined locations on the plantar aspect. The advantages of discrete devices are that they are small in size and affordable. The disadvantages are that they can act as a foreign body in the shoe and alter the mechanics of the foot/shoe interface. Moreover, discrete systems might be prone to inaccuracies due to incorrect or subjective positioning of the sensors. Researchers have used different methods for determining accurate sensor placements such as inked mats, X-rays and palpation of bony landmarks. The sensors might also displace due to shear stress (Cavanagh, et al., 1992). This problem might be overcome by placing the sensors inside the shoe insole. However, this might create a new problem when feet of different morphologies are analyzed with the same sensor configuration.

Matrix devices consist of numerous sensing elements arranged in rows and columns. Compared to discrete devices, this system allows for the collection of a greater area, usually the whole plantar surface. As a result, there is no need to customize the sensor placements for different subjects. Insoles using the matrix system can have at least 80 sensing areas which cover on average 1.5cm^2. There are calibration techniques so that each sensing element can be calibrated individually. One such example of a system that uses a matrix device is the F-Scan manufactured by Tekscan. The F-scan contains 960 sensing elements and is extremely thin (0.15mm).

.

The matrix devices offer a significant advantage because of the increased surface area captured. However, because of the high number of sensing areas, it is difficult to collect data at a high frequency which might not make it ideal for the study of high speed

movements such as ice hockey skating. These technologies have yet to be used inside hockey skates.

2.4.2 Validating Plantar Pressure Measures

Accurate plantar pressure measurement is required in both clinical and research settings. However, there has not been standardization processes or defined reliable reference datasets. The accuracy and reliability of existing pressure measurement devices vary widely due to different sensor technology, spatial resolution, pressure range, sampling rate and calibration and processing procedures (Giacomozzi, 2010). A study looked at the concurrent validity of a Parotec System which has 24 sensors areas. A force plate was used to compare the COP from both systems. It was found that the correlation coefficients comparing COP displacement calculated from the two systems were greater than 0.70 for 52/67 trials (78%) in the ML direction and were greater than 0.90 for 67/67 trials (100%) in the AP direction. The mean RMS error for COP displacement in the ML direction was 0.56 ± 0.3 cm. The mean RMS error for COP displacement in the AP direction was 1.37 ± 0.59 cm.

A research group designed an in-shoe plantar pressure measurement and analysis system based on a textile fabric sensor array. The system consisted of a 6 strategically placed sensors inside an insole and the signals could be transmitted wirelessly through Bluetooth.

In order to validate it, the insole was placed on a force plate. The insole coordinates were matched with the force platform before it was fixed on the platform. The subjects were required to do four tasks: normal standing, standing on one leg, heel strike and push off. The relative differences in COP were measured. The average

differences during heel-strike and push-off tests are lower than 3% and the differences in normal standing and one leg standing tests were higher. The results show that with these six pressure points, the measurement error in COP is relatively low. These results confirm the importance of these pressure points for COP measurement.

2.4.3 Applications of Plantar Pressure Measures in Sports

The centre of pressure is the instantaneous point of application of the ground reaction force. During locomotion, this point of application usually moves in a heel-to-toe direction during the stance phase with smaller displacements observed in the medial-lateral direction (De Cock, Vanrenterghem, Willems, Witvrouw, & De Clercq, 2008). One study was done on barefoot running using a pressure platform. A medially oriented peak in medial-lateral COP velocity was found, which may reflect the fast initial pronation. A laterally oriented second peak in both medial-lateral and anterior-posterior COP indicated a fast forward shift of the COP over the lateral border of the foot during forefoot contact phase. During the forefoot push off phase, at the level of the metatarsals, anterior velocities of the COP were low. This illustrates the role of the forefoot during the push-off. The authors also studied the effects of foot arch type on the displacement of COP. It was found that the low arch subjects had a greater displacement in the M-L COP. However, earlier studies have shown that there was a greater displacement in the M-L COP in high arch feet during walking (Nigg, Cole, & Nachbauer, 1993; Williams, McClay, & Hamill, 2001).

Plantar pressure distribution patterns during soccer movements have been studied. The Pedal Mobile system was used. It is a matrix system containing 99 sensing areas

which can collect at frequency of 50 Hz. The foot was separated in 10 different areas. The soccer-specific movements studied were sprinting, cutting and kicking the soccer ball and were compared to normal running. It was found that loading patterns with higher pressure values than those observed during normal run were found. In cutting and sprinting, the medial part of the foot was predominantly loaded while in kicking, the lateral part of the foot was predominantly loaded. No global effect of the two surfaces on pressure parameters was found. Also, two different playing surfaces were studied: grass and red cinder. No significant differences were found between the two surfaces. (Eils, et al., 2004)

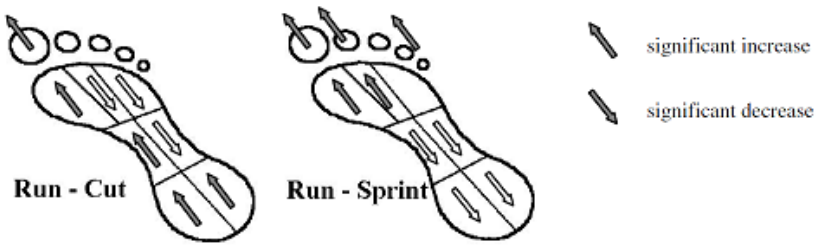

Figure 2.3: Relative peak pressures in selected soccer tasks as compared to running (adapted from Eils et al., 2004)

Another study also looked at plantar pressure in soccer-related movements. In this study, the authors compared the preferred foot and the non-preferred foot. Four movements were analyzed: running (at 3.3 m/s), sideward cutting, 45 degrees cutting and landing from a vertical jump. In general, it was found that the preferred foot had a higher overall plantar pressure. In each of the four movements, a higher pressure was found in the preferred foot during the take-off phase. However, a higher pressure was found in the non-preferred foot during the landing phase. This suggests that the preferred foot has a

bigger role for higher motion force while the non-preferred foot has a greater role for body stabilization (Wong et al., 2007).

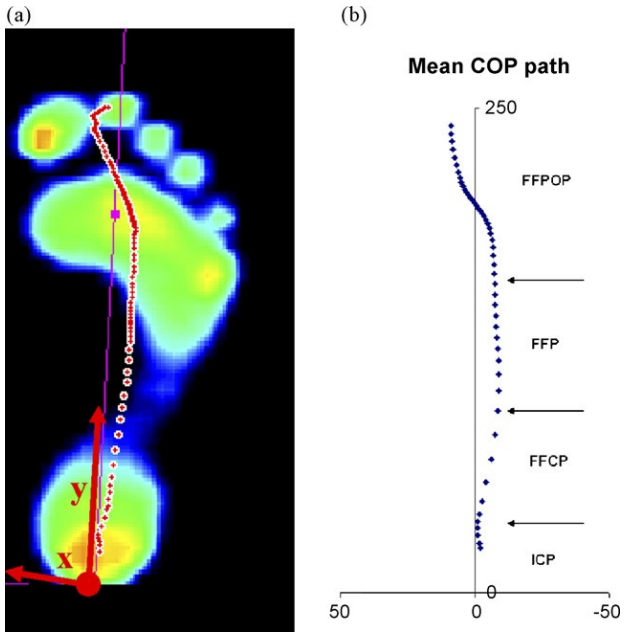

Figure 2.4: COP path during barefoot during barefoot running (adapted from De Cock, 2008)

These studies can give an insight on the structures in the foot that are being used for the different tasks. As a result, a better understanding of the mechanical demands of these tasks can be achieved. No similar studies have been done on ice hockey skating. Therefore, it will be interesting to see the difference in the COP displacement in ice skating compared to other tasks such as running, sprinting, cutting or jumping. For example, in cutting in soccer, the load is shifted from the lateral parts of the midfoot and

forefoot to the medial parts of the foot (Eils, et al., 2004) and it is possible that there are similarities with forward skating in ice hockey.

3. Methods

3.1 Subjects

Healthy, experienced adult male hockey players aged 18-28 years of age were recruited for this study. A sample size of 10 subjects was recruited to voluntarily participate in the study. The subjects had to complete an informed consent form before participating in the study.

3.1.1. Ethical Considerations

The risks associated with this study are minimal. The subjects recruited to participate in this study were proficient at the skating skills necessary to successfully perform the required tasks. Furthermore, they were executing movements similar to those used in hockey practice and game situations.

All of the personal information collected during the study was encoded in order to keep the subjects' information confidential. These records are maintained at the Biomechanics Laboratory by the principal investigator and faculty supervisor for five years after the completion of the project, and will be destroyed afterwards. Only members of the research team have access to the information. In case of presentation or publication of the results of this study, nothing will allow the identification of subjects who participated. The records are maintained through the use of an identification code consisting of the subject's number in chronological order of the date of the experiment.

The subjects were asked to complete an informed consent form. The subjects were informed that the participation in this study is entirely voluntary. The subjects were

also informed that they may withdraw from the study at any time. The consent form outlined the basic methods and explained any risks associated with the experiment. The consent forms are attached. This project has been approved by the McGill University Research Ethics Board (REB file number 270-0112).

3.2 Equipment

The pressure measurement system consists of an insole with pressure sensors taped under the sole.

Figure 5: FSA sensors fitted under the insole

3.2.1 FSA sensors

There are a variety of pressure sensors available but the Force Sensitive Application Array (FSA) sensors were chosen for this project in order to create an instrumented insole. The FSA sensors (ISS-O) (Vista Medical, Winnipeg, Manitoba) are thin, flexible piezo-resistive force sensors. The sensors for this project need to be thin and light so that they do not interfere with the natural motion of ice skating. Since the sensors are placed under the insole, it will not affect the foot/insole interface. The sensors must be placed under the insole to ensure there is no displacement during the procedures. The wires need to be flexible and need to be resistant to bending and twisting because they must pass through the underside of the insole into the back of the skating boot. The FSA sensors satisfy both of these conditions. Furthermore, the FSA sensors are coated with Teflon which makes them more durable.

Many of these systems can only collect at a lower frequency (~50-100 Hz) because of the high number of sensors collecting simultaneously. The FSA sensors are 1.7 cm x 1.5 cm in dimension and have an active sensing area of 0.64 cm x 0.64 cm. A 32-channel amplifier was developed and connected to a data acquisition device (DAQ) to allow a sampling rate of 1000 Hz. The amplifier was designed using PCB Artist software (Advanced Circuits, Aurora, CO) assembled in lab using two custom printed circuit boards manufactured by Advanced Circuits (Aurora, CO) and surface mounted electronics to minimize size and weight. The FSA sensors' leads were connected to a ribbon cable (UL Style 2651 300 Volt Max, Phalo Corporation, Manchester, NH) leading to the amplifier. In turn, the amplifier is in series with a data acquisition device (cDAQ-9174, National Instruments, Austin, TX) linked by an USB cable to a computer using the

LabVIEW™ Version 10.0 (National Instruments®, Austin, Texas) software to the record the sensors' voltages. The amplifier and DAQ board are driven by 5V DC.

3.2.2 Instrumented Insole

The foot can be separated into 15 major pressure points: the heel (points 1-3), midfoot (points 4-5), metatarsals (points 6-10), and toes (points 11-15). These areas support most of the body weight and can be used to derive information of the lower limb and body as a whole (Shu et al., 2010). However, since no study has measured plantar pressure in an ice hockey skating boot the exact locations of the sensors were selected through trial and error to find the locations that provided the optimal responses. Since the sensors are set at a fixed location under the insole, the sensor configuration is the same for different subjects. However, subjects of different foot sizes and morphologies were tested in order to optimize the placement of the FSA sensors.

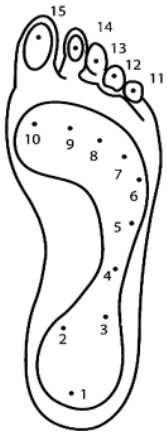

Figure 3.1: Foot anatomical areas (adapted from Shu, 2010)

Two perpendicular lines were drawn under the insole to represent x and y axis. The sensors were wired to a 16-channel custom-built amplifier using fixed resistances of 3kΩ using PC ribbon cable. The amplified signal was output to a PC USB data acquisition device (DAQ) (NI USB-6210, National Instruments, Austin, TX) where data were sampled at 1000 Hz per channel at 16-bit resolution. The program Labview provided a visual interface with a live display.

Figure 3.2: LabView 2010 interface for data collection

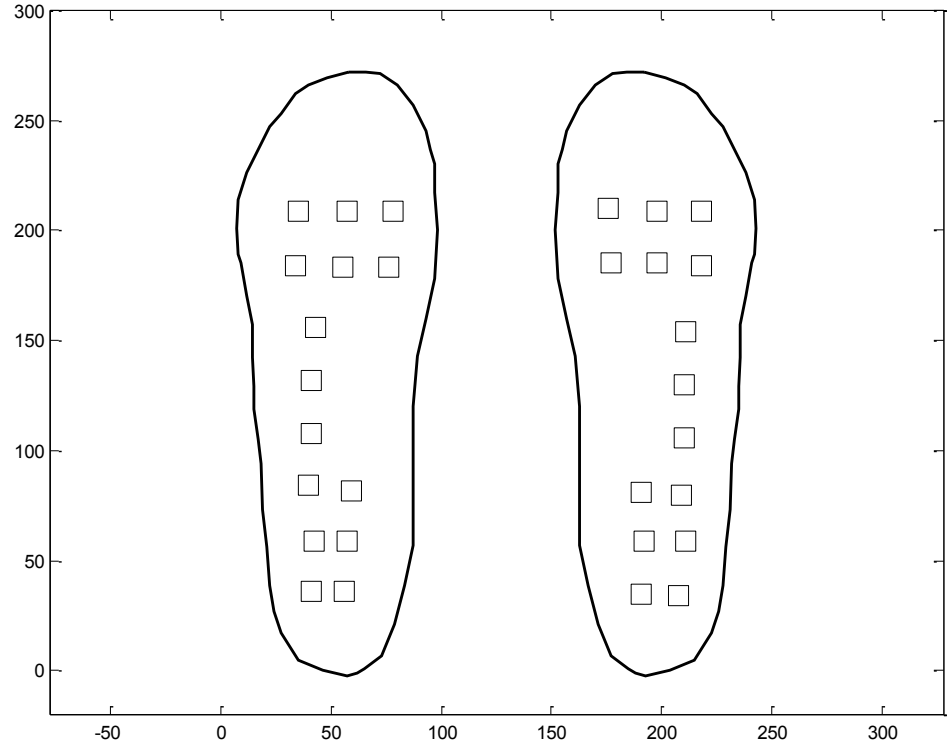

Figure 3.3: Sensor placement as shown in MATLAB

3.2.3 Sensor Calibration

The DAQ board supplies each sensor with a voltage of 5V. The sensor has a variable resistance to current, depending on the amount of force on the sensor. In order to convert voltage into force, an individual calibration for each sensor is needed. The FSA sensors read forces that are perpendicular to the sensor plane. Each sensor was calibrated using a static stepwise calibration using a force plate (4060-10, Bertec, Columbus, OH). This method was used to eliminate loading rate, creep and hysteresis. A wooden board acting as a lever served as the platform for the calibration weights. The board was

secured on an elevated floor at one end and the other end rested over the force plate where the weights were added during calibration. A plastic "puck" matching the size of the active-sensing area was fixed to the bottom of the platform to ensure even and full surface contact with the sensor. The FSA sensor was then taped to the "puck" using double sided tape and the board was then placed so that it rested on a piezoelectric force plate (Bertec FP4060-10). Each sensor was calibrated starting with the weight of the platform and with the addition of 1 kg weights using six weights in total for a total of 7 force plateaus per trial. Each calibration trial was repeated five times. All the data was filtered using a 4^{th} order Butterworth filter with a 14 Hz cut off. A cubic relationship for force vs. voltage was then derived.

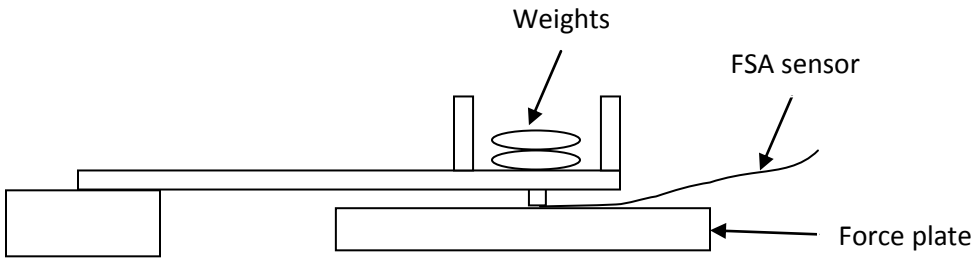

Figure 3.4a: Setup for calibration of FSA sensors

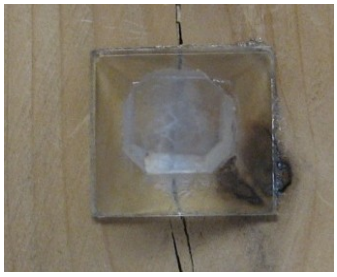

Figure 3.4b: A "puck" was stuck under the platform to ensure even surface contact with sensor

Each FSA sensor was individually calibrated. A polynomial cubic equation and its corresponding R^2 value were obtained for each sensor. A very high correlation ($R^2 > 0.98$)

was obtained for each sensor. An example of the calibration curve obtained for one sensor is provided in Fig 3.6.

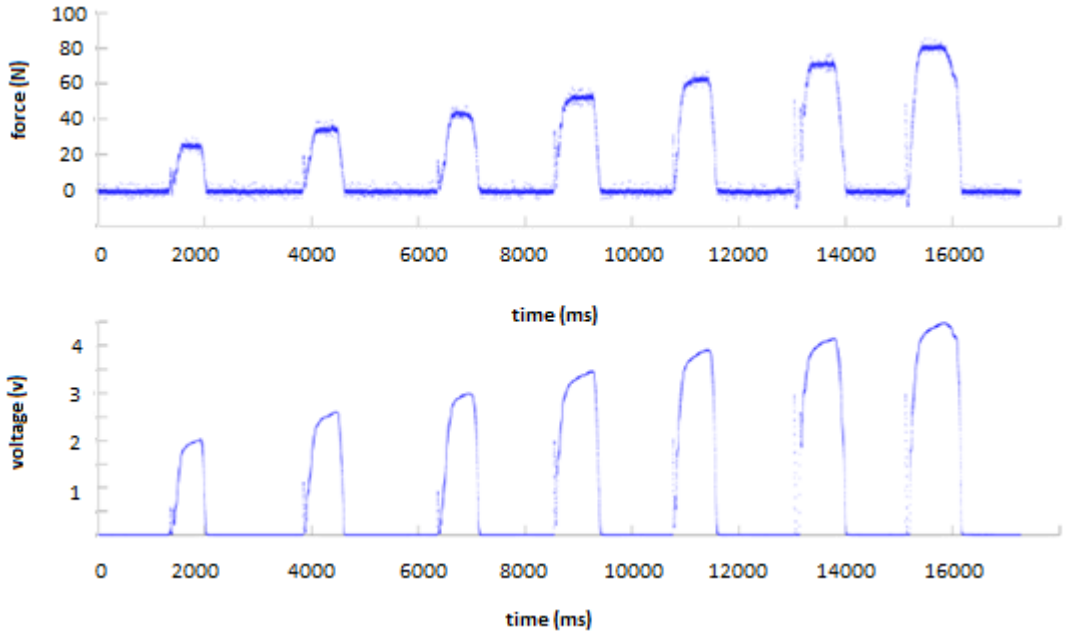

Figure 3.5: Example of FSA sensor calibration trial

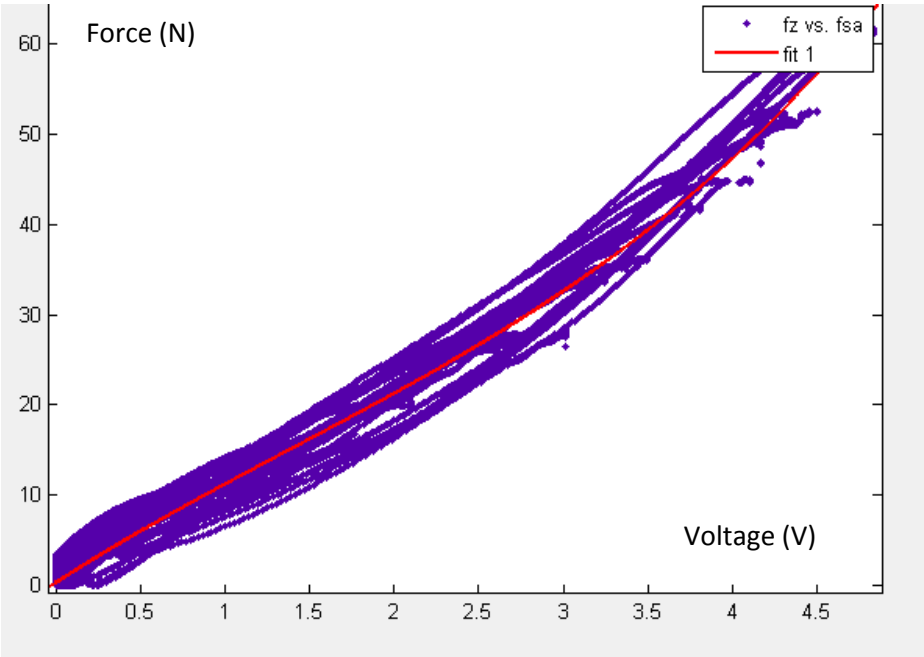

Figure 3.6: Calibration curve of a FSA sensor
$F(v) = 0.3588v^3 - 1.527v^2 + 12.13v + 0.2989$)

3.2.4 Data Acquisition and Processing

The software LabVIEW™ Version 10.0 (National Instruments®, Austin, Texas) was used to collect all the sensors and force plate outputs. The data was filtered using a 4^{th} order Butterworth filter with a 14 Hz cut-off frequency. MATLAB (Ver 7.10.0, R2010a, MathWorks, Inc., Massachusetts, U.S.A.) software was used to process the data and perform statistical analyses.

3.2.5 Types of Skates

Two different types of skates were utilized in order to examine the effects of skate design on centre of pressure. The first skate model used was a regular Bauer One95 skate (Bauer Hockey Corp). The second skate used was a modified Bauer One95 with a flexible tendon guard to allow for more dorsiflexion and plantar flexion.

Figure 3.7a: Medial and posterior view of the regular Bauer One95 skate

Figure 3.7b: Medial and posterior view of the modified Bauer One95 skate

3.3. Validation of the Centre of Pressure Measurement System

Figure 3.8: COP measurement system inside the boot

The concurrent validity between the COP calculated from the sensors and COP measured by a Bertec force plate was measured. The subjects were fitted with the instrumented insole in a skate boot with the blade removed. Insoles were taped on the force plate in order to align the force plate coordinate system to the instrumented insole coordinate system. The subjects were instructed to place their left foot on the force plate and their right foot on a platform at the same level as the force plate. First, the subjects shifted their weight in the medial-lateral (ML) plane without lifting their foot out of the insole. This was repeated for 5 trials. Subsequently, subjects shifted their weight in the anterior-posterior (AP) plane without lifting the boot out of the insole.

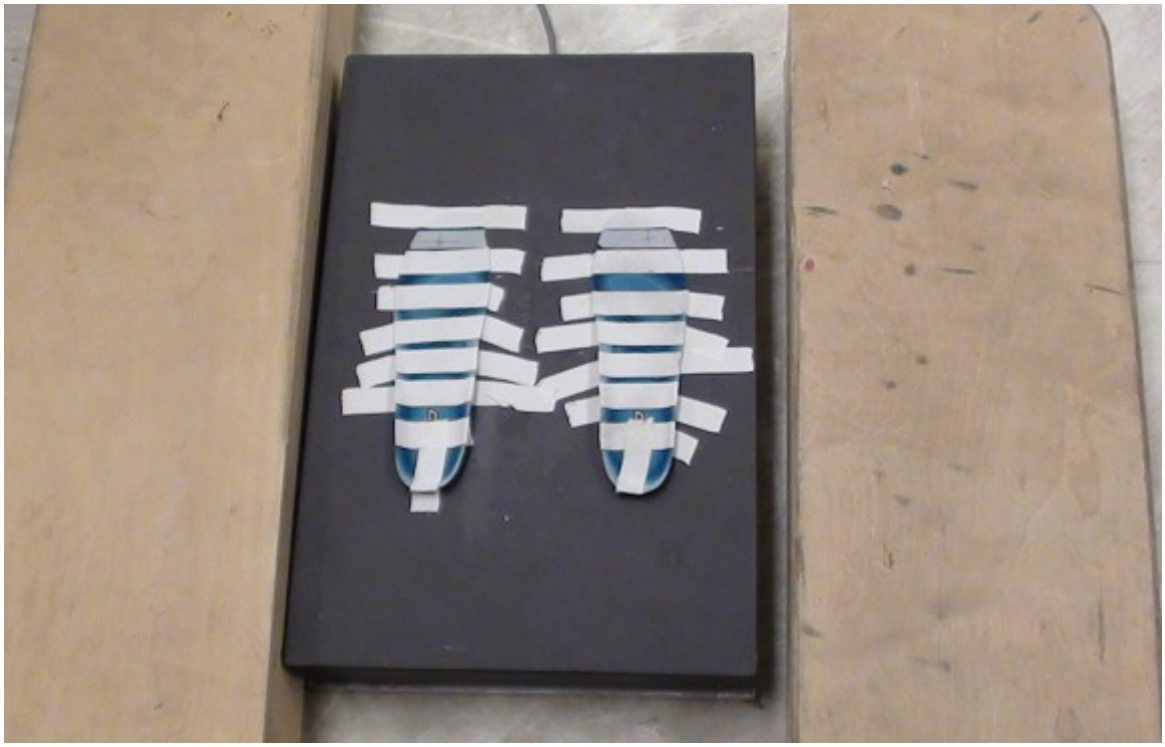

Figure 3.9: Setup using force plate for COP validation

The COP on the force plate was measured using **FPCOPx** = -My/Fz and **FPCOPy** = Mx/Fz. The COP of the combined sensors was measured using a combined weighted average of each individual sensor using their coordinates. The COP of the combined FSA sensors at any instant in time is given by **COPx** = $\frac{\sum_{i=1}^{8} F_i x_i}{\sum_{i=1}^{8} F_i}$ and similarly **COPy** = $\frac{\sum_{i=1}^{8} F_i y_i}{\sum_{i=1}^{8} F_i}$, where x_i represents the x-coordinate of sensor i, y_i the y coordinate of sensor i and F_i represents the value in force of sensor i after using the calibration equations.

Pearson correlation coefficients comparing COP displacement in the medial-lateral and anterior-posterior direction were calculated from the two systems. For each ML and AP trial, a coefficient of correlation was calculated. While the COP under the foot inside the boot might not be the same as the COP under the boot on the force plate, the pattern should be the same. Therefore, as long as a high correlation value is observed, it is acceptable to use the system as a measure of centre of pressure.

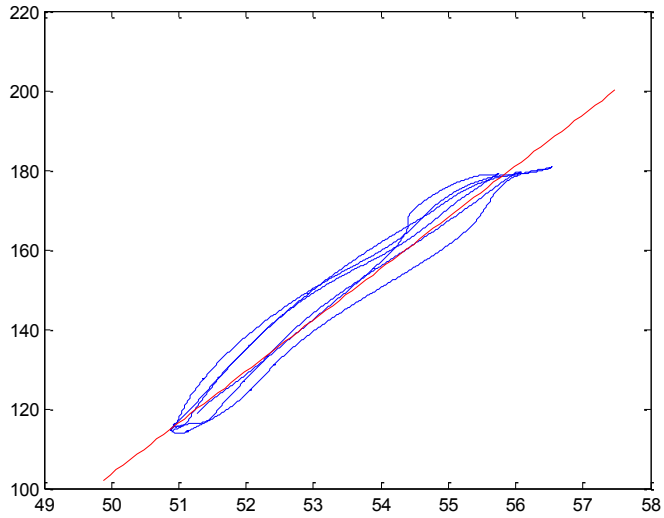

Fig 3.10a: Example of Medial-Lateral Trial, a linear line of best fit was used to calculate correlation

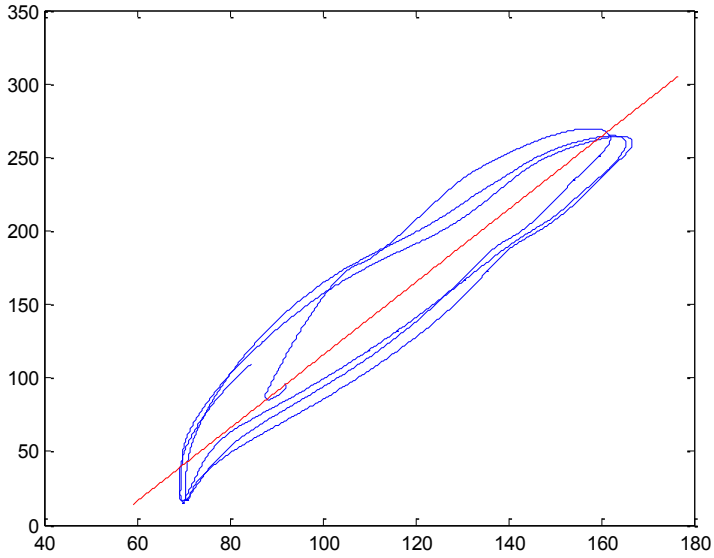

Fig 3.10b: Example of Anterior-Posterior Trial, a linear line of best fit was used to calculate correlation

	Medial-Lateral Direction			Anterior Posterior Direction		
	Min R^2	Max R^2	Average R^2	Min R^2	Max R^2	Average R^2
Subject 1	0.8697	0.9642	0.9251	0.8696	0.9047	0.8833
Subject 2	0.9345	0.9685	0.9542	0.9445	0.9551	0.9513
Subject 3	0.8807	0.9465	0.9213	0.9233	0.9348	0.9294
Subject 4	0.8723	0.9488	0.9217	0.8256	0.9506	0.8949
Subject 5	0.9427	0.9801	0.9222	0.9175	0.9610	0.9438
Subject 6	0.9334	0.9424	0.9368	0.9643	0.9472	0.9468
Subject 7	0.9506	0.9688	0.9622	0.9767	0.9463	0.9809
Subject 8	0.8409	0.9239	0.8772	0.9515	0.9649	0.9640
Subject 9	0.9339	0.9466	0.9411	0.9511	0.9551	0.9731
Average (sd)	0.9065 (0.040)	0.9544 (0.017)	0.9291 (0.024)	0.9249 (0.049)	0.9466 (0.018)	0.9408 (0.033)

Table 3.1: Coefficients of determination between centre of pressure of force plate and centre of pressure of insole System

The coefficient of determination R^2 was calculated for a total of 9 subjects for both the medial-lateral centre of pressure and the anterior-posterior centre of pressure. For the M-L COP, a R^2 value of 0.9291 ± 0.025 was found and for the A-P COP, a R^2 value of 0.9408 ± 0.033 was found. Both these values are high and show that the insole system can detect the changes in COP in the same way the force plate can detect the changes in COP. Therefore, the insole system can be used as a reliable tool to measure centre of pressure.

3.4 Experimental Protocol

3.4.1 Testing Location

The testing was done at the McGill McConnell Arena.

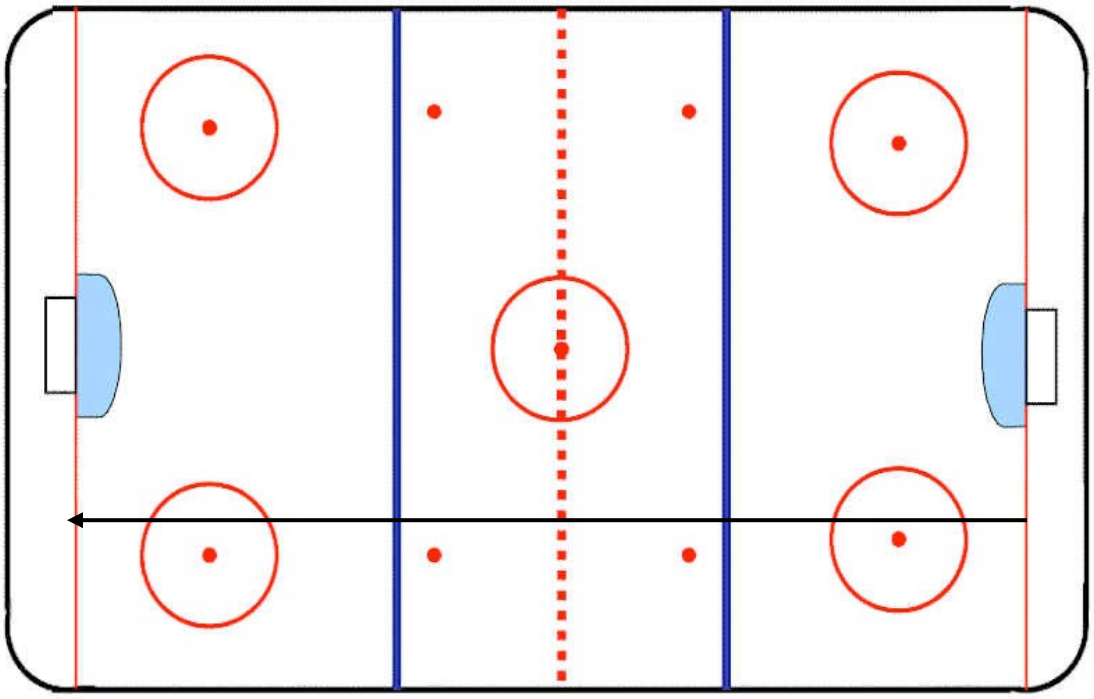

Figure 3.11: The path of the skater during the forward skating task. The arrow represents the direction of skating (Adapted from Lachaine, 2010)

3.4.2 Subject Preparation

The subjects wore size 8.5 or size 9 skates, which correspond to shoe size 10-10.5 with the instrumented insoles placed in the skates. The sensor wires were fit into a wireless data acquisition board, which was placed in a backpack which was worn on the shoulders of the subject. The weight of the backpack including containing the equipment

is 2.4 kg. The subjects were given a warm-up to get accustomed to skating with the equipment on.

3.4.3 Tasks

The subjects completed a forward skating task from one goal line to another. The distance covered was 50 m on an official North American ice hockey rink. The subjects were instructed to skate at maximal speed. Three trials were taken for each condition. The subjects had to maintain a linear trajectory while covering this distance. A camera followed the skater using a sagittal view. The order of the two conditions were randomized between subjects.

3.5 Data Processing

Figure 3.12 displays a filtered voltage response from all the sensors of the left foot during a trial. It can be seen that for that particular trial, 10 complete strides were captured.

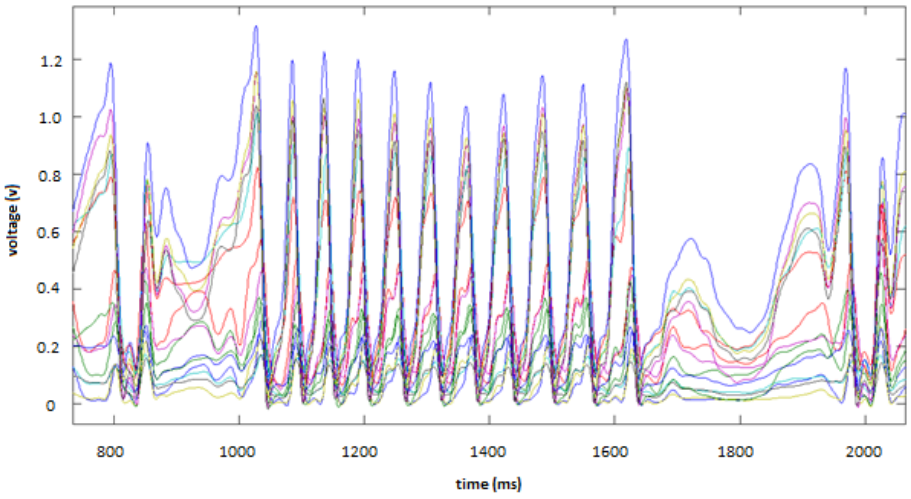

Fig 3.12: The voltage response from the left foot (15 sensors) for one full trial, including jump, forward skating, braking and jump

Figure 3.13 illustrates the relationship between the displacement of the centre of pressure in the anterior-posterior direction and the magnitude of the vertical force acting on the skate during a stride. The blue line represents the vertical channel of the left skate strain gauge. The green line represents the anterior-posterior component of the centre of pressure. The purple lines represent the channels 1-6 which are located in the anterior compartment of the boot. The thin red line presents the other FSA channels

All the units are put on a relative scale in order to show on the same graph.

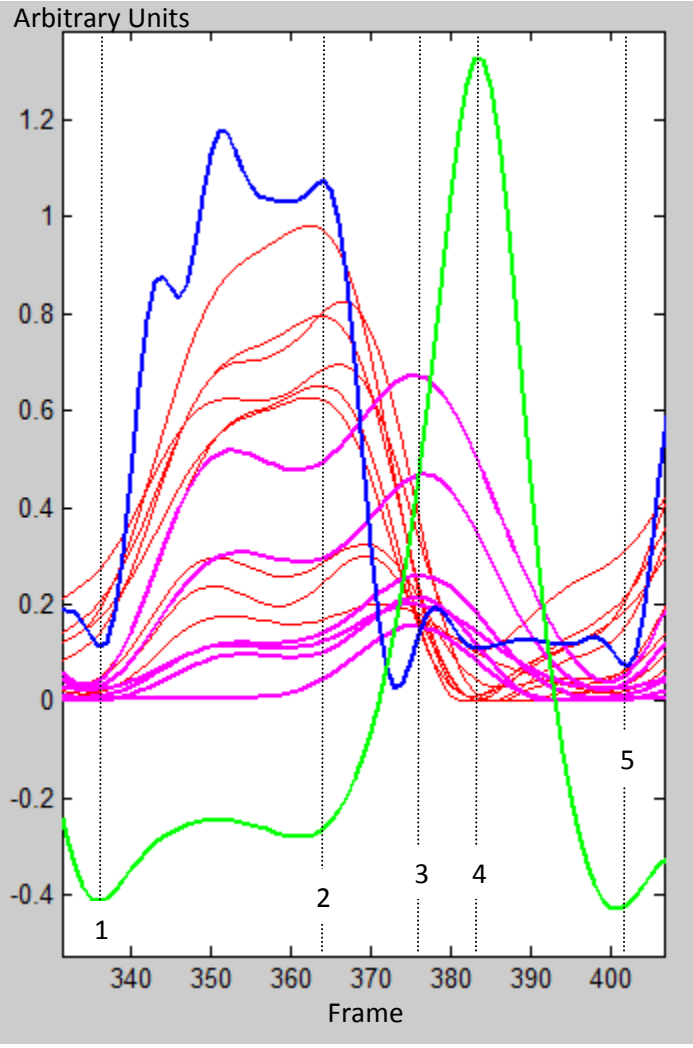

Fig 3.13: Analysis of a single stride

1. The skate hits the ice, the centre of pressure is located at the heel of the foot and stays at the heel for almost the entire duration is on the ice

2. As the skate begins to get lifted, the centre of pressure shifts towards the anterior direction

3. The sensors at the front of the foot peak but the rest of the sensors have not completely unloaded which put the location of the COP at the midfoot

4. The sensors of at the back of the foot have completely unloaded but the sensors at the front are still loaded which puts the COP at the anterior portion of the foot under the forefoot

5. Start of next stride

Figure 3.14 shows the force distribution for both skates during a stride. It can be observed that as the skate hits the ice while the weight is at the heel of the foot. The weight then travels to the front of the foot as the skate begins to lift and the other skate hits the ice.

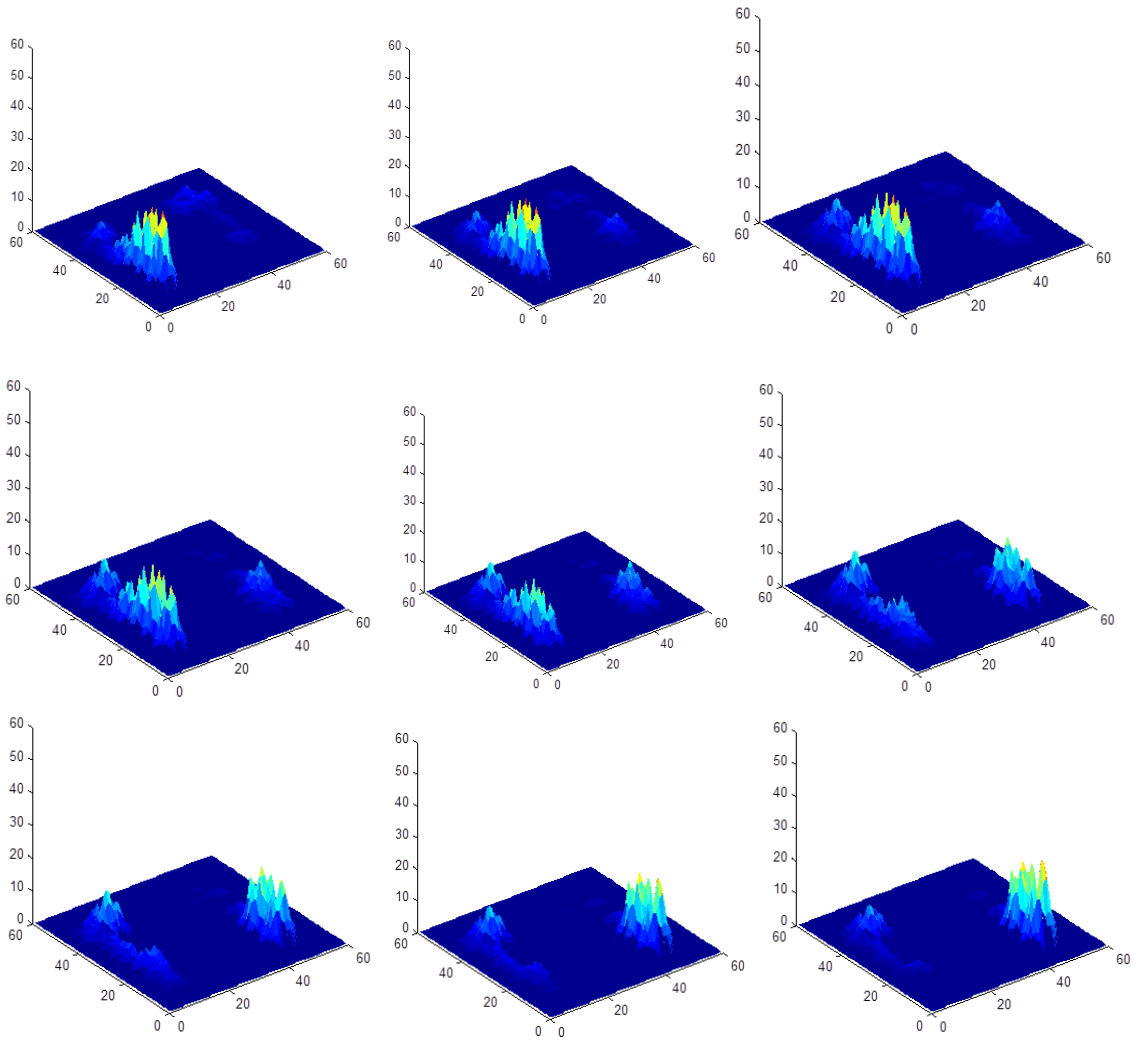

Figure 3.14: Pressure distribution over time of a single stride for left and right feet, the color red represents the highest force application. Each picture is separated by a time frame of 0.1sec

3.6 Research Design and Statistical Analysis

Variable	Type	Scale	Definition
Task	Independent variable	Categorical	- Forward Skating - Acceleration - Steady-State - Deceleration
Skate Type	Independent variable	Categorical	- One95 skate - Modified One95 skate
Time Measures	Dependent variable	Continuous	- Contact Time - Stride Rate
Kinetic Variables	Dependent variable	Continuous	-Vertical Force - Impulse - Work - Power
Centre of Pressure	Dependent variable	Continuous	- Centre of Pressure - Anterior-Posterior - Medial-Lateral - Sensor Force Values

Table 3.2: List of variables

A two-way multivariate analysis of variance (MANOVA) with repeated measures was conducted to compare the differences between the skate models. Statistical significance was set at $\alpha = 0.05$.

4. Results

Descriptive and inferential statistics of these dependant variables are presented below in graphical format including means and standard deviations (SD). Significant differences set to $\alpha = 0.05$ are identified in the graphs with an asterisk. The MANOVA tables are presented in the appendix. Kinetic data from the strain gauge and centre of pressure data from the insole system were collected successfully on 5 subjects on both left and right skates.

All the trials were separated into three phases: acceleration, steady state and deceleration. Each trial consisted of 8-11 strides for both the left and right skates. The acceleration phase was defined as the first three strides of the trial. The deceleration phase was defined as the last three strides of the trial. The steady state phase was defined as all the strides between the acceleration and deceleration phase. Because of the differences in the technique used by the subjects during the deceleration phase, only the acceleration and steady state phases were considered for the analyses. The following graphs show the steady state phase. Complete results are included in tables after the graphs.

Time Measures

No significant differences were observed for contact time and stride rate between the two skate models ($p > .05$).

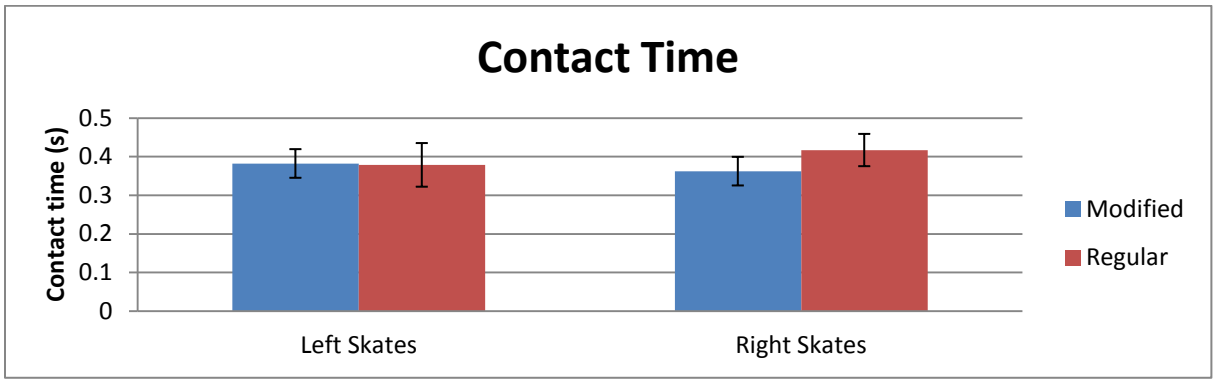

Figure 4.1a: Contact time per stride during steady state skating

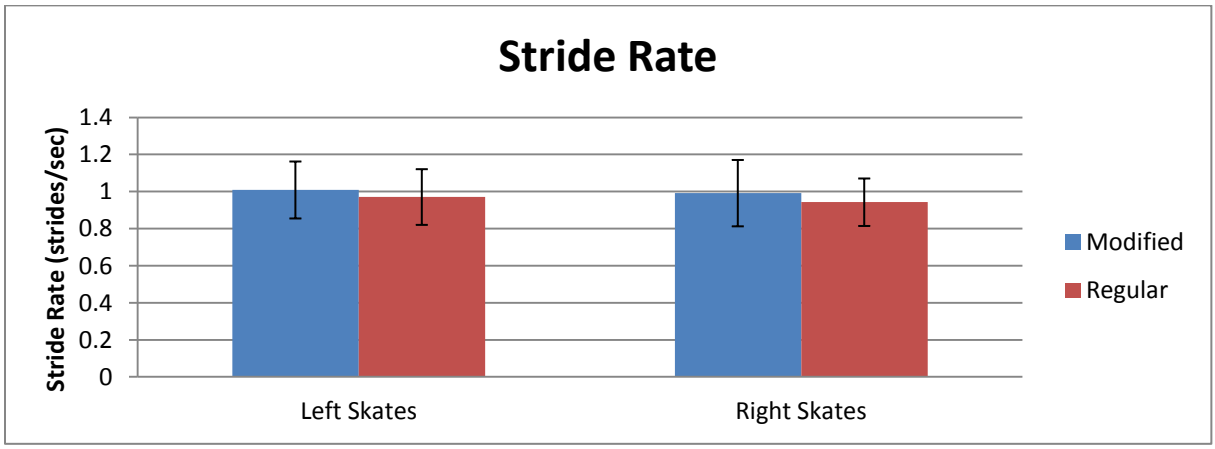

Figure 4.1b: Stride rate over entire trial

	Left Skates				Right Skates			
Skating Task	Acceleration		Steady State		Acceleration		Steady State	
Skate Type	Modified	Regular	Modified	Regular	Modified	Regular	Modified	Regular
Contact Time (s)	0.325 (0.056)	0.326 (0.056)	0.382 (0.0371)	0.378 (0.056)	0.301 (0.048)	0.343 (0.044)	0.362 (0.037)	0.417 (0.042)
	p = .977		*p = .907*		*p = .189*		*p = .060*	
Skating Task	Entire Trial				Entire Trial			
Skate Type	Modified		Regular		Modified		Regular	
Stride Rate (strides/s)	1.009 (0.153)		0.971 (0.150)		0.992 (0.179)		0.943 (0.128)	
	p = .703				*p = .633*			

Table 4.1: Time measures (n=5)

Kinetic Variables

The force values were normalized as a percentage of body weight in order to compare all the subjects. The kinetic variables include average vertical force, peak vertical force, impulse, work and power. The impulse was significantly higher in the regular model for the right skates during the steady state phase ($p < .05$) but not for the acceleration phase ($p > .05$). The regular model also had significantly higher power and work values than the modified skate model ($p < .05$).

The peak force ranged from 113% to 124% of bodyweight for the left skates and 122% to 135% of bodyweight for the right skates. However, there were no differences between the skate models.

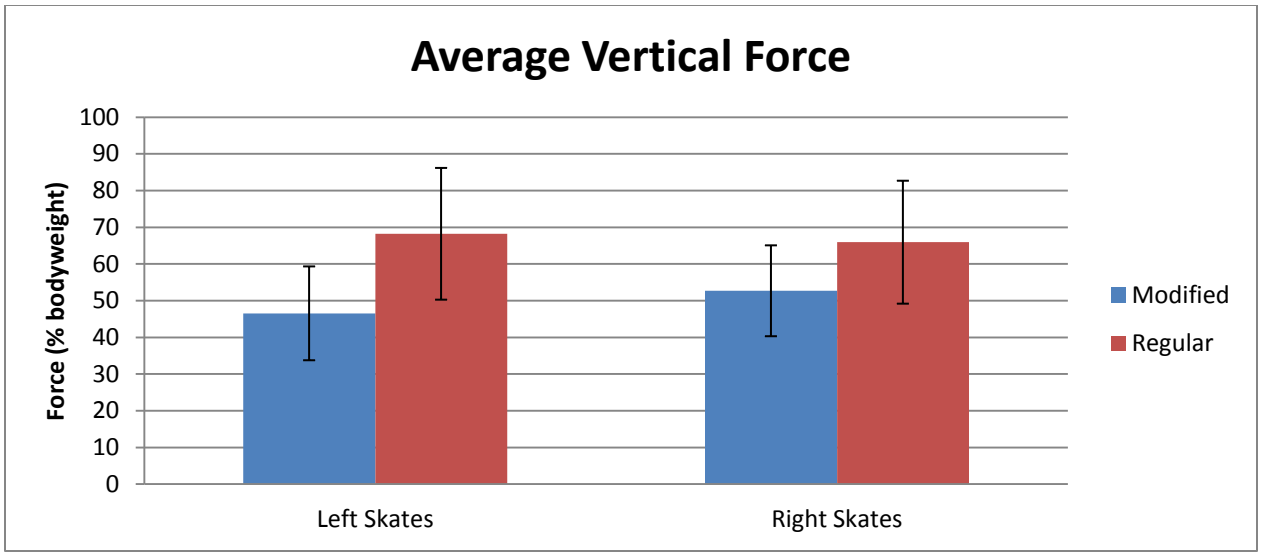

Figure 4.2a: Average Vertical For per Stride during Steady State

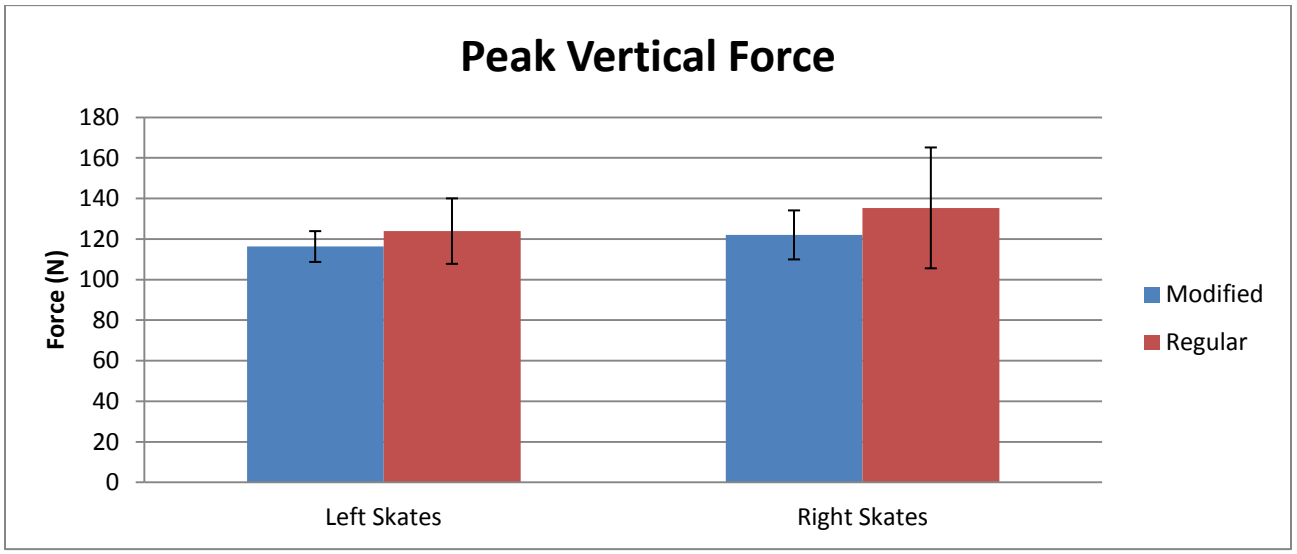

Figure 4.2b: Peak vertical force per stride during steady state

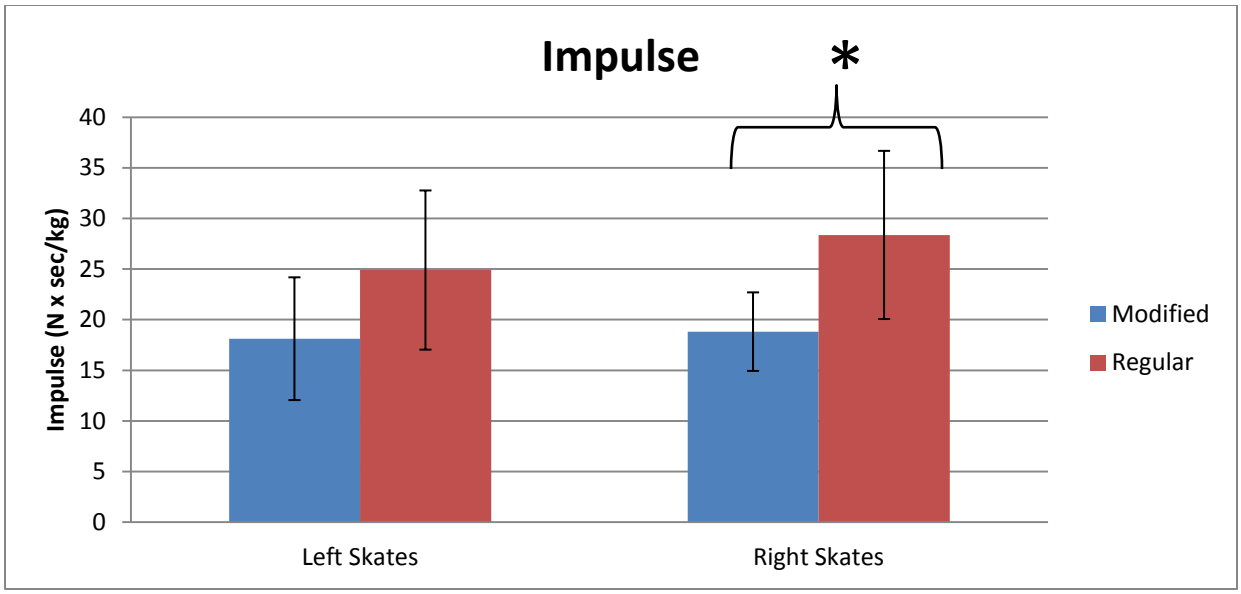

Figure 4.2c: Impulse per stride during steady state. Statistical significance is denoted by * (p < .05)

	Left Skates				Right Skates			
Skating Task	Acceleration		Steady State		Acceleration		Steady State	
Skate Type	Modified	Regular	Modified	Regular	Modified	Regular	Modified	Regular
Average Vertical Force	51.54 (5.52)	54.72 (19.81)	46.56 (12.79)	68.23 (17.95)	52.09 (9.42)	60.41 (18.98)	52.70 (12.38)	65.94 (16.75)
	p = .738		*p = .059*		*p =.406*		*p = .193*	
Peak Vertical Force	124.2 (6.0)	113.3 (30.4)	116.3 (7.6)	123.9 (16.1)	125.3 (10.3)	128.3 (28.4)	122.0 (12.1)	135.3 (29.8)
	p = .456		*p = .368*		*p = .831*		*p = .381*	
Impulse	17.20 (3.90)	17.57 (8.77)	18.13 (6.06)	24.90 (7.86)	15.89 (3.69)	21.93 (8.46)	18.82 (3.88)	28.37 (8.31)
	p = .934		*p = .165*		*p = .181*		***p = .048***	

Table 4.2a: Kinetic variables: force and impulse (n=5)

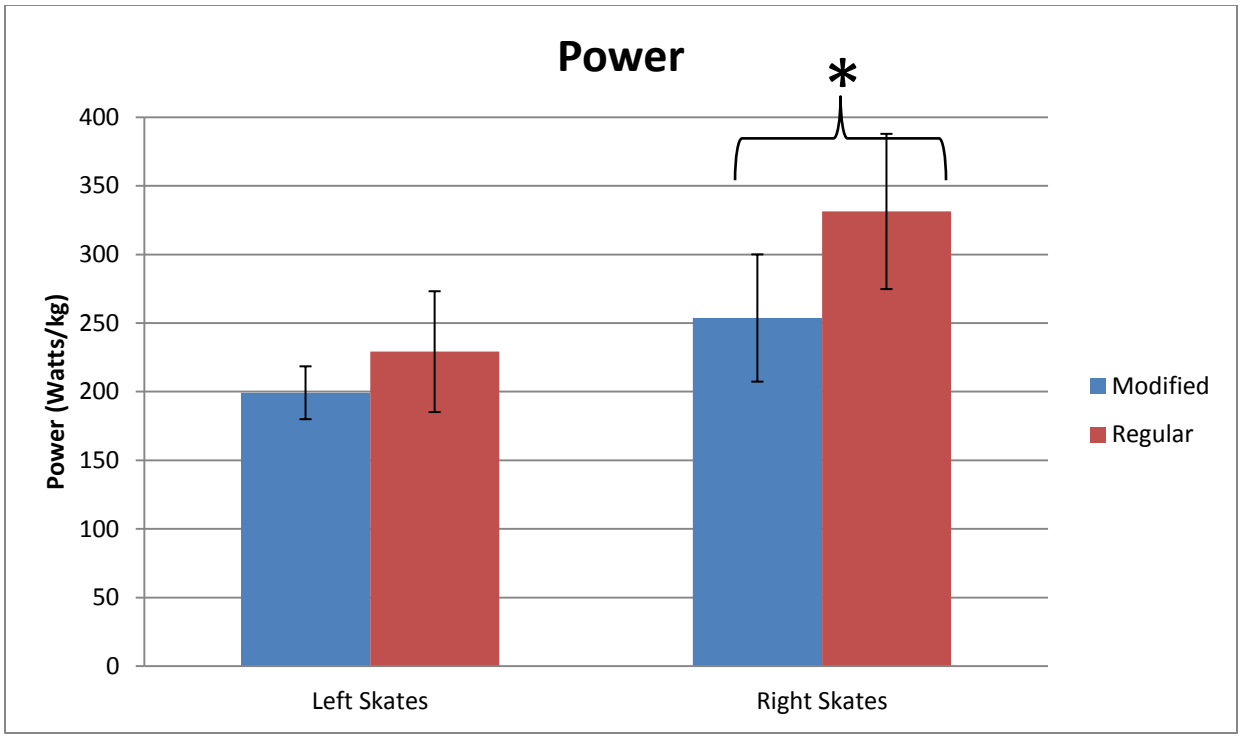

Figure 4.2d: Power Output during Entire Trial. Statistical significance is denoted by * ($p < .05$)

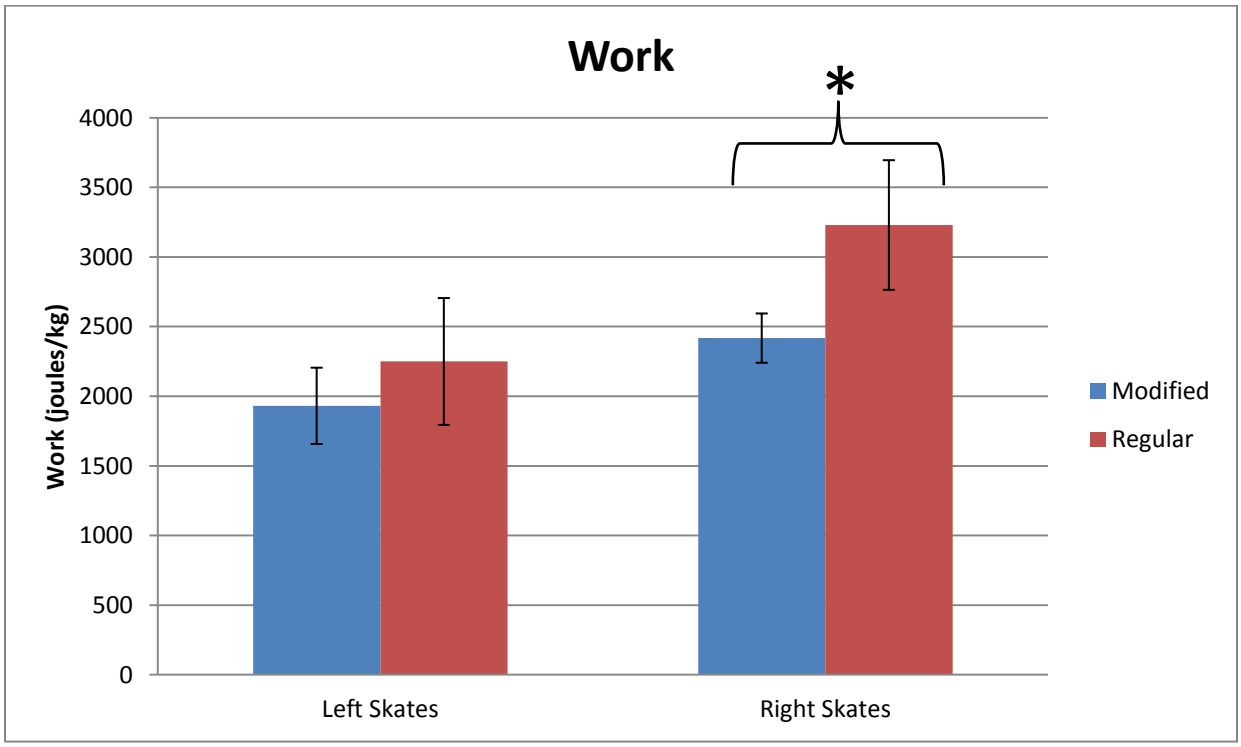

Figure 4.2e: Work done per Skate over Entire Trial. Statistical significance is denoted by * ($p < .05$)

	Left Skates		Right Skates	
Skating Task	Entire Trial		Entire Trial	
Skate Type	Modified	Regular	Modified	Regular
Power	199.2 (19.3)	229.2 (44.0)	253.7 (46.4)	331.3 (56.6)
	p = .201		***p = .045***	
Work	1931.4 (274.1)	2250.1 (455.4)	2417.9 (177.0)	3230.0 (465.5)
	p = .217		***p = .007***	

Table 4.2b: Kinetic variables: power and work (n=5)

Centre of Pressure Measures

Anterior Posterior COP

There was a significant difference for the total anterior posterior (AP) excursion between the modified and regular skates ($p < .05$). The regular skate had a higher AP excursion than the modified skate in both the left skates (20mm) and the right skates (15mm). There was no significant difference in the minimal AP between the skate models. However, there was a significant difference in the maximal AP for the left skates and the right skates. The regular skate had a higher maximal AP value than the modified skate, by 20mm and 17mm ($p < .05$). This shows that the increase in anterior posterior excursion occurs is at the anterior part rather than the posterior part.

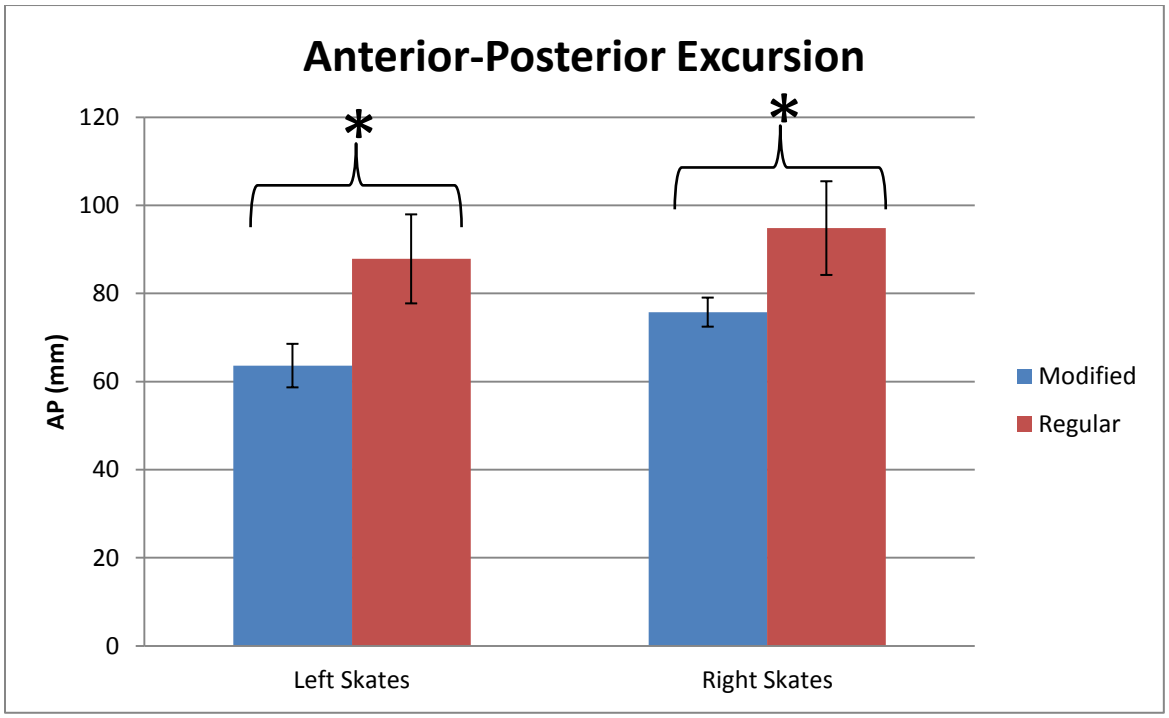

Figure 4.3a: Anterior-Posterior Centre of Pressure Excursion per Stride during Steady State. Statistical significance is denoted by * ($p < .05$)

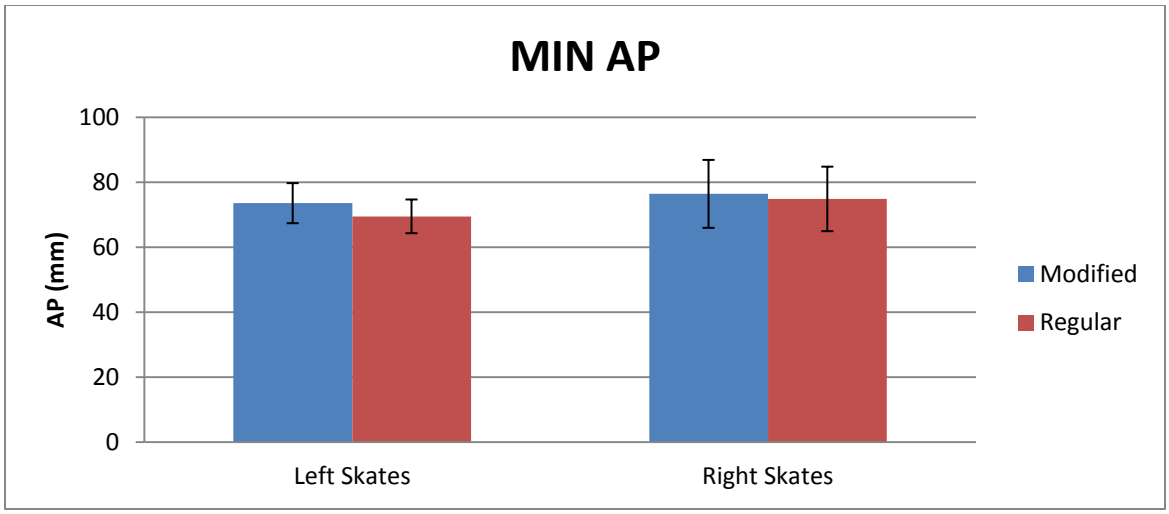

Figure 4.3b: Minimal Anterior-posterior centre of pressure value in left and right skates by skate type

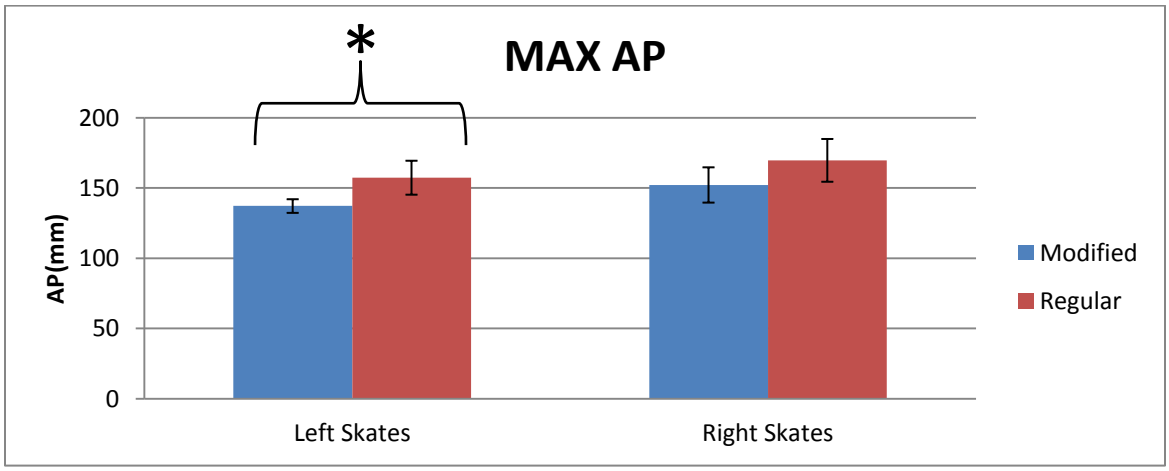

Figure 4.3c: Maximal Anterior-posterior centre of pressure value in left and right skates by skate type. Statistical significance is denoted by * ($p < .05$)

	Left Skates				Right Skates			
Skating Task	Acceleration		Steady State		Acceleration		Steady State	
Skate Type	Modified	Regular	Modified	Regular	Modified	Regular	Modified	Regular
AP excursion	67.3 (7.0)	87.1 (9.0)	63.6 (4.9)	87.9 (10.1)	81.0 (6.4)	95.5 (8.0)	75.8 (3.3)	94.8 (10.6)
	p = .005		***p =.001***		***p = .013***		***p = .005***	
AP min	72.1 (5.7)	69.3 (4.9)	73.5 (6.2)	69.5 (5.2)	75.0 (9.7)	73.9 (8.0)	76.4 (10.5)	74.8 (9.9)
	p =.426		*p =.313*		*p = .851*		*p = .816*	
AP max	139.5 (7.0)	156.4 (9.1)	137.2 (4.9	157.3 (10.1)	156.0 (6.4)	169.5 (8.0)	152.2 (3.3)	169.7 (10.6)
	p =.012		***p =.009***		*p = 0.54*		*p = .083*	

Table 4.3a: Centre of pressure measures: anterior-posterior (n=5)

Medial Lateral COP

There were no significant differences in either the total ML excursion as well as the minimal and maximal values (p> .05).

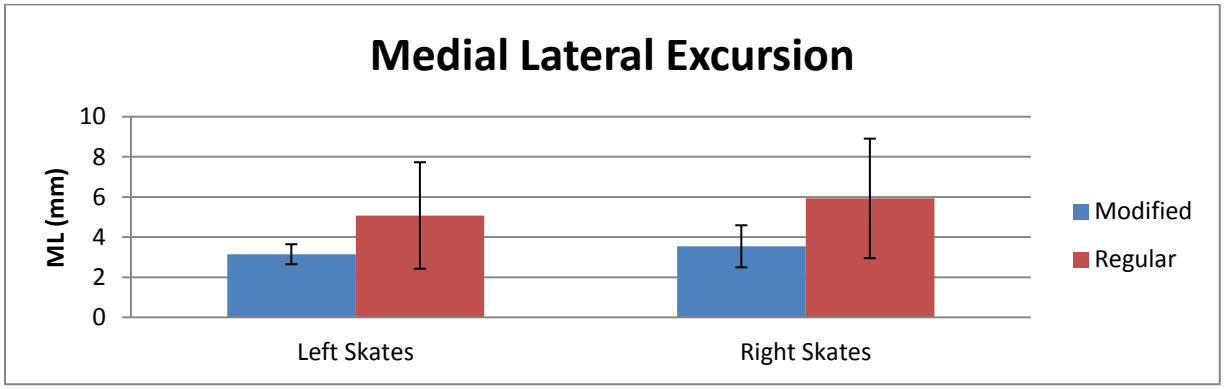

Figure 4.3d: Anterior-Posterior centre of pressure excursion

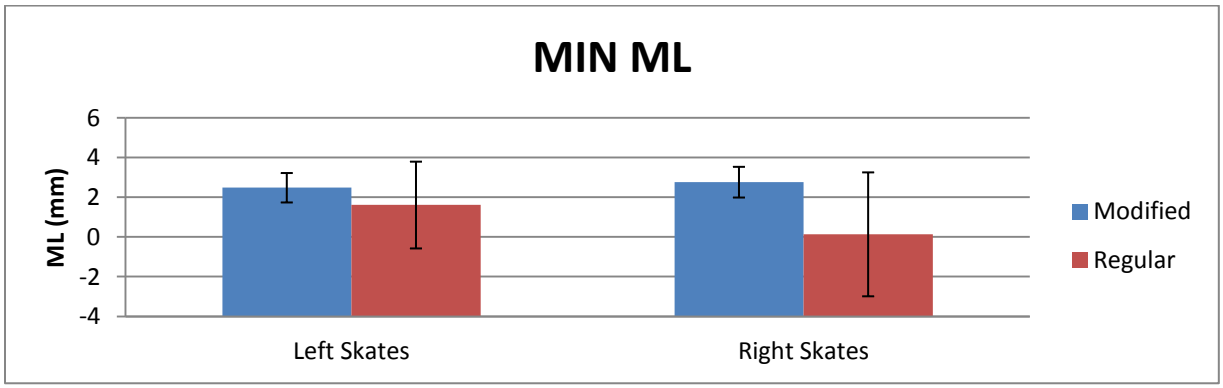

Figure 4.3e: Minimal medial-lateral centre of pressure value

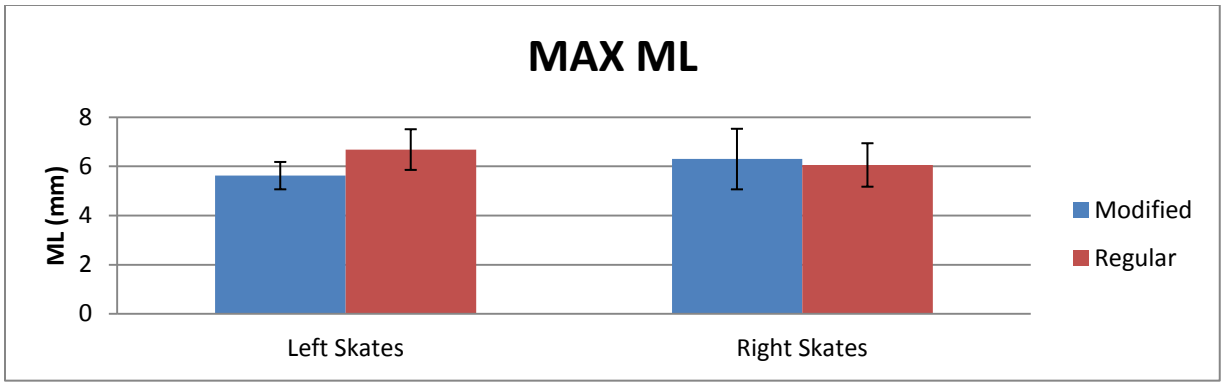

Figure 4.3f: Maximal medial-lateral centre of pressure value

	Left Skates				Right Skates			
Skating Task	Acceleration		Steady State		Acceleration		Steady State	
Skate Type	Modified	Regular	Modified	Regular	Modified	Regular	Modified	Regular
ML	3.3 (0.5)	4.9 (2.0)	3.1 (0.5)	5.1 (2.6)	3.4 (0.8)	5.7 (3.0)	3.5 (1.0)	5.9 (3.0)
	p = .122		*p = .148*		*p = .143*		*p = .130*	
ML min	2.1 (0.7)	1.5 (1.8)	2.5 (0.7)	1.6 (2.2)	2.7 (0.7)	0.0 (2.7)	2.8 (0.8)	0.1 (3.1)
	p = .535		*p = .423*		*p = .069*		*p =.105*	
ML max	5.4 (0.5)	6.4 (0.7)	5.6 (0.6)	6.7 (0.8)	6.1 (1.0)	5.7 (0.4)	6.3 (1.2)	6.1 (0.9)
	p = .022		*p = .055*		*p =.416*		*p =.732*	

Table 4.3b: Centre of pressure measures: medial-lateral (n=5)

Sensor Region Force Measures

The sensors in the insole were grouped into three regions: heel, midfoot and toe. The average force per sensor per region was then calculated. The average force during the contact time and whole stride were measured. The peak force during the stride was also measured. There were no significant differences when comparing between the skate models for both the average forces and peak force values in all regions. However, when comparing the left and right skates, the right foot had significantly higher peak and average force for the midfoot region for both skate models.

There was no significant difference in the average force and peak forces between the skate models for the heel region ($p > .05$).

There was a significant difference in the average force for the midfoot region for both during the stride as well as during the contact time between the left and right foot for both skate models. There was also a significant difference in the peak force for the midfoot region between the left and right skates for both skate models ($p < .05$).

There was no significant difference in the average force and peak forces between the skate models for the midfoot region.

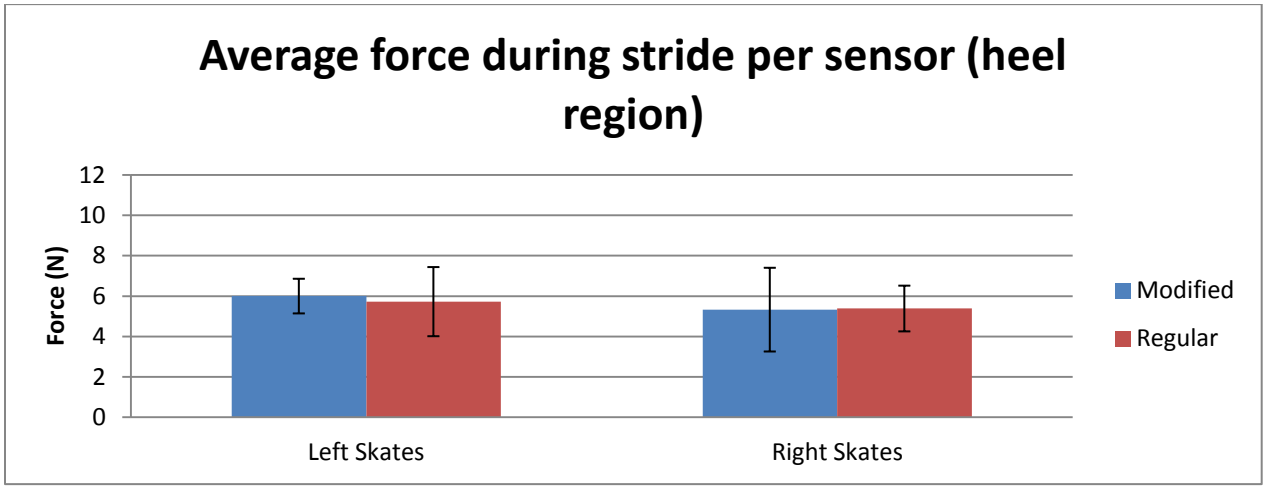

Figure 4.4a: Average Force during Stride per Sensor (Heel Region)

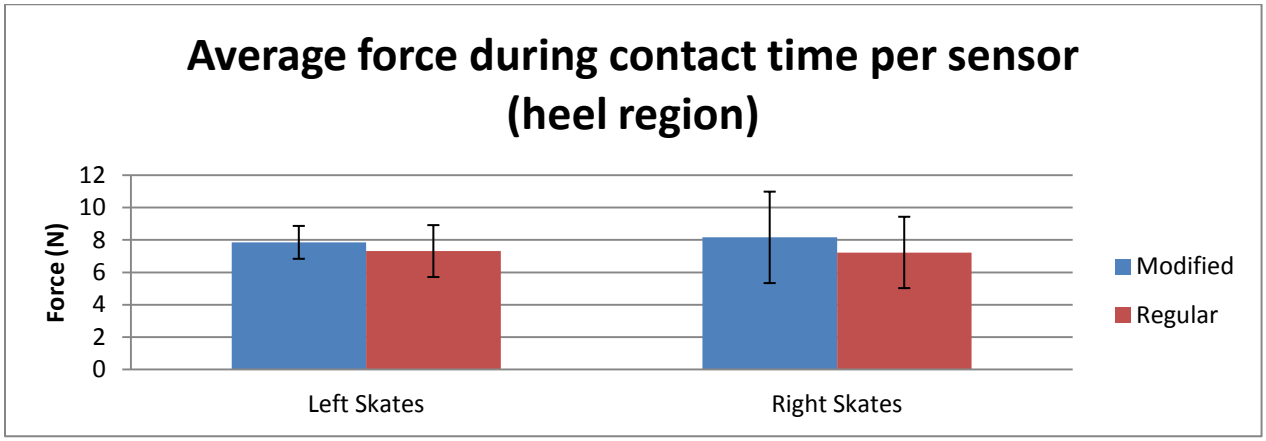

Figure 4.4b: Average Force during Contact Time per Sensor (Heel Region)

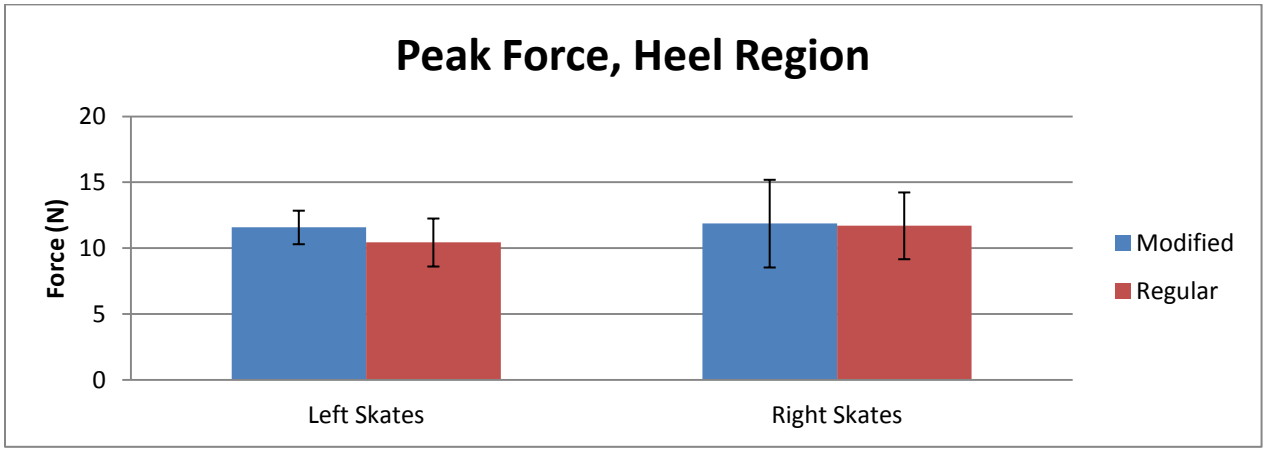

Figure 4.4c: Peak Force, Heel Region

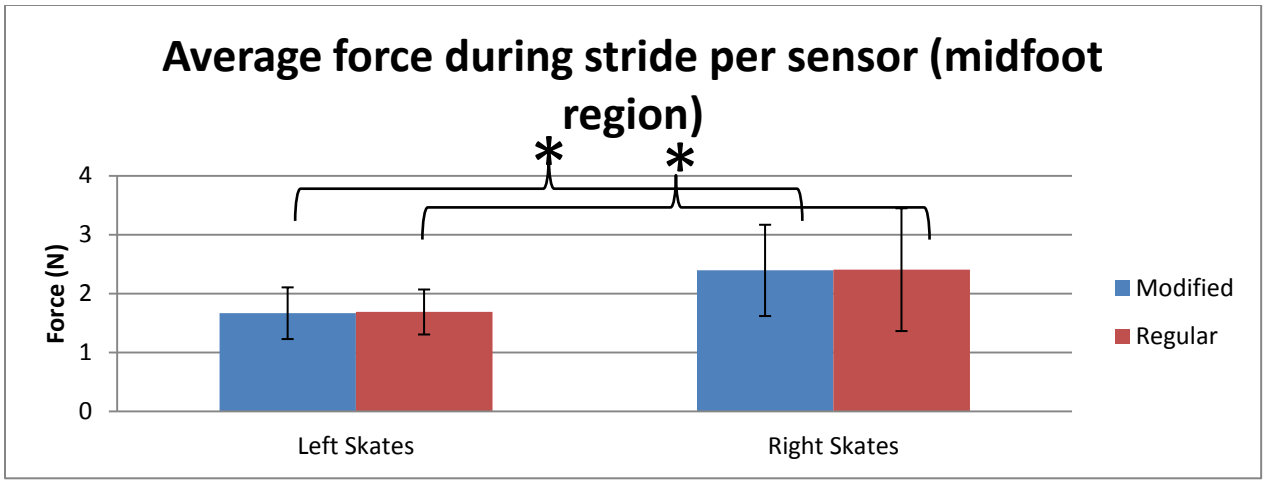

Figure 4.4d: Average force during Stride per Sensor (Midfoot Region) . Statistical significance is denoted by * (p < .05)

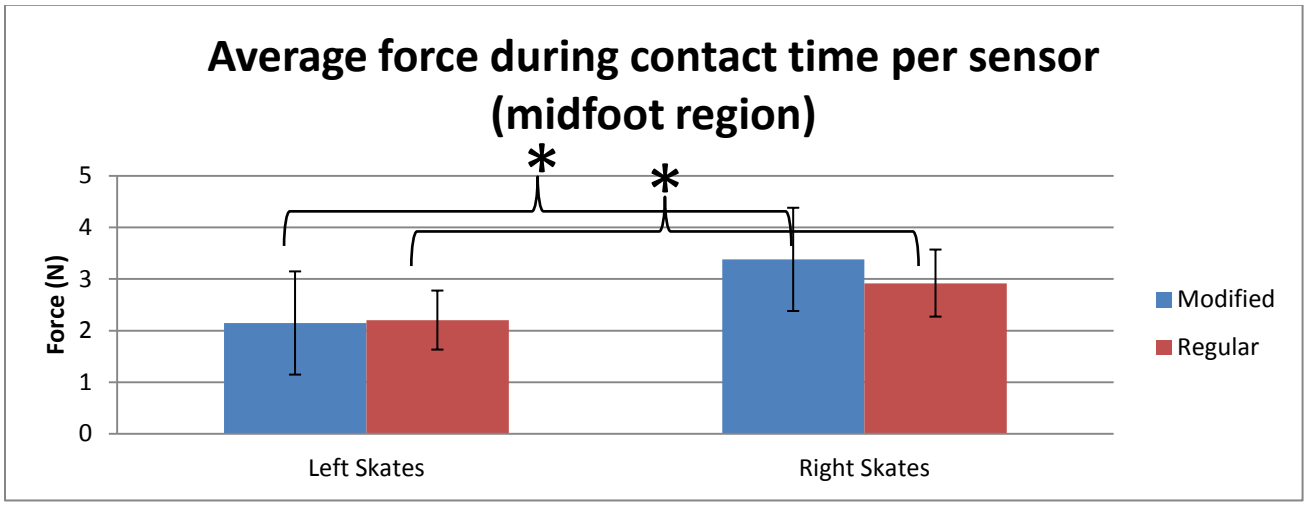

Figure 4.4e: Average Force during Contact Time per Sensor (Midfoot Region). Statistical significance is denoted by * (p < .05)

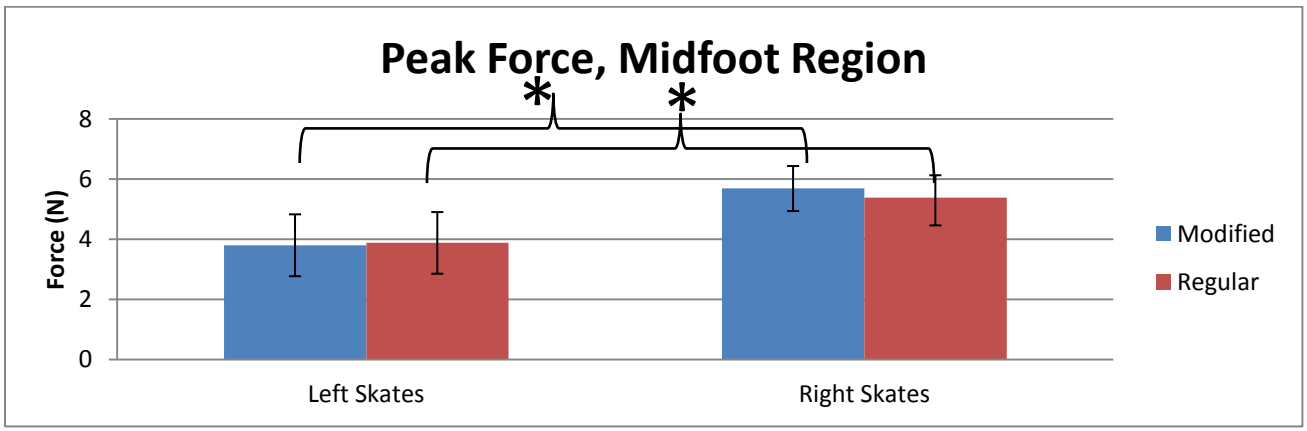

Figure 4.4f: Peak Force, Midfoot Region. Statistical significance is denoted by * (p < .05)

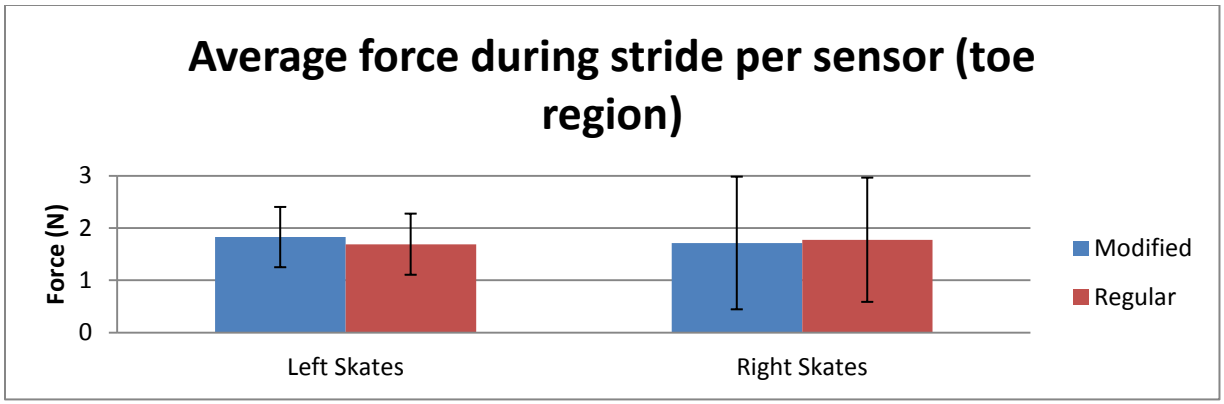

Figure 4.4g: Average Force during Stride per Sensor (Toe Region)

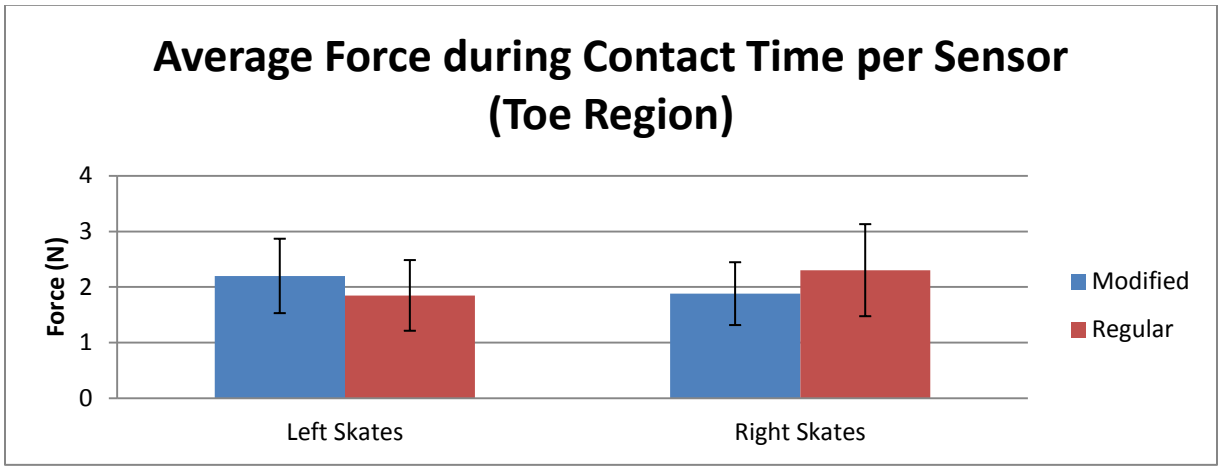

Figure 4.4h: Average Force during Contact Time per Sensor (Toe Region)

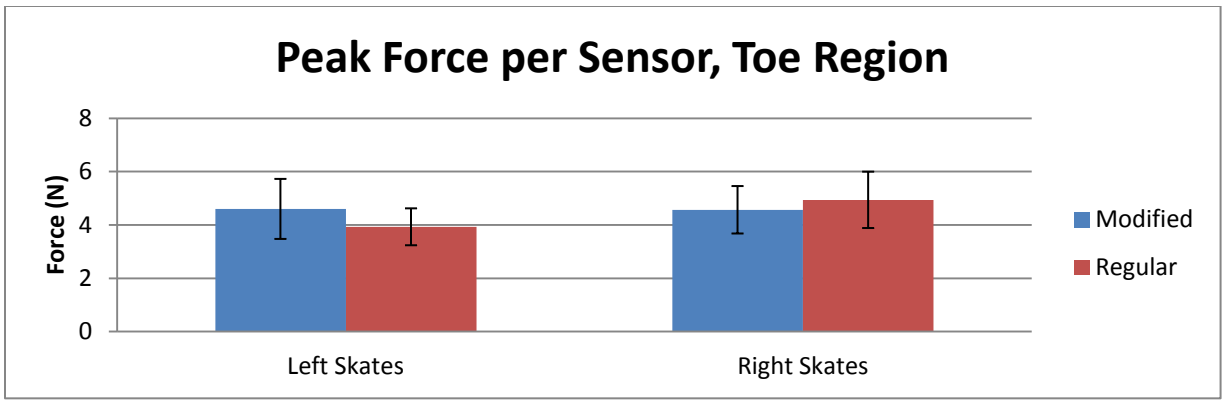

Figure 4.4i: Peak Force per Sensor, Toe Region

	Left Skates				Right Skates			
Skating Task	Acceleration		Steady State		Acceleration		Steady State	
Skate Type	Modified	Regular	Modified	Regular	Modified	Regular	Modified	Regular
Heel Region Peak Force	11.10 (0.65)	10.11 (1.34)	11.58 (1.27)	10.44 (1.82)	12.37 (3.97)	11.48 (2.65)	11.87 (3.33)	11.71 (2.54)
	p = .173		*p = .283*		*p = .688*		*p = .931*	
Heel Region Average Force during Contact Time	7.47 (0.67	6.91 (1.17)	7.85 (1.01)	7.31 (1.60)	8.27 (3.04)	7.00 (2.30)	8.15 (2.82)	7.22 (2.20)
	p = .379		*p = .543*		*p = .480*		*p = .577*	
Heel Region Average Force during Stride	5.77 (1.11	5.78 (2.29)	6.00 (0.86)	5.73 (1.71)	5.22 (1.96)	5.06 (1.17)	5.33 (2.07)	5.39 (1.13)
	p = .994		*p = .756*		*p = .881*		*p = .960*	
Midfoot Region Peak Force	3.70 (0.99)	3.90 (0.97)	3.80 (1.03)	3.88 (1.02)	5.73 (0.62)	5.30 (0.79)	5.69 (0.75)	5.38 (0.92)
	p = .765		*p = .910*		*p = .369*		*p = .578*	
Midfoot Region Average Force during Contact Time	2.14 (0.68)	2.20 (0.57)	2.14 (0.63)	2.20 (0.48)	3.33 (0.79)	2.97 (0.65)	3.38 (0.36)	2.92 (0.90)
	p = .891		*p = .204*		*p = .368*		*p = .344*	
Midfoot Region Average Force during Stride	1.60 (0.53)	1.59 (0.38)	1.67 (0.48)	1.69 (0.52)	2.29 (0.85)	2.33 (1.04)	2.39 (1.09)	2.41 (1.26)
	p = .946		*p = .411*		*p = .941*		*p = .984*	
Toe Region Peak Force	5.06 (1.37)	4.09 (0.99)	4.60 (1.12)	3.93 (0.69)	4.54 (0.95)	4.86 (1.00)	4.57 (0.90)	4.94 (1.06)
	p = .234		*p = .289*		*p = .616*		*p = .564*	
Toe Region Average Force during Contact Time	2.35 0.63	1.86 0.61	2.20 0.68	1.85 0.57	1.91 0.54	2.49 0.66	1.88 0.79	2.30 0.65
	p = .204		*p = .421*		*p = .224*		*p = .374*	
Toe Region Average Force during Stride	1.85 0.44	1.57 0.33	1.83 0.53	1.69 0.38	1.63 0.77	1.80 1.01	1.71 0.85	1.78 1.04
	p = .411		*p = .720*		*p = .825*		*p = .938*	

Table 4.4: Sensor region force measures

Sensor Temporal Measures

The timing of the peak force per region (heel, midfoot and toe) was compared between the regular and the modified skates. In the right skate, there was a significant difference in the timing of the force peaks. The heel, midfoot and toe regions peaked earlier in the regular skate compared to the modified skate ($p < .05$). During the acceleration phase, the heel, midfoot and toe regions peaked at 62-75%, 80-94% and 85-

100% respectively. During the steady state phase they peaked at 67-81%, 82-96% and 89-103% respectively.

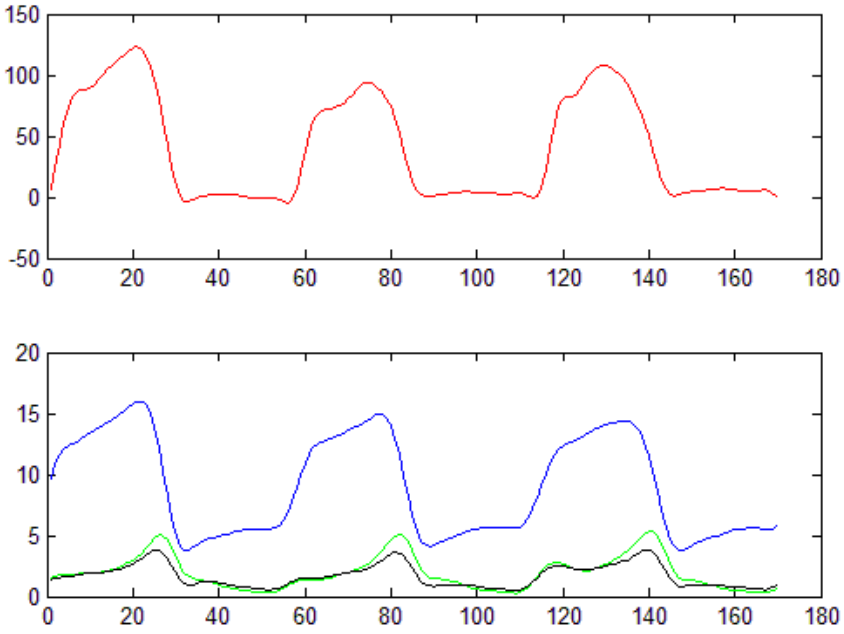

Figure 4.5a: Vertical force in bodyweight percentage (red) and force in N by region: toe (green), midfoot (black) and heel (blue) for three strides

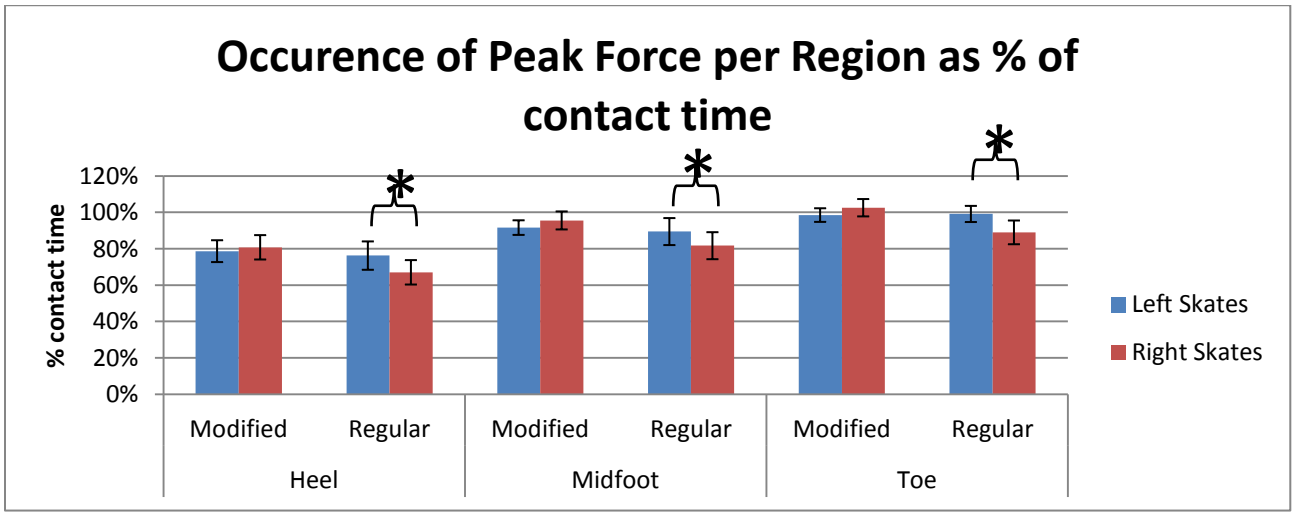

Figure 4.5b: Occurrence of peak force per region as percentage of contact time. Statistical significance is denoted by * ($p < .05$)

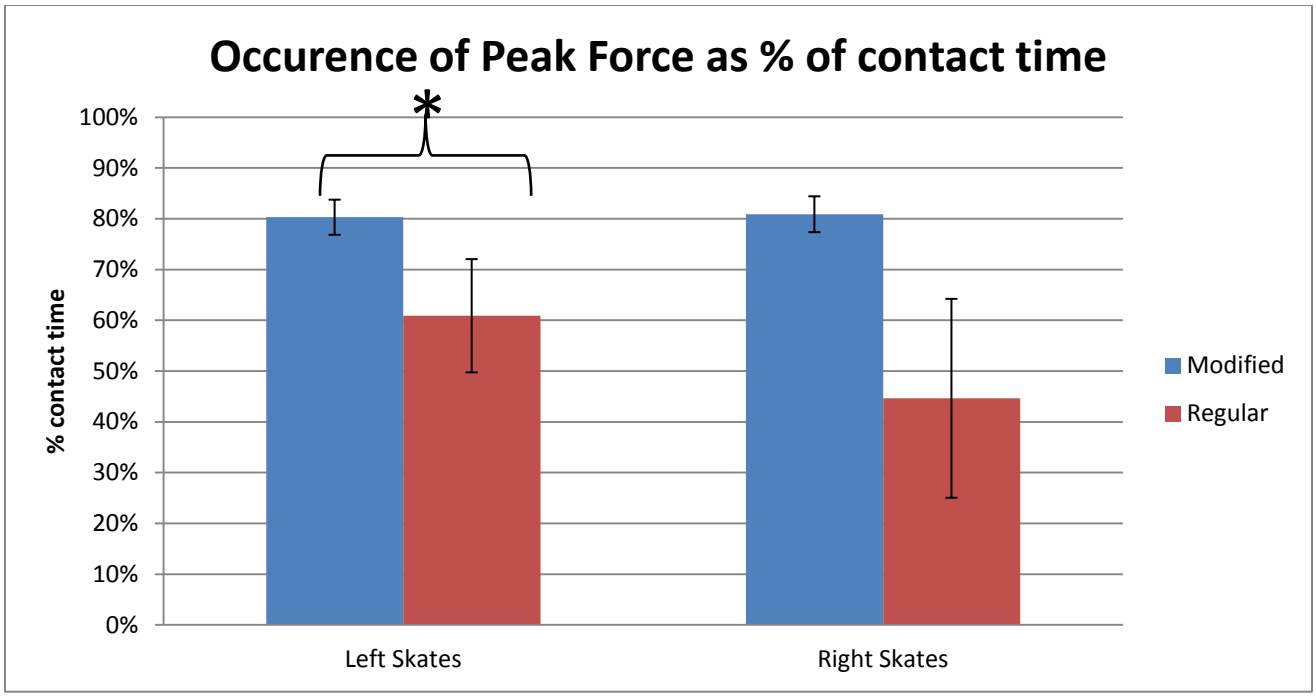

Figure 4.5c: Occurrence of peak force as percentage of contact time. Statistical significance is denoted by * ($p < .05$)

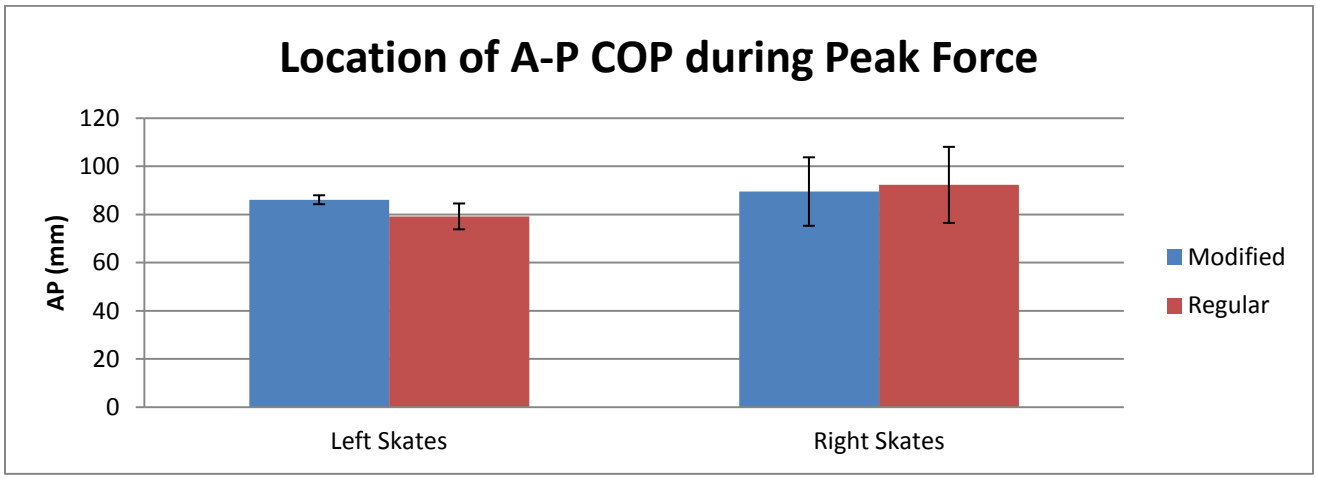

Figure 4.5d: Location of anterior-posterior centre of pressure during peak force

	Left Skates				Right Skates			
Skating Task	Acceleration		Steady State		Acceleration		Steady State	
Skate Type	Modified	Regular	Modified	Regular	Modified	Regular	Modified	Regular
Time of Heel Peak Force	72.9 (5.9)	70.6 (10.9)	78.7 (6.0)	76.3 (7.8)	75.3 (6.9)	61.8 (5.4)	80.8 (6.7)	67.0 (6.7)
	p = .690		*p = .596*		***p = .008***		***p = .012***	
Time of Midfoot Peak Force	89.4 (8.1)	89.9 (11.9)	91.7 (4.0)	89.5 (7.4)	94.6 (8.2)	80.2 (7.8)	95.6 (4.9)	81.7 (7.4)
	p = .943		*p = .579*		***p = .025***		***p = .008***	
Time of Toe Peak Force	95.0 (4.2)	98.1 (7.7)	98.5 (3.7)	99.1 (4.4)	100.5 (5.4)	85.3 (7.4)	102.6 (4.8)	89.0 (6.5)
	p = .441		*p = .816*		***p = .006***		***p = .006***	
Time of Vertical Peak Force	72.8 (5.8)	55.7 (13.0)	80.3 (3.5)	60.9 (11.2)	74.0 (3.9)	44.6 (15.8)	80.9 (3.5)	44.6 (19.6)
	p = .028		***p = .006***		***p = .004***		***p = .004***	

Table 4.5: Sensor temporal measures

Discussion

The purpose of this study was to compare a regular skate and a modified skate which allows for more ankle motion during a forward skating trial by using kinetic and centre of pressure measurements. Previous research has shown that significant improvements in skating performance could be achieved by improved skate design (de Koning, et al., 2000). The regular skate and modified skate were compared by measuring the vertical force applied on the ice by the skate through the use of strain gauges and by measuring the plantar centre of pressure through the use of an instrumented insole. The main finding of this study is that there is a significant decrease in anterior-posterior (AP) centre of pressure excursion, more specifically at the forefoot, in the modified skate when compared to the regular skate ($p < .05$). In comparison, the medial-lateral centre of pressure excursion shows no differences ($p < .05$). However, changes in the centre of pressure in the medial-lateral plane were not expected to be found because the skate modifications should not have an impact on the medial-lateral plane. Additionally, for the right skates, the modified skate showed a lower impulse during the steady state phase, and a lower work and power output during the entire trial ($p < .05$). However, the peak vertical force per stride was the same for both skates ($p > .05$).

The forward skating stride can be divided into four phases: initial contact, glide, push-off and swing (Figure 5.1). At the initial contact, the ankle is in a dorsiflexed position (Lachaîne, 2010) and the centre of pressure under the foot is at its most posterior part, over the heel region. It is then followed by the glide phase in which weight acceptance occurs and the orientation of the blade steers the body movement but no propulsion occurs. During the push-off phase, the blade is turned outward due to hip

abduction and external rotation and propulsion is created through extension of the hip, knee and ankle joints. It is followed by plantarflexion and the skate is then lifted from the ice (D. J. Pearsall, et al., 2000). The swing phase then occurs where the skate is lifted off the ice in order to prepare for the next stride. Maximal ankle dorsiflexion occurs at initial contact and maximal ankle plantarflexion occurs at the end of the push-off (Lachaine, 2009).

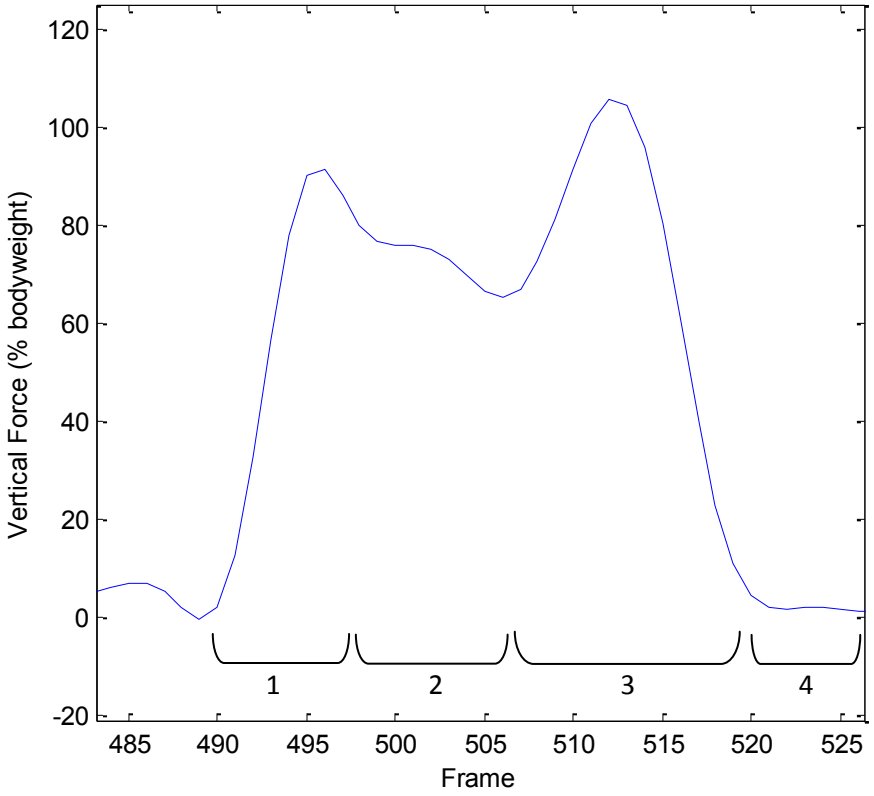

Figure 5.1: Sample Stride: Vertical force during the contact time of the skate with the ice illustrating the initial contact (1) represented by the initial increase in force, followed by the glide (2), the push-off phase (3) represented by the second force peak followed by the swing (4)

The modified skate contains two modifications that affect the ankle motion when compared to a standard skate. The first modification is the elevated eyelet placement at the metatarsal guard which allows for more dorsiflexion. The second modification is a more flexible Achilles' tendon guard at the back of the skate which allows for more plantarflexion. Since the maximal dorsiflexion occurs during the initial contact, the changes at the eyelet configuration should affect mainly the beginning of the stride. Similarly, since maximal plantarflexion occurs at end of the push-off, the changes at the tendon guard should affect the end of the push-off phase and the initiation of the swing phase. During the initial contact, due to the changes at the metatarsal guard in the modified skate, the ankle is allowed to be in a more dorsiflexed position. In the right skate, the modified skate showed significantly lower values of impulse, work and power ($p < .05$). Since these values are calculated from the vertical force applied to the ice during both weight acceptance and propulsion, less force during the weight acceptance phase would result in lower values of impulse, work and power. Generally, a double peak pattern is observed in the vertical force applied to the ice during the contact phase. These two peaks represent respectively the weight acceptance and the propulsion. In the modified skate, it appears that the peak vertical force consistently occurred at the propulsion phase of the stride. The peak vertical force occurred at a different time when comparing the two skate models ($p < .05$). In the modified skate, the peak force occurred at 80.3% ± 3.5% and 80.9% ± 3.5% of the stride for the left and right skates, respectively (Figure 5.2). In the regular skate, many of the weight acceptance peaks were recorded as the peak vertical force was attained during the trial (Figure 5.3), resulting in earlier peak

forces values in the regular skate. In the regular skate, the peak force occurs at 60.0% ± 11.2% and 44.6% ± 19.6% of the stride for the left and right skates, respectively.

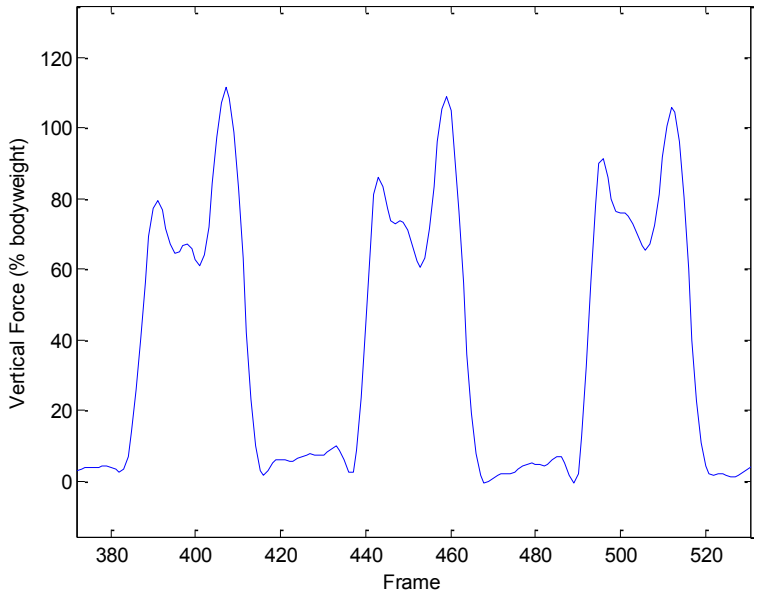

Figure 5.2: Three strides during steady state in a modified skate showing higher force peaks during push off

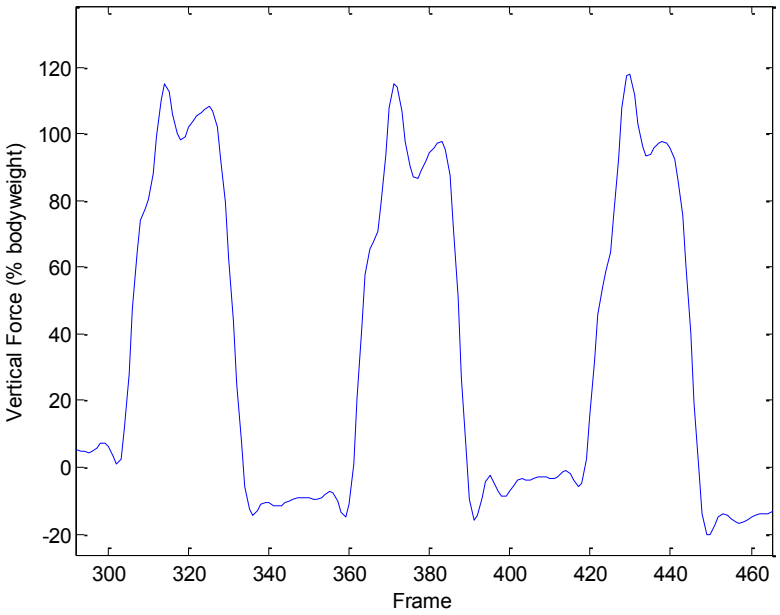

Figure 5.3: Three strides during steady state in a regular skate showing higher force peaks during weight acceptance

The modified skate seemed to allow the ankle to be in a more dorsiflexed position which might have resulted in a smoother weight acceptance by having the blade at a more horizontal level as it contacts the ice. This might result in less forceful impact which results in less vertical force registered by the strain gauge system during weight acceptance. This may in turn explain the lower values of impulse, work and power as well as the consistent peak vertical force during the propulsion phase of the stride. However, there was no significant difference between the two skate models in the peak vertical force ($p > .05$) during a stride indicating that the skate model did not have an influence on the capacity to generate maximal push-off force. While less force was registered in the modified skate during the weight acceptance, it did not seem to affect the center of pressure during initial contact as the minimal centre of pressure in the AP direction were similar for both skate models ($p > .05$). This means that during the weight acceptance phase, the location of the force application under the skater's foot seems to be the same.

During the end of push off phase, the ankle goes into plantarflexion. In a normal skate, the tendon guard is rigid and therefore allows the skater to use the back of the leg to push against it. This force is then transferred to the anterior portion at the bottom of foot. Since there is a less rigid structure at the back of the ankle in the modified skate, the skater cannot push against it in order to transfer forces to the toe region. It was observed that that there was a significant decrease in the AP centre of pressure in the total excursion in the modified skates when compared to the regular skates ($p < 0.05$) for both the left and right skates. More specifically, there was a significant decrease (1.7-2.0 cm)

in the maximal AP value observed in the modified skate in the left skate ($p < .05$). The same trend (1.3-1.7 cm) was also observed in the right skate ($p < .05$). It has been shown that the modified skate could allow for more 4 degrees of dorsiflexion during forward skating (Lachaine 2009). Since the center of pressure is closer to the ankle joint, it might allow for greater stability and control. However, an analysis of lower limbs and upper body kinematics during skating is warranted in order to analyze the exact changes in the skating technique due to the skate modifications. There was no difference in the minimal AP centre of pressure value ($p > .05$). This suggests that the skate modifications only influence the AP centre of pressure at the anterior part of the foot, similar to the findings of Pearsall et al. when the different skate boots were tested into a dynamometer (David J. Pearsall, et al., 2012).

Figure 5.4 shows the centre of pressure part during a whole trial for both skate models for the same subject. It can be seen that the modified skate has a reduced centre of pressure excursion in the anterior posterior direction. It seems that the centre of pressure during skating does not travel to the extreme anterior and posterior regions of the foot, since the foot is in a non-compliant boot as opposed to barefoot or shoed running (De Cock, et al., 2008). Moreover, the interaction between the skater and the ice surface occurs on an already profiled surface due to the blade radius of curvature.

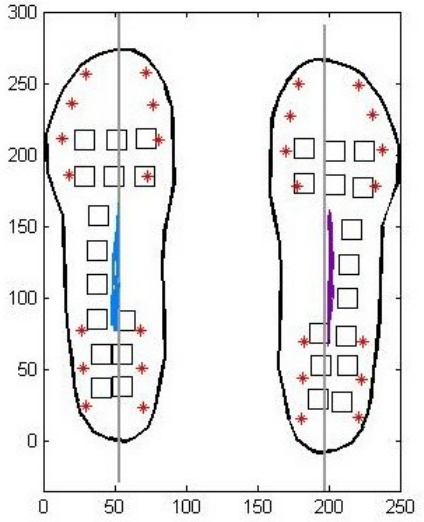

Figure 5.4a: Centre of pressure excursion during entire trial: Regular skates

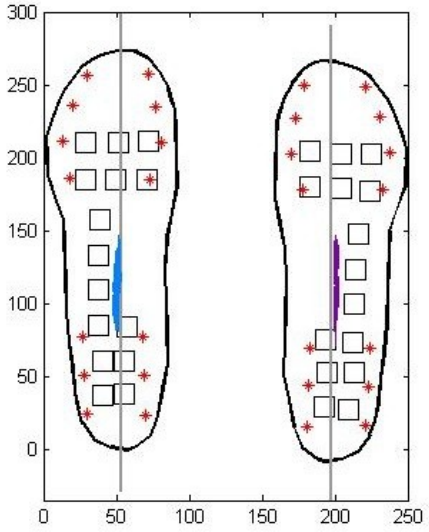

Figure 5.4b: Centre of pressure excursion entire whole trial: Modified skates

While significant differences in the AP centre of pressure were detected, the ML centre of pressure excursion was not significantly different ($p > .05$). The changes in ML centre of pressure might have been harder to detect due to the lower resolution in the ML

range. A greater number of sensors might be needed in future studies if a better resolution in the medial lateral range was required. Moreover, since ice skating occurs in a more rigid boot compared to a shoe which is a more flexible structure, it is possible that the boot allows the skater to use other parts of the foot to apply pressure other than the plantar surface of the foot. In future studies, it might be relevant to place sensors on the inside surface of a skating boot in order to detect the forces of the feet pressing against the lateral sides and the top portions of the boot.

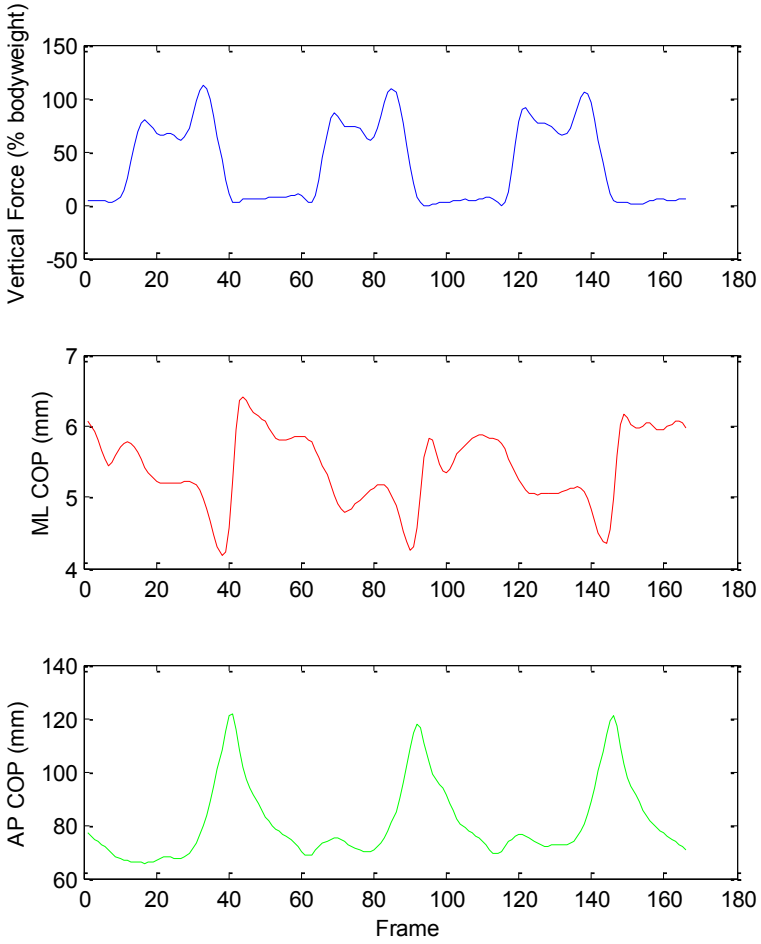

Figure 5.5: Three strides during steady state showing Vertical Force, ML COP and AP COP, minimal (most medial) ML COP and maximal (most anterior) AP COP occurs at the end of push off

The sensors in the insole were grouped into three regions: heel, midfoot and toe. The average force per sensor per region was then calculated. The average and peak sensor force during the contact time and whole stride were measured. The heel region had highest average and peak force. This suggests that during the stride as well as during the push-off, most of the force is transferred through the heel region of the foot. There were no noticeable differences between the skate models for both the average force and peak force values ($p > .05$). However, when comparing the left and right skates, the right foot had significant higher peak and average force for the midfoot region for both skate models ($p < .05$). This seems to be consistent because the right foot also showed a trend towards higher vertical force. However, foot dominance might have influenced the results. No significant difference in force values were detected by the pressure sensors between the skate models ($p > .05$).

However, there was a difference in the timing of the peak force per region (heel, midfoot and toe). In the right skate, there was a significant difference in the timing of the force peaks. As a percentage of the total contact time, the heel, midfoot and toe region peaked earlier in the regular skate compared to the modified skate ($p < 0.05$). This might suggest that, when using the modified skate, there might be some differences in how the skaters modify their skating pattern according to the dominance of their foot in response.

Future Directions

While this study has shown that the skate modifications should have an impact on the centre of pressure during forward skating, there is still information that is missing in

order to get a more complete picture. In addition to the centre of pressure under the foot, it would be interesting to be able to measure pressure in all the areas around the foot, including at the back of the foot and at the top of the foot. Furthermore, it would be ideal to also look at whole body kinematics during skating in order to perform a complete analysis. In order for the skater to manipulate the centre of pressure during skating, there must be changes in body kinematics. Also, it would be interesting to look at other skating tasks to see how they are affected.

Conclusion

It was shown that the modifications on the modified skate have an impact on the center of pressure during forward skating. The modified skate showed a reduction in total AP center of pressure excursion, characterized by a smaller displacement towards the anterior part of the skate. The results are the opposite of what was initially hypothesized. It was hypothesized that a modified skate that allowed for greater dorsiflexion and plantarflexion would show an increase in anterior posterior centre of pressure excursion. Instead, the results showed a decrease. This may provide insight that could help coaches and athletes better understand the mechanics of ice skating. Furthermore, by studying different skate models, this study also has the potential to provide information that could lead to improved skate design.

However, the changes in peak force produced as well as the forces detected by the sensors were not significant. These results show that the modified skates can change a skater's centre of pressure and possibly movement pattern which might result in positive changes but might not have a direct impact on the amount of force generated. In order to truly determine the modified skate's benefit and the exact changes in the skater's technique, a kinematic study of the lower limbs and upper body will be required.

References

Bracko, M. R. (2001). On-ice performance characteristics of elite and non-elite women's ice hockey players. *J Strength Cond Res, 15*(1), 42-47.

Cavanagh, P. R., Hewitt Jr, F. G., & Perry, J. E. (1992). In-shoe plantar pressure measurement: a review. *The Foot, 2*(4), 185-194. doi: 10.1016/0958-2592(92)90047-s

Chesnin, K. J., Selby-Silverstein, L., & Besser, M. P. (2000). Comparison of an in-shoe pressure measurement device to a force plate: concurrent validity of center of pressure measurements. *Gait Posture, 12*(2), 128-133. doi: S0966-6362(00)00071-0 [pii]

de Boer, R. W., Cabri, J., Vaes, W., Clarijs, J. P., Hollander, A. P., de Groot, G., & van Ingen Schenau, G. J. (1987). Moments of force, power, and muscle coordination in speed-skating. *Int J Sports Med, 8*(6), 371-378. doi: 10.1055/s-2008-1025688

de Boer, R. W., Schermerhorn, P., Gademan, J., De Groot, G., & van Ingen Schenau, G. J. (1986). Characteristic stroke mechanics of elite and trained male speed skaters. *International Journal of Sport Biomechanics, 2*, 175-185.

De Cock, A., Vanrenterghem, J., Willems, T., Witvrouw, E., & De Clercq, D. (2008). The trajectory of the centre of pressure during barefoot running as a potential measure for foot function. *Gait Posture, 27*(4), 669-675.

de Koning, J. J., de Groot, G., & van Ingen Schenau, G. J. (1992). Ice friction during speed skating. *J Biomech, 25*(6), 565-571. doi: 0021-9290(92)90099-M [pii]

de Koning, J. J., Houdijk, H., de Groot, G., & Bobbert, M. F. (2000). From biomechanical theory to application in top sports: the klapskate story. *J Biomech, 33*(10), 1225-1229. doi: S0021-9290(00)00063-4 [pii]

de Koning, J. J., Thomas, R., Berger, M., de Groot, G., & van Ingen Schenau, G. J. (1995). The start in speed skating: from running to gliding. *Med Sci Sports Exerc, 27*(12), 1703-1708.

Eils, E., Streyl, M., Linnenbecker, S., Thorwesten, L., Volker, K., & Rosenbaum, D. (2004). Characteristic plantar pressure distribution patterns during soccer-specific movements. *Am J Sports Med, 32*(1), 140-145.

Formenti, F., & Minetti, A. E. (2007). Human locomotion on ice: the evolution of ice-skating energetics through history. *J Exp Biol, 210*(Pt 10), 1825-1833.

Formenti, F., & Minetti, A. E. (2008). The first humans travelling on ice: an energy-saving strategy? *Biological Journal of the Linnean Society, 93*, 1-7.

Giacomozzi, C. (2010). Appropriateness of plantar pressure measurement devices: a comparative technical assessment. *Gait Posture, 32*(1), 141-144. doi: S0966-6362(10)00084-6 [pii]

Hoshizaki, T. B., Kirchner, G., Hall, K. (1989). Kinematic analysis of the talocrural and subtalar joints during the hockey skating stride.

Houdijk, H., de Koning, J. J., de Groot, G., Bobbert, M. F., And, & van Ingen Schenau, G. J. (2000). Push-off mechanics in speed skating with conventional skates and klapskates. *Med Sci Sports Exerc, 32*(3), 635-641.

Jobse, H., Schuurhof, R., Cserep, F., Schreurs, A. W., & De Koning, J. J. (1990). Measurement of Push-Off Force and Ice Friction during Speed Skating. *International Journal of Sport Biomechanics, 6*(1), 92-100.

Lachaîne, X. (2010). Force measurement and ankle motion of the forward skating and crossover with a standard hockey skate and a modified hockey state.

Lafontaine, D. (2007). Three-dimensional kinematics of the knee and ankle joints for three consecutive push-offs during ice hockey skating starts. *Sports Biomech, 6*(3), 391-406.

Marino, G. W. (1977). Kinematics of ice skating at different velocities. *Res Q, 48*(1), 93-97.

Marino, G. W. (1979). Acceleration-time relationships in an ice skating start. *Res Q, 50*(1), 55-59.

Marino, G. W. (1983). Selected mechanical factors associated with acceleration in ice skating. *Research quarterly for exercise and sport, 54*(3), 234-238.

Marino, G. W., & Weese, R. G. (1979). A kinematic analysis of the ice skating stride.

Nigg, B. M., Cole, G. K., & Nachbauer, W. (1993). Effects of arch height of the foot on angular motion of the lower extremities in running. *J Biomech, 26*(8), 909-916. doi: 0021-9290(93)90053-H [pii]

Pearsall, D. J., Paquette, Y. M., Baig, Z., Albrecht, J., & Turcotte, R. A. (2012). Ice hockey skate boot mechanics: Direct torque and contact pressure measures. *Procedia Engineering, 34*(0), 295-300. doi: 10.1016/j.proeng.2012.04.051

Pearsall, D. J., Turcotte, R. A., Lefebvre, R., Bateni, H., Nicolaou, M., & Montgomery, D. (2001). *Kinematics of the foot and ankle in forward ice hockey skating*. Paper presented at the XIX International Symposium on Biomechanics in Sports, ISBS, San Francisco.

Pearsall, D. J., Turcotte, R. A., & Murphy, S. D. (2000). Biomechanics of ice hockey. In W. W. Lippincott (Ed.), *Exercise and Sport Science* (pp. 675-692). Philadelphia: W.E Garrett Jr. and D.T. Kirkendall (Eds.).

Queen, R. M., Haynes, B. B., Hardaker, W. M., & Garrett, W. E., Jr. (2007). Forefoot loading during 3 athletic tasks. *Am J Sports Med, 35*(4), 630-636. doi: 0363546506295938 [pii]

10.1177/0363546506295938

Rosenbaum, D., & Becker, H. P. (1997). Plantar pressure distribution measurements. Technical background and clinical applications. *Foot and Ankle Surgery, 3*(1), 1-14. doi: 10.1046/j.1460-9584.1997.00043.x

Shu, L., Hua, T., Wang, Y., Qiao Li, Q., Feng, D. D., & Tao, X. (2010). In-shoe plantar pressure measurement and analysis system based on fabric pressure sensing array. *IEEE Trans Inf Technol Biomed, 14*(3), 767-775. doi: 10.1109/TITB.2009.2038904

Stidwill, T. J., Turcotte, R. A., Dixon, P., & Pearsall, D. J. (2010). Force transducer system for measurement of ice hockey skating force. *Sports Engineering, 12*(2), 63-68. doi: 10.1007/s12283-009-0033-4

Upjohn, T., Turcotte, R., Pearsall, D. J., & Loh, J. (2008). Three-dimensional kinematics of the lower limbs during forward ice hockey skating. *Sports Biomechanics, 7*(2), 206-221. doi: 10.1080/14763140701841621

van Ingen Schenau, G. J., De Boer, R. W., & De Groot, G. (1989). Biomechanics of speed skating. In C. L. Vaughn (Ed.), *Biomechanics of sport* (pp. 121-167). Boca Raton, FL: CRC Press.

Van Ingen Schenau, G. J., de Groot, G., & de Boer, R. W. (1985). The control of speed in elite female speed skaters. *J Biomech, 18*(2), 91-96.

Williams, D. S., 3rd, McClay, I. S., & Hamill, J. (2001). Arch structure and injury patterns in runners. *Clin Biomech (Bristol, Avon), 16*(4), 341-347. doi: S0268003301000055 [pii]

Wong, P. L., Chamari, K., Chaouachi, A., Mao de, W., Wisloff, U., & Hong, Y. (2007). Difference in plantar pressure between the preferred and non-preferred feet in four soccer-related movements. *Br J Sports Med, 41*(2), 84-92. doi: bjsm.2006.030908 [pii]

Appendix 1: Complete Results

		Left Skates	Left std	Right Skates	Right std
AP COP excursion (acceleration)	Modified	67.3452	7.03502	80.9628	6.43065
	Regular	87.0997	8.9744	95.5244	8.02795
AP COP excursion (steady state)	Modified	63.6334	4.93981	75.7706	3.29936
	Regular	87.8574	10.10331	94.8409	10.63698
———Average Vertical Force (acceleration)	Modified	51.5427	5.51566	52.0902	9.42329
	Regular	54.7223	19.80939	60.4086	18.9786
Average Vertical Force (steady state)	Modified	46.5579	12.78852	52.7023	12.38054
	Regular	68.2312	17.94938	65.9403	16.75152
Average Heel Region Force – Contact Time (acceleration)	Modified	7.4718	0.68004	8.2677	3.04236
	Regular	6.9081	1.17192	7.0046	2.3002
Average Heel Region Force – Stride (acceleration)	Modified	5.7677	1.11024	5.2196	1.96473
	Regular	5.777	2.28733	5.0615	1.166
Average Heel Region Force – Contact Time (steady state)	Modified	7.8461	1.01477	8.1534	2.82287
	Regular	7.3075	1.60275	7.2227	2.20244
Average Heel Region Force – Stride (steady state)	Modified	6.002	0.8578	5.331	2.07221
	Regular	5.7273	1.71129	5.3861	1.13213
Average Midfoot Region Force – Contact Time (acceleration)	Modified	2.1424	0.6275	3.3318	0.54019
	Regular	2.2026	0.60711	2.9663	0.6647
Average Midfoot Region Force – Stride (acceleration)	Modified	1.5953	0.43857	2.2856	0.77457
	Regular	1.5852	0.32988	2.3291	1.01358
Average Midfoot Region Force – Contact Time (steady state)	Modified	2.1445	0.68208	3.3772	0.78862
	Regular	2.201	0.57179	2.9179	0.64982
Average Midfoot Region Force – Stride (steady state)	Modified	1.668	0.53382	2.3947	0.8512
	Regular	1.6886	0.38175	2.407	1.04195
Average Toe Region Force – Contact Time (acceleration)	Modified	2.3476	0.62594	1.9126	0.35795
	Regular	1.8599	0.48088	2.4855	0.90476
Average Toe Region Force – Stride (acceleration)	Modified	1.845	0.47632	1.6322	1.09392
	Regular	1.5722	0.51776	1.8027	1.25503
Average Toe Region Force – Contact Time (steady state)	Modified	2.1967	0.66915	1.8781	0.56523
	Regular	1.8463	0.63578	2.3001	0.82798
Average Toe Region Force – Stride (steady state)	Modified	1.8279	0.57644	1.7148	1.26892
	Regular	1.6916	0.58452	1.7769	1.18875
Contact Time (acceleration)	Modified	0.32483	0.056502	0.30144	0.048067
	Regular	0.3259	0.056576	0.34327	0.043996
Contact Time	Modified	0.38218	0.037115	0.36228	0.037045
	Regular	0.37853	0.056536	0.41698	0.041797

Impulse (acceleration)	Modified	17.2045	3.8962	15.8913	3.68802
	Regular	17.5687	8.77161	21.9305	8.45734
Impulse	Modified	18.1246	6.06043	18.8194	3.87878
	Regular	24.904	7.86051	28.371	8.30565
Max AP COP (acceleration)	Modified	139.455610	6.2091699	155.9801479	8.1840704
	Regular	156.408805	9.9551056	169.451702	10.5782903
Max AP COP (steady state)	Modified	137.183177	4.8594134	152.178165	12.5584418
	Regular	157.344617	12.0880173	169.694308	15.229769
Max ML COP (acceleration)	Modified	5.376531	0.4597361	6.082680	.9707853
	Regular	6.404994	0.6731819	5.682980	.3770043
Max ML COP (steady state)	Modified	5.622727	0.5566051	6.296940	1.2321415
	Regular	6.683158	0.8271734	6.056800	.8841727
Min AP COP (acceleration)	Modified	72.110419	5.6707461	75.016428	9.7279005
	Regular	69.30883	4.8585215	73.927566	7.9550713
Min AP COP (steady state)	Modified	73.549138	6.1657806	76.407965	10.4544162
	Regular	69.487513	5.193509	74.853638	9.9284423
Min ML COP (acceleration)	Modified	2.073568	0.7004194	2.682680	0.6619502
	Regular	1.521305	1.7708339	.020980	2.762411
Min ML COP (steady state)	Modified	2.477169	0.7404541	2.756940	0.7726702
	Regular	1.606649	2.1837451	.132800	3.1181794
ML COP Excursion (acceleration)	Modified	3.303	0.54683	3.4014	0.82804
	Regular	4.8837	1.97247	5.661	3.00236
ML COP Excursion (steady state)	Modified	3.1456	0.49884	3.5408	1.04726
	Regular	5.0765	2.65022	5.9256	2.9779
Power	Modified	199.2246	19.26035	253.685	46.35977
	Regular	229.1945	44.00766	331.323	56.55304
Peak Vertical Force (acceleration)	Modified	124.1901	5.96921	125.323	10.28714
	Regular	113.3415	30.39621	128.2925	28.35019
Peak Vertical Force (steady state)	Modified	116.2775	7.60181	122.0093	12.08542
	Regular	123.8881	16.13917	135.3442	29.79991
Location of AP COP during Peak Vertical Force(acceleration)	Modified	89.913193	2.3312442	90.092109	14.673618
	Regular	77.651366	5.3478633	91.369205	16.8390052
Location of AP COP during Peak Vertical Force(steady state)	Modified	86.08676	1.8539723	89.50032	14.2100673
	Regular	79.170985	5.3709906	92.261571	15.7854623
Peak Heel Region Force (acceleration)	Modified	11.1015	0.64562	12.3689	3.97634
	Regular	10.106	1.34041	11.4791	2.65095
Peak Heel Region Force (steady state)	Modified	11.5824	1.27344	11.8715	3.32868
	Regular	10.4387	1.82181	11.7054	2.53503
Peak Midfoot Region Force (acceleration)	Modified	3.7047	0.98881	5.7263	0.6236
	Regular	3.8964	0.97057	5.298	0.78992
Peak Midfoot Region	Modified	3.8006	1.02842	5.6863	0.74835

Force (steady state)	Regular	3.8758	1.02188	5.3789	0.91828
Peak Toe Region Force (acceleration)	Modified	5.068	1.37361	4.5401	0.94689
	Regular	4.0927	0.9898	4.8621	1.00352
Peak Toe Region Force (steady state)	Modified	4.5981	1.12578	4.5662	0.88937
	Regular	3.9272	0.692	4.9381	1.05707
Peak Heel Region Force % of Stride (acceleration)	Modified	0.7286	0.05936	0.7536	0.06919
	Regular	0.7056	0.10903	0.6181	0.05339
Peak Heel Region Force % of Stride (steady state)	Modified	0.7869	0.06003	0.8081	0.06697
	Regular	0.7625	0.07796	0.6706	0.06712
Peak Midfoot Region Force % of Stride (acceleration)	Modified	0.8942	0.08077	0.9406	0.08197
	Regular	0.8989	0.11887	0.8018	0.07762
Peak Midfoot Region Force % of Stride (steady state)	Modified	0.9165	0.04016	0.9558	0.04948
	Regular	0.8946	0.07422	0.817	0.07432
Peak Vertical Force % of Stride (acceleration)	Modified	0.7283	0.05802	0.7397	0.03932
	Regular	0.5573	0.13015	0.4463	0.15825
Peak Vertical Force % of Stride (steady state)	Modified	0.803	0.03459	0.8089	0.0353
	Regular	0.6089	0.11152	0.4463	0.1959
Peak Toe Region Force % of Stride (acceleration)	Modified	0.9496	0.04237	1.0047	0.05422
	Regular	0.9815	0.07729	0.853	0.07389
Peak Toe Region Force % of Stride (steady state)	Modified	0.9853	0.03749	1.0258	0.0477
	Regular	0.9915	0.04434	0.8902	0.06526
Stride Rate	Modified	1.0092	0.15369	0.9921	0.179
	Regular	0.9712	0.15033	0.9431	0.12814
Work	Modified	1931.4208	274.05243	2417.8725	176.9605
	Regular	2250.1474	455.37895	3230.0369	465.52842

Appendix 2.1: MANOVA table, left skates: regular vs. modified skates

Tests of Between-Subjects Effects

Source	Dependent Variable	Type III Sum of Squares	df	Mean Square	F	Sig.
Corrected Model	AP_ACCav	975.606[a]	1	975.606	15.006	.005
	avf_ACCav	25.274[b]	1	25.274	.120	.738
	AP_STDav	1466.998[c]	1	1466.998	23.198	.001
	avf_STDav	1174.324[d]	1	1174.324	4.835	.059
	avgheel_ACCav	.794[e]	1	.794	.865	.379
	avgheel_ACCstride	.000[f]	1	.000	.000	.994
	avgheel_STDav	.725[g]	1	.725	.403	.543
	avgheel_STDstride	.189[h]	1	.189	.103	.756
	avgmid_ACCav	.009[i]	1	.009	.024	.881
	avgmid_ACCstride	.000[j]	1	.000	.002	.968
	avgmid_STDav	.008[k]	1	.008	.020	.891
	avgmid_STDstride	.001[l]	1	.001	.005	.946
	avgtop_ACCav	.595[m]	1	.595	1.909	.204
	avgtop_ACCstride	.186[n]	1	.186	.752	.411
	avgtop_STDav	.307[o]	1	.307	.721	.421
	avgtop_STDstride	.046[p]	1	.046	.138	.720
	ct_ACCav	2.846E-6[q]	1	2.846E-6	.001	.977
	ct_STDav	3.321E-5[r]	1	3.321E-5	.015	.907
	i_ACCav	.332[s]	1	.332	.007	.934
	i_STDav	114.901[t]	1	114.901	2.333	.165
	MAXAP_ACCav	718.527[u]	1	718.527	10.439	.012
	MAXAP_STDav	1016.209[v]	1	1016.209	11.974	.009
	maxML_ACCav	2.644[w]	1	2.644	7.959	.022
	maxML_STDav	2.811[x]	1	2.811	5.656	.045
	MINAP_ACCav	19.622[y]	1	19.622	.704	.426
	MINAP_STDav	41.242[z]	1	41.242	1.162	.313
	minML_ACCav	.762[aa]	1	.762	.421	.535
	minML_STDav	1.895[ab]	1	1.895	.713	.423
	ML_ACCav	6.247[ac]	1	6.247	2.982	.122
	ML_STDav	9.321[ad]	1	9.321	2.563	.148

	P	2245.481[ae]	1	2245.481	1.946	.201
	p_ACCav	294.234[af]	1	294.234	.613	.456
	p_STDav	144.804[ag]	1	144.804	.910	.368
	PEAKAP_ACCav	375.881[ah]	1	375.881	22.088	.002
	PEAKAP_STDav	119.570[ai]	1	119.570	7.407	.026
	peakheel_ACCav	2.478[aj]	1	2.478	2.239	.173
	peakheel_STDav	3.270[ak]	1	3.270	1.324	.283
	peakmid_ACCav	.092[al]	1	.092	.096	.765
	peakmid_STDav	.014[am]	1	.014	.013	.910
	peakML_ACCav	.418[an]	1	.418	1.209	.303
	peakML_STDav	.001[ao]	1	.001	.003	.961
	peaktop_ACCav	2.378[ap]	1	2.378	1.659	.234
	peaktop_STDav	1.125[aq]	1	1.125	1.289	.289
	percentheel_ACCav	.001[ar]	1	.001	.171	.690
	percentheel_STDav	.001[as]	1	.001	.305	.596
	percentmid_ACCav	5.616E-5[at]	1	5.616E-5	.005	.943
	percentmid_STDav	.001[au]	1	.001	.335	.579
	percentpeak_ACCav	.073[av]	1	.073	7.206	.028
	percentpeak_STDav	.094[aw]	1	.094	13.829	.006
	percenttop_ACCav	.003[ax]	1	.003	.657	.441
	percenttop_STDav	9.779E-5[ay]	1	9.779E-5	.058	.816
	sr	.004[az]	1	.004	.156	.703
	W	253966.598[ba]	1	253966.598	1.798	.217
Intercept	AP_ACCav	59633.085	1	59633.085	917.211	.000
	avf_ACCav	28230.642	1	28230.642	133.531	.000
	AP_STDav	57373.675	1	57373.675	907.247	.000
	avf_STDav	32941.354	1	32941.354	135.638	.000
	avgheel_ACCav	516.954	1	516.954	563.177	.000
	avgheel_ACCstride	333.198	1	333.198	103.085	.000
	avgheel_STDav	574.084	1	574.084	319.065	.000
	avgheel_STDstride	343.938	1	343.938	187.721	.000
	avgmid_ACCav	47.197	1	47.197	123.821	.000
	avgmid_ACCstride	25.289	1	25.289	167.938	.000
	avgmid_STDav	47.210	1	47.210	119.190	.000
	avgmid_STDstride	28.166	1	28.166	130.794	.000
	avgtop_ACCav	44.259	1	44.259	142.073	.000

	avgtop_ACCstride	29.194	1	29.194	117.964	.000
	avgtop_STDav	40.865	1	40.865	95.931	.000
	avgtop_STDstride	30.967	1	30.967	91.898	.000
	ct_ACCav	1.059	1	1.059	331.167	.000
	ct_STDav	1.447	1	1.447	632.608	.000
	i_ACCav	3022.943	1	3022.943	65.629	.000
	i_STDav	4628.662	1	4628.662	93.967	.000
	MAXAP_ACCav	218839.380	1	218839.380	3179.467	.000
	MAXAP_STDav	216866.553	1	216866.553	2555.369	.000
	maxML_ACCav	347.011	1	347.011	1044.378	.000
	maxML_STDav	378.587	1	378.587	761.725	.000
	MINAP_ACCav	49998.510	1	49998.510	1793.263	.000
	MINAP_STDav	51148.709	1	51148.709	1440.725	.000
	minML_ACCav	32.308	1	32.308	17.818	.003
	minML_STDav	41.694	1	41.694	15.683	.004
	ML_ACCav	167.553	1	167.553	79.984	.000
	ML_STDav	169.006	1	169.006	46.478	.000
	P	458857.239	1	458857.239	397.686	.000
	p_ACCav	141053.170	1	141053.170	293.995	.000
	p_STDav	144198.814	1	144198.814	906.169	.000
	PEAKAP_ACCav	70194.703	1	70194.703	4124.934	.000
	PEAKAP_STDav	68275.305	1	68275.305	4229.570	.000
	peakheel_ACCav	1124.401	1	1124.401	1015.937	.000
	peakheel_STDav	1212.321	1	1212.321	490.754	.000
	peakmid_ACCav	144.441	1	144.441	150.479	.000
	peakmid_STDav	147.320	1	147.320	140.178	.000
	peakML_ACCav	201.670	1	201.670	583.124	.000
	peakML_STDav	213.415	1	213.415	424.963	.000
	peaktop_ACCav	209.799	1	209.799	146.379	.000
	peaktop_STDav	181.701	1	181.701	208.104	.000
	percentheel_ACCav	5.142	1	5.142	667.335	.000
	percentheel_STDav	6.002	1	6.002	1239.836	.000
	percentmid_ACCav	8.039	1	8.039	778.410	.000
	percentmid_STDav	8.200	1	8.200	2302.998	.000
	percentpeak_ACCav	4.132	1	4.132	406.970	.000
	percentpeak_STDav	4.984	1	4.984	731.135	.000
	percenttop_ACCav	9.322	1	9.322	2399.703	.000
	percenttop_STDav	9.769	1	9.769	5795.244	.000

	sr	9.804	1	9.804	424.237	.000
	W	43713782.886	1	43713782.886	309.506	.000
Conditiondrom1reg2	AP_ACCav	975.606	1	975.606	15.006	.005
	avf_ACCav	25.274	1	25.274	.120	.738
	AP_STDav	1466.998	1	1466.998	23.198	.001
	avf_STDav	1174.324	1	1174.324	4.835	.059
	avgheel_ACCav	.794	1	.794	.865	.379
	avgheel_ACCstride	.000	1	.000	.000	.994
	avgheel_STDav	.725	1	.725	.403	.543
	avgheel_STDstride	.189	1	.189	.103	.756
	avgmid_ACCav	.009	1	.009	.024	.881
	avgmid_ACCstride	.000	1	.000	.002	.968
	avgmid_STDav	.008	1	.008	.020	.891
	avgmid_STDstride	.001	1	.001	.005	.946
	avgtop_ACCav	.595	1	.595	1.909	.204
	avgtop_ACCstride	.186	1	.186	.752	.411
	avgtop_STDav	.307	1	.307	.721	.421
	avgtop_STDstride	.046	1	.046	.138	.720
	ct_ACCav	2.846E-6	1	2.846E-6	.001	.977
	ct_STDav	3.321E-5	1	3.321E-5	.015	.907
	i_ACCav	.332	1	.332	.007	.934
	i_STDav	114.901	1	114.901	2.333	.165
	MAXAP_ACCav	718.527	1	718.527	10.439	.012
	MAXAP_STDav	1016.209	1	1016.209	11.974	.009
	maxML_ACCav	2.644	1	2.644	7.959	.022
	maxML_STDav	2.811	1	2.811	5.656	.045
	MINAP_ACCav	19.622	1	19.622	.704	.426
	MINAP_STDav	41.242	1	41.242	1.162	.313
	minML_ACCav	.762	1	.762	.421	.535
	minML_STDav	1.895	1	1.895	.713	.423
	ML_ACCav	6.247	1	6.247	2.982	.122
	ML_STDav	9.321	1	9.321	2.563	.148
	P	2245.481	1	2245.481	1.946	.201
	p_ACCav	294.234	1	294.234	.613	.456
	p_STDav	144.804	1	144.804	.910	.368
	PEAKAP_ACCav	375.881	1	375.881	22.088	.002
	PEAKAP_STDav	119.570	1	119.570	7.407	.026
	peakheel_ACCav	2.478	1	2.478	2.239	.173

	peakheel_STDav	3.270	1	3.270	1.324	.283
	peakmid_ACCav	.092	1	.092	.096	.765
	peakmid_STDav	.014	1	.014	.013	.910
	peakML_ACCav	.418	1	.418	1.209	.303
	peakML_STDav	.001	1	.001	.003	.961
	peaktop_ACCav	2.378	1	2.378	1.659	.234
	peaktop_STDav	1.125	1	1.125	1.289	.289
	percentheel_ACCav	.001	1	.001	.171	.690
	percentheel_STDav	.001	1	.001	.305	.596
	percentmid_ACCav	5.616E-5	1	5.616E-5	.005	.943
	percentmid_STDav	.001	1	.001	.335	.579
	percentpeak_ACCav	.073	1	.073	7.206	.028
	percentpeak_STDav	.094	1	.094	13.829	.006
	percenttop_ACCav	.003	1	.003	.657	.441
	percenttop_STDav	9.779E-5	1	9.779E-5	.058	.816
	sr	.004	1	.004	.156	.703
	W	253966.598	1	253966.598	1.798	.217
Error	AP_ACCav	520.125	8	65.016		
	avf_ACCav	1691.337	8	211.417		
	AP_STDav	505.914	8	63.239		
	avf_STDav	1942.905	8	242.863		
	avgheel_ACCav	7.343	8	.918		
	avgheel_ACCstride	25.858	8	3.232		
	avgheel_STDav	14.394	8	1.799		
	avgheel_STDstride	14.657	8	1.832		
	avgmid_ACCav	3.049	8	.381		
	avgmid_ACCstride	1.205	8	.151		
	avgmid_STDav	3.169	8	.396		
	avgmid_STDstride	1.723	8	.215		
	avgtop_ACCav	2.492	8	.312		
	avgtop_ACCstride	1.980	8	.247		
	avgtop_STDav	3.408	8	.426		
	avgtop_STDstride	2.696	8	.337		
	ct_ACCav	.026	8	.003		
	ct_STDav	.018	8	.002		
	i_ACCav	368.486	8	46.061		
	i_STDav	394.066	8	49.258		
	MAXAP_ACCav	550.632	8	68.829		

	MAXAP_STDav	678.936	8	84.867		
	maxML_ACCav	2.658	8	.332		
	maxML_STDav	3.976	8	.497		
	MINAP_ACCav	223.050	8	27.881		
	MINAP_STDav	284.017	8	35.502		
	minML_ACCav	14.506	8	1.813		
	minML_STDav	21.268	8	2.659		
	ML_ACCav	16.759	8	2.095		
	ML_STDav	29.090	8	3.636		
	P	9230.541	8	1153.818		
	p_ACCav	3838.244	8	479.781		
	p_STDav	1273.042	8	159.130		
	PEAKAP_ACCav	136.137	8	17.017		
	PEAKAP_STDav	129.139	8	16.142		
	peakheel_ACCav	8.854	8	1.107		
	peakheel_STDav	19.763	8	2.470		
	peakmid_ACCav	7.679	8	.960		
	peakmid_STDav	8.408	8	1.051		
	peakML_ACCav	2.767	8	.346		
	peakML_STDav	4.018	8	.502		
	peaktop_ACCav	11.466	8	1.433		
	peaktop_STDav	6.985	8	.873		
	percentheel_ACCav	.062	8	.008		
	percentheel_STDav	.039	8	.005		
	percentmid_ACCav	.083	8	.010		
	percentmid_STDav	.028	8	.004		
	percentpeak_ACCav	.081	8	.010		
	percentpeak_STDav	.055	8	.007		
	percenttop_ACCav	.031	8	.004		
	percenttop_STDav	.013	8	.002		
	sr	.185	8	.023		
	W	1129898.894	8	141237.362		
Total	AP_ACCav	61128.816	10			
	avf_ACCav	29947.252	10			
	AP_STDav	59346.587	10			
	avf_STDav	36058.583	10			
	avgheel_ACCav	525.092	10			
	avgheel_ACCstride	359.056	10			

	avgheel_STDav	589.204	10			
	avgheel_STDstride	358.784	10			
	avgmid_ACCav	50.255	10			
	avgmid_ACCstride	26.494	10			
	avgmid_STDav	50.387	10			
	avgmid_STDstride	29.890	10			
	avgtop_ACCav	47.346	10			
	avgtop_ACCstride	31.360	10			
	avgtop_STDav	44.580	10			
	avgtop_STDstride	33.709	10			
	ct_ACCav	1.084	10			
	ct_STDav	1.465	10			
	i_ACCav	3391.761	10			
	i_STDav	5137.629	10			
	MAXAP_ACCav	220108.539	10			
	MAXAP_STDav	218561.699	10			
	maxML_ACCav	352.313	10			
	maxML_STDav	385.374	10			
	MINAP_ACCav	50241.183	10			
	MINAP_STDav	51473.968	10			
	minML_ACCav	47.576	10			
	minML_STDav	64.857	10			
	ML_ACCav	190.559	10			
	ML_STDav	207.417	10			
	P	470333.262	10			
	p_ACCav	145185.649	10			
	p_STDav	145616.660	10			
	PEAKAP_ACCav	70706.722	10			
	PEAKAP_STDav	68524.014	10			
	peakheel_ACCav	1135.733	10			
	peakheel_STDav	1235.354	10			
	peakmid_ACCav	152.212	10			
	peakmid_STDav	155.742	10			
	peakML_ACCav	204.855	10			
	peakML_STDav	217.434	10			
	peaktop_ACCav	223.643	10			
	peaktop_STDav	189.811	10			
	percentheel_ACCav	5.205	10			

	percentheel_STDav	6.042	10			
	percentmid_ACCav	8.121	10			
	percentmid_STDav	8.230	10			
	percentpeak_ACCav	4.286	10			
	percentpeak_STDav	5.132	10			
	percenttop_ACCav	9.356	10			
	percenttop_STDav	9.783	10			
	sr	9.993	10			
	W	45097648.377	10			
Corrected Total	AP_ACCav	1495.731	9			
	avf_ACCav	1716.611	9			
	AP_STDav	1972.912	9			
	avf_STDav	3117.229	9			
	avgheel_ACCav	8.138	9			
	avgheel_ACCstride	25.858	9			
	avgheel_STDav	15.119	9			
	avgheel_STDstride	14.846	9			
	avgmid_ACCav	3.058	9			
	avgmid_ACCstride	1.205	9			
	avgmid_STDav	3.177	9			
	avgmid_STDstride	1.724	9			
	avgtop_ACCav	3.087	9			
	avgtop_ACCstride	2.166	9			
	avgtop_STDav	3.715	9			
	avgtop_STDstride	2.742	9			
	ct_ACCav	.026	9			
	ct_STDav	.018	9			
	i_ACCav	368.818	9			
	i_STDav	508.967	9			
	MAXAP_ACCav	1269.159	9			
	MAXAP_STDav	1695.145	9			
	maxML_ACCav	5.302	9			
	maxML_STDav	6.787	9			
	MINAP_ACCav	242.673	9			
	MINAP_STDav	325.259	9			
	minML_ACCav	15.268	9			

	minML_STDav	23.163	9			
	ML_ACCav	23.005	9			
	ML_STDav	38.411	9			
	P	11476.023	9			
	p_ACCav	4132.478	9			
	p_STDav	1417.846	9			
	PEAKAP_ACCav	512.018	9			
	PEAKAP_STDav	248.709	9			
	peakheel_ACCav	11.332	9			
	peakheel_STDav	23.033	9			
	peakmid_ACCav	7.771	9			
	peakmid_STDav	8.422	9			
	peakML_ACCav	3.185	9			
	peakML_STDav	4.019	9			
	peaktop_ACCav	13.844	9			
	peaktop_STDav	8.110	9			
	percentheel_ACCav	.063	9			
	percentheel_STDav	.040	9			
	percentmid_ACCav	.083	9			
	percentmid_STDav	.030	9			
	percentpeak_ACCav	.154	9			
	percentpeak_STDav	.149	9			
	percenttop_ACCav	.034	9			
	percenttop_STDav	.014	9			
	sr	.188	9			
	W	1383865.491	9			

Appendix 2.2: MANOVA table, right skates: regular vs. modified skates

Tests of Between-Subjects Effects

Source	Dependent Variable	Type III Sum of Squares	df	Mean Square	F	Sig.
Corrected Model	AP_ACCav	530.102[a]	1	530.102	10.021	.013
	avf_ACCav	172.988[b]	1	172.988	.771	.406
	AP_STDav	909.187[c]	1	909.187	14.661	.005
	avf_STDav	438.115[d]	1	438.115	2.019	.193
	avgheel_ACCav	3.988[e]	1	3.988	.548	.480
	avgheel_ACCstride	.062[f]	1	.062	.024	.881
	avgheel_STDav	2.165[g]	1	2.165	.338	.577
	avgheel_STDstride	.008[h]	1	.008	.003	.960
	avgmid_ACCav	.334[i]	1	.334	.910	.368
	avgmid_ACCstride	.005[j]	1	.005	.006	.941
	avgmid_STDav	.527[k]	1	.527	1.010	.344
	avgmid_STDstride	.000[l]	1	.000	.000	.984
	avgtop_ACCav	.821[m]	1	.821	1.733	.224
	avgtop_ACCstride	.073[n]	1	.073	.052	.825
	avgtop_STDav	.445[o]	1	.445	.886	.374
	avgtop_STDstride	.010[p]	1	.010	.006	.938
	ct_ACCav	.004[q]	1	.004	2.060	.189
	ct_STDav	.007[r]	1	.007	4.796	.060
	i_ACCav	91.177[s]	1	91.177	2.142	.181
	i_STDav	228.085[t]	1	228.085	5.429	.048
	MAXAP_ACCav	453.707[u]	1	453.707	5.073	.054
	MAXAP_STDav	767.038[v]	1	767.038	3.937	.083
	maxML_ACCav	.399[w]	1	.399	.737	.416
	maxML_STDav	.144[x]	1	.144	.125	.732
	MINAP_ACCav	2.964[y]	1	2.964	.038	.851
	MINAP_STDav	6.040[z]	1	6.040	.058	.816
	minML_ACCav	17.712[aa]	1	17.712	4.390	.069
	minML_STDav	17.215[ab]	1	17.215	3.336	.105
	ML_ACCav	12.765[ac]	1	12.765	2.632	.143
	ML_STDav	14.219[ad]	1	14.219	2.854	.130

	P	15069.115[ae]	1	15069.115	5.636	.045
	p_ACCav	22.045[af]	1	22.045	.048	.831
	p_STDav	444.552[ag]	1	444.552	.860	.381
	PEAKAP_ACCav	4.077[ah]	1	4.077	.016	.901
	PEAKAP_STDav	19.061[ai]	1	19.061	.085	.779
	peakheel_ACCav	1.980[aj]	1	1.980	.173	.688
	peakheel_STDav	.069[ak]	1	.069	.008	.931
	peakmid_ACCav	.459[al]	1	.459	.906	.369
	peakmid_STDav	.236[am]	1	.236	.337	.578
	peakML_ACCav	2.142[an]	1	2.142	3.674	.092
	peakML_STDav	2.341[ao]	1	2.341	3.258	.109
	peaktop_ACCav	.259[ap]	1	.259	.272	.616
	peaktop_STDav	.346[aq]	1	.346	.362	.564
	percentheel_ACCav	.046[ar]	1	.046	12.009	.008
	percentheel_STDav	.047[as]	1	.047	10.506	.012
	percentmid_ACCav	.048[at]	1	.048	7.561	.025
	percentmid_STDav	.048[au]	1	.048	12.078	.008
	percentpeak_ACCav	.215[av]	1	.215	16.183	.004
	percentpeak_STDav	.329[aw]	1	.329	16.596	.004
	percenttop_ACCav	.058[ax]	1	.058	13.704	.006
	percenttop_STDav	.046[ay]	1	.046	14.072	.006
	sr	.006[az]	1	.006	.247	.633
	W	1649027.561[ba]	1	1649027.561	13.297	.007
Intercept	AP_ACCav	77869.320	1	77869.320	1471.993	.000
	avf_ACCav	31639.918	1	31639.918	140.940	.000
	AP_STDav	72770.678	1	72770.678	1173.426	.000
	avf_STDav	35190.154	1	35190.154	162.207	.000
	avgheel_ACCav	583.103	1	583.103	80.169	.000
	avgheel_ACCstride	264.249	1	264.249	101.250	.000
	avgheel_STDav	591.056	1	591.056	92.213	.000
	avgheel_STDstride	287.135	1	287.135	102.994	.000
	avgmid_ACCav	99.166	1	99.166	270.342	.000
	avgmid_ACCstride	53.239	1	53.239	65.433	.000
	avgmid_STDav	99.070	1	99.070	189.756	.000
	avgmid_STDstride	57.640	1	57.640	63.684	.000
	avgtop_ACCav	48.356	1	48.356	102.156	.000

	avgtop_ACCstride	29.498	1	29.498	21.284	.002
	avgtop_STDav	43.644	1	43.644	86.849	.000
	avgtop_STDstride	30.480	1	30.480	20.163	.002
	ct_ACCav	1.039	1	1.039	489.453	.000
	ct_STDav	1.518	1	1.518	973.350	.000
	i_ACCav	3576.225	1	3576.225	84.020	.000
	i_STDav	5567.327	1	5567.327	132.510	.000
	MAXAP_ACCav	264764.722	1	264764.722	2960.262	.000
	MAXAP_STDav	259004.722	1	259004.722	1329.387	.000
	maxML_ACCav	346.077	1	346.077	638.191	.000
	maxML_STDav	381.537	1	381.537	331.781	.000
	MINAP_ACCav	55460.784	1	55460.784	702.412	.000
	MINAP_STDav	57200.181	1	57200.181	550.349	.000
	minML_ACCav	18.274	1	18.274	4.529	.066
	minML_STDav	20.876	1	20.876	4.046	.079
	ML_ACCav	205.316	1	205.316	42.334	.000
	ML_STDav	224.030	1	224.030	44.965	.000
	P	855585.865	1	855585.865	319.996	.000
	p_ACCav	160802.093	1	160802.093	353.583	.000
	p_STDav	165577.073	1	165577.073	320.237	.000
	PEAKAP_ACCav	82320.521	1	82320.521	330.030	.000
	PEAKAP_STDav	82593.462	1	82593.462	366.181	.000
	peakheel_ACCav	1421.814	1	1421.814	124.509	.000
	peakheel_STDav	1389.676	1	1389.676	158.761	.000
	peakmid_ACCav	303.836	1	303.836	599.964	.000
	peakmid_STDav	306.093	1	306.093	436.259	.000
	peakML_ACCav	317.882	1	317.882	545.268	.000
	peakML_STDav	332.745	1	332.745	463.101	.000
	peaktop_ACCav	221.003	1	221.003	232.189	.000
	peaktop_STDav	225.831	1	225.831	236.673	.000
	percentheel_ACCav	4.704	1	4.704	1231.620	.000
	percentheel_STDav	5.467	1	5.467	1216.137	.000
	percentmid_ACCav	7.590	1	7.590	1191.075	.000
	percentmid_STDav	7.856	1	7.856	1971.124	.000
	percentpeak_ACCav	3.516	1	3.516	264.506	.000
	percentpeak_STDav	3.939	1	3.939	198.836	.000
	percenttop_ACCav	8.628	1	8.628	2054.623	.000
	percenttop_STDav	9.177	1	9.177	2808.790	.000

	sr	9.363	1	9.363	386.400	.000
	W	79747201.173	1	79747201.173	643.040	.000
Conditiondrom1reg2	AP_ACCav	530.102	1	530.102	10.021	.013
	avf_ACCav	172.988	1	172.988	.771	.406
	AP_STDav	909.187	1	909.187	14.661	.005
	avf_STDav	438.115	1	438.115	2.019	.193
	avgheel_ACCav	3.988	1	3.988	.548	.480
	avgheel_ACCstride	.062	1	.062	.024	.881
	avgheel_STDav	2.165	1	2.165	.338	.577
	avgheel_STDstride	.008	1	.008	.003	.960
	avgmid_ACCav	.334	1	.334	.910	.368
	avgmid_ACCstride	.005	1	.005	.006	.941
	avgmid_STDav	.527	1	.527	1.010	.344
	avgmid_STDstride	.000	1	.000	.000	.984
	avgtop_ACCav	.821	1	.821	1.733	.224
	avgtop_ACCstride	.073	1	.073	.052	.825
	avgtop_STDav	.445	1	.445	.886	.374
	avgtop_STDstride	.010	1	.010	.006	.938
	ct_ACCav	.004	1	.004	2.060	.189
	ct_STDav	.007	1	.007	4.796	.060
	i_ACCav	91.177	1	91.177	2.142	.181
	i_STDav	228.085	1	228.085	5.429	.048
	MAXAP_ACCav	453.707	1	453.707	5.073	.054
	MAXAP_STDav	767.038	1	767.038	3.937	.083
	maxML_ACCav	.399	1	.399	.737	.416
	maxML_STDav	.144	1	.144	.125	.732
	MINAP_ACCav	2.964	1	2.964	.038	.851
	MINAP_STDav	6.040	1	6.040	.058	.816
	minML_ACCav	17.712	1	17.712	4.390	.069
	minML_STDav	17.215	1	17.215	3.336	.105
	ML_ACCav	12.765	1	12.765	2.632	.143
	ML_STDav	14.219	1	14.219	2.854	.130
	P	15069.115	1	15069.115	5.636	.045
	p_ACCav	22.045	1	22.045	.048	.831
	p_STDav	444.552	1	444.552	.860	.381
	PEAKAP_ACCav	4.077	1	4.077	.016	.901
	PEAKAP_STDav	19.061	1	19.061	.085	.779
	peakheel_ACCav	1.980	1	1.980	.173	.688

	peakheel_STDav	.069	1	.069	.008	.931
	peakmid_ACCav	.459	1	.459	.906	.369
	peakmid_STDav	.236	1	.236	.337	.578
	peakML_ACCav	2.142	1	2.142	3.674	.092
	peakML_STDav	2.341	1	2.341	3.258	.109
	peaktop_ACCav	.259	1	.259	.272	.616
	peaktop_STDav	.346	1	.346	.362	.564
	percentheel_ACCav	.046	1	.046	12.009	.008
	percentheel_STDav	.047	1	.047	10.506	.012
	percentmid_ACCav	.048	1	.048	7.561	.025
	percentmid_STDav	.048	1	.048	12.078	.008
	percentpeak_ACCav	.215	1	.215	16.183	.004
	percentpeak_STDav	.329	1	.329	16.596	.004
	percenttop_ACCav	.058	1	.058	13.704	.006
	percenttop_STDav	.046	1	.046	14.072	.006
	sr	.006	1	.006	.247	.633
	W	1649027.561	1	1649027.561	13.297	.007
Error	AP_ACCav	423.205	8	52.901		
	avf_ACCav	1795.943	8	224.493		
	AP_STDav	496.125	8	62.016		
	avf_STDav	1735.565	8	216.946		
	avgheel_ACCav	58.187	8	7.273		
	avgheel_ACCstride	20.879	8	2.610		
	avgheel_STDav	51.277	8	6.410		
	avgheel_STDstride	22.303	8	2.788		
	avgmid_ACCav	2.935	8	.367		
	avgmid_ACCstride	6.509	8	.814		
	avgmid_STDav	4.177	8	.522		
	avgmid_STDstride	7.241	8	.905		
	avgtop_ACCav	3.787	8	.473		
	avgtop_ACCstride	11.087	8	1.386		
	avgtop_STDav	4.020	8	.503		
	avgtop_STDstride	12.093	8	1.512		
	ct_ACCav	.017	8	.002		
	ct_STDav	.012	8	.002		
	i_ACCav	340.512	8	42.564		
	i_STDav	336.115	8	42.014		
	MAXAP_ACCav	715.517	8	89.440		

	MAXAP_STDav	1558.641	8	194.830		
	maxML_ACCav	4.338	8	.542		
	maxML_STDav	9.200	8	1.150		
	MINAP_ACCav	631.661	8	78.958		
	MINAP_STDav	831.475	8	103.934		
	minML_ACCav	32.277	8	4.035		
	minML_STDav	41.280	8	5.160		
	ML_ACCav	38.799	8	4.850		
	ML_STDav	39.859	8	4.982		
	P	21389.898	8	2673.737		
	p_ACCav	3638.235	8	454.779		
	p_STDav	4136.368	8	517.046		
	PEAKAP_ACCav	1995.469	8	249.434		
	PEAKAP_STDav	1804.427	8	225.553		
	peakheel_ACCav	91.355	8	11.419		
	peakheel_STDav	70.026	8	8.753		
	peakmid_ACCav	4.051	8	.506		
	peakmid_STDav	5.613	8	.702		
	peakML_ACCav	4.664	8	.583		
	peakML_STDav	5.748	8	.719		
	peaktop_ACCav	7.615	8	.952		
	peaktop_STDav	7.634	8	.954		
	percentheel_ACCav	.031	8	.004		
	percentheel_STDav	.036	8	.004		
	percentmid_ACCav	.051	8	.006		
	percentmid_STDav	.032	8	.004		
	percentpeak_ACCav	.106	8	.013		
	percentpeak_STDav	.158	8	.020		
	percenttop_ACCav	.034	8	.004		
	percenttop_STDav	.026	8	.003		
	sr	.194	8	.024		
	W	992126.918	8	124015.865		
Total	AP_ACCav	78822.628	10			
	avf_ACCav	33608.848	10			
	AP_STDav	74175.989	10			
	avf_STDav	37363.834	10			
	avgheel_ACCav	645.279	10			
	avgheel_ACCstride	285.190	10			

	avgheel_STDav	644.499	10			
	avgheel_STDstride	309.446	10			
	avgmid_ACCav	102.435	10			
	avgmid_ACCstride	59.753	10			
	avgmid_STDav	103.775	10			
	avgmid_STDstride	64.882	10			
	avgtop_ACCav	52.964	10			
	avgtop_ACCstride	40.658	10			
	avgtop_STDav	48.109	10			
	avgtop_STDstride	42.583	10			
	ct_ACCav	1.060	10			
	ct_STDav	1.538	10			
	i_ACCav	4007.915	10			
	i_STDav	6131.527	10			
	MAXAP_ACCav	265933.946	10			
	MAXAP_STDav	261330.402	10			
	maxML_ACCav	350.815	10			
	maxML_STDav	390.881	10			
	MINAP_ACCav	56095.409	10			
	MINAP_STDav	58037.696	10			
	minML_ACCav	68.263	10			
	minML_STDav	79.372	10			
	ML_ACCav	256.881	10			
	ML_STDav	278.107	10			
	P	892044.878	10			
	p_ACCav	164462.373	10			
	p_STDav	170157.994	10			
	PEAKAP_ACCav	84320.067	10			
	PEAKAP_STDav	84416.951	10			
	peakheel_ACCav	1515.148	10			
	peakheel_STDav	1459.771	10			
	peakmid_ACCav	308.346	10			
	peakmid_STDav	311.943	10			
	peakML_ACCav	324.687	10			
	peakML_STDav	340.834	10			
	peaktop_ACCav	228.877	10			
	peaktop_STDav	233.811	10			
	percentheel_ACCav	4.780	10			

	percentheel_STDav	5.550	10			
	percentmid_ACCav	7.689	10			
	percentmid_STDav	7.937	10			
	percentpeak_ACCav	3.838	10			
	percentpeak_STDav	4.426	10			
	percenttop_ACCav	8.719	10			
	percenttop_STDav	9.250	10			
	sr	9.562	10			
	W	82388355.652	10			
Corrected Total	AP_ACCav	953.307	9			
	avf_ACCav	1968.931	9			
	AP_STDav	1405.311	9			
	avf_STDav	2173.680	9			
	avgheel_ACCav	62.176	9			
	avgheel_ACCstride	20.941	9			
	avgheel_STDav	53.443	9			
	avgheel_STDstride	22.311	9			
	avgmid_ACCav	3.269	9			
	avgmid_ACCstride	6.514	9			
	avgmid_STDav	4.704	9			
	avgmid_STDstride	7.241	9			
	avgtop_ACCav	4.607	9			
	avgtop_ACCstride	11.160	9			
	avgtop_STDav	4.465	9			
	avgtop_STDstride	12.103	9			
	ct_ACCav	.021	9			
	ct_STDav	.020	9			
	i_ACCav	431.690	9			
	i_STDav	564.200	9			
	MAXAP_ACCav	1169.224	9			
	MAXAP_STDav	2325.679	9			
	maxML_ACCav	4.738	9			
	maxML_STDav	9.344	9			
	MINAP_ACCav	634.625	9			
	MINAP_STDav	837.515	9			
	minML_ACCav	49.989	9			

	minML_STDav	58.495	9			
	ML_ACCav	51.564	9			
	ML_STDav	54.077	9			
	P	36459.013	9			
	p_ACCav	3660.280	9			
	p_STDav	4580.920	9			
	PEAKAP_ACCav	1999.546	9			
	PEAKAP_STDav	1823.489	9			
	peakheel_ACCav	93.335	9			
	peakheel_STDav	70.095	9			
	peakmid_ACCav	4.510	9			
	peakmid_STDav	5.849	9			
	peakML_ACCav	6.806	9			
	peakML_STDav	8.089	9			
	peaktop_ACCav	7.874	9			
	peaktop_STDav	7.979	9			
	percentheel_ACCav	.076	9			
	percentheel_STDav	.083	9			
	percentmid_ACCav	.099	9			
	percentmid_STDav	.080	9			
	percentpeak_ACCav	.321	9			
	percentpeak_STDav	.487	9			
	percenttop_ACCav	.091	9			
	percenttop_STDav	.072	9			
	sr	.200	9			
	W	2641154.479	9			